NATIONAL TECHNICAL UNIVERSITY OF ATHENS
CROSS-DEPARTMENTAL POSTGRADUATE PROGRAMME OF STUDIES
«DESIGN AND CONSTRUCTION OF UNDERGROUND WORKS»
SCHOOL OF CIVIL ENGINEERING
DEPARTMENT OF GEOTECHNICAL ENGINEERING

# EFFECT OF HYDRAULIC CONDITIONS ON CONTROLLING THE EXCAVATION FACE OF SHALLOW, EPB-BORED TUNNELS

A Postgraduate Thesis by

**PAPADAKOS ANASTASIOS**
Civil Engineer, D.U.TH

**Supervisor:** M. Kavvadas, Assistant Professor, N.T.U.A

ATHENS, JULY 2015

# ACKNOWLEDGMENTS

First things first, I would like to thank all the staff of the Geotechnical Engineering Department for their general assistance during my postgraduate course of studies and especially my supervisor, Mr. M. Kavvadas[1], for giving me also the opportunity to fulfill this project.

Additionally, I am indebted to Litsas Dimitrios[2] and Panagiotis Sitarenios[3], for their constant desire to assist and support this work, for the patience they showed and also for their time and cooperation. Also, I would like to thank ATTIKO METRO S.A. and the contractor JV of the Line 3 Project: "Extension to Piraeus" for the information they provided us after the fruitful visit we took at the worksite of Ag. Varvara Station.

Finally, I am more than grateful to my family for all kind of support throughout my studies. Consequently, this Thesis is dedicated to them.

Papadakos Anastasios

Civil Engineer, D.U.TH.

Athens, July 2015

[1] Assistant Professor, Department of Geotechnical Engineering, N.T.U.A

[2] , [3] Ph.D. Candidates, Department of Geotechnical Engineering, N.T.U.A

# TABLE OF CONTENTS

# ΕΚΤΕΝΗΣ ΕΛΛΗΝΙΚΗ ΠΕΡΙΛΗΨΗ

Η παρούσα Μεταπτυχιακή Διπλωματική Εργασία πραγματεύεται το ζήτημα της απαίτησης ευστάθειας του μετώπου σήραγγας, σε πλήρως κορεσμένο έδαφος, υπό μηχανοποιημένη διάνοιξη. Πιο συγκεκριμένα, διερευνήθηκε η επιρροή των υδραυλικών συνθηκών στην ευστάθεια του μετώπου αβαθούς σήραγγας, διανοιγμένης με μηχάνημα εξισορρόπησης της εδαφικής πίεσης (EPB), σε πλήρως κορεσμένο, αργιλικό έδαφος κατά την φάση της εκσκαφής.

Η προαναφερθείσα διερεύνηση συντελέστηκε μέσω ενενήντα τριών (93) τρισδιάστατων, συζευγμένων-αριθμητικών αναλύσεων με το λογισμικό πεπερασμένων στοιχείων «Abaqus v.11.1». Η μηχανοποιημένη όρυξη με EPB προσομοιώθηκε μόνο ως μια ισοδύναμη πίεση μετώπου δηλαδή χωρίς να ληφθούν υπόψη παράμετροι όπως πχ τα κενά μεταξύ ασπίδας και εδάφους/προκατασκευασμένου στοιχείου, το βάρος του μηχανήματος, η γεωμετρία της ασπίδας, ο θάλαμος εκσκαφής, η ενεμάτωση κλπ. καθώς έχει αποδειχτεί από πρόσφατες αναλύσεις ευαισθησίας[4] ότι η επιρροή τους στην ευστάθεια του μετώπου είναι αμελητέα. Οι συζευγμένες αναλύσεις αφορούν συγκεκριμένα γεωμετρικά χαρακτηριστικά, καθώς εξετάστηκε ένας (1) λόγος υπερκειμένου προς τη διάμετρο της διατομής (H/D) και συγκεκριμένο αρχικό εντατικό πεδίο.

Η ευστάθεια του μετώπου ποσοτικοποιήθηκε με τη χρήση της εξώθησης της επιφάνειας και της ακτινικής σύγκλισης των τοιχωμάτων της διατομής στη θέση του μετώπου. Οι παράμετροι που μεταβάλλονταν σε κάθε ομάδα αναλύσεων είναι τα γεωτεχνικά στοιχεία του εδάφους (c, ϕ, E, δ) με βάση το κριτήριο αστοχίας Mohr Coulomb. Οι παράμετροι των οποίων η υδραυλική επιρροή διερευνήθηκε ήταν κυρίως:

- η ασκούμενη πίεση υποστήριξης,
- η διαπερατότητα του εδάφους και
- ο ρυθμός εκσκαφής (ή ρυθμός προχώρησης)

Η ασκούμενη πίεση μετώπου λαμβάνει τραπεζοειδή κατανομή με κλίση ίση και σταθερή με την πυκνότητα του υλικού εκσκαφής, η οποία θεωρήθηκε 15KN/m$^3$. Η τιμή

[4] (Kavvadas M., Litsas D., Sitarenios P., Chortis P., Kalos A., Rachmani A. , 2015)

αναφοράς στη στέψη της σήραγγας εκφράστηκε ως συνάρτηση της υδροστατικής πίεσης μέσω ενός αδιάστατου παράγοντα Α. Βασική παραδοχή των αναλύσεων είναι πως το υλικό εκσκαφής συμπεριφέρεται ως ιξώδες ρευστό λόγω της χρήσης ρυθμιστικών προσθέτων κάτι που από γεωτεχνικής απόψεως σημαίνει ότι δεν αναπτύσσονται ενεργές τάσεις στο θάλαμο και άρα η ασκούμενη πίεση (ολική) «μεταφράζεται» ως συνοριακή πίεση πόρων στο μέτωπο εκσκαφής. Ωστόσο, επειδή η προαναφερθείσα θεώρηση παραπέμπει σε ιδανικές συνθήκες βελτίωσης του εκσκαπτόμενου υλικού διενεργήθηκε μια ομάδα αναλύσεων όπου εξετάστηκε η επιρροή της ανάπτυξης ενεργών τάσεων στο υλικό.

Η αποτίμηση των αποτελεσμάτων (εξώθηση, ακτινική σύγκλιση) στη ευστάθεια του μετώπου εκσκαφής έγινε λαμβάνοντας υπόψη και υδρο-μηχανικά φαινόμενα όπως οι πιέσεις πόρων που αναπτύσσονται μπροστά από το μέτωπο, πιθανή ανάπτυξη συρτικών δυνάμεων ροής προς το μέτωπο, μύζηση κλπ. Τα αποτελέσματα παρουσιάζονται σε διαγράμματα αδιαστατοποιημένης εξώθησης/σύγκλισης σε σχέση με τον προτεινόμενο δείκτη ευστάθειας $2C_u/\gamma' H$. Η χρήση της αστράγγιστης διατμητικής αντοχής του εδάφους ($C_u$) υποδηλώνει αστράγγιστες συνθήκες παραμόρφωσης. Πράγματι, ενδελεχής εξέταση της μεταβολής του λόγου κενών σε όλες τις αναλύσεις έδειξε ότι η ογκομετρική παραμόρφωση ήταν αμελητέα. Τα σημεία-κλειδιά στα οποία αξίζει να σταθεί κανείς είναι τα εξής:

- Αποδείχτηκε πως η ασκούμενη πίεση μετώπου αποτελεί καθοριστική παράμετρο της ευστάθειας του μετώπου. Αυτό πρακτικά σημαίνει πως είναι σημαντικό να αποφεύγονται και να προλαμβάνονται διακυμάνσεις πίεσης καθώς μπορεί να αποτυπωθούν άμεσα στις μετακινήσεις. Πίεση μετώπου κατώτερη της υδροστατικής ($A<1.0$) σε συνδυασμό με πτωχά γεωτεχνικά χαρακτηριστικά ($2C_u/\gamma' H<1.0$) μπορεί να οδηγήσει σε συνθήκες καθολικής αστάθειας. Αντίθετα, πίεση μετώπου ίση ή μεγαλύτερη της υδροστατικής ακόμα και σε μη ευνοϊκές γεωτεχνικές συνθήκες θεωρείται ικανή να διασφαλίσει την ευστάθειά του. Η παραμόρφωση (εξώθηση, ακτινική σύγκλιση) φαίνεται να συγκεντρώνεται στο άνω μισό της διατομής λόγω της μειωμένης υποστήριξης σε σχέση με τον πυθμένα.
- Η μεταβολή της διαπερατότητας στα πλαίσια των λεπτόκοκκων υλικών έδειξε ότι δεν ήταν ικανή ώστε να μεταβάλλει τις συνθήκες στράγγισης. Παρόλα

αυτά προέκυψε ότι η ευστάθεια του μετώπου μπορεί ν' «απειληθεί» με την αύξηση της διαπερατότητας σε εδάφη με πτωχά γεωτεχνικά χαρακτηριστικά ακόμη και όταν η πίεση του μετώπου είναι μεγαλύτερη της υδροστατικής. Το μέγεθος της επιρροής εξαρτάται σε μεγάλο βαθμό από τις υδραυλικές συνοριακές συνθήκες, ήτοι τις πιέσεις πόρων στην επιφάνεια του μετώπου καθώς καθορίζουν την υδραυλική βαθμίδα και τις επαγόμενες δυνάμεις ροής. Οι συνοριακές πιέσεις πόρων με τη σειρά τους εξαρτώνται από τη συμπεριφορά του εκσκαπτόμενου υλικού καταδεικνύοντας έτσι τη μεγάλη σημασία της αποτελεσματικής βελτίωσης στη μείωση του υδραυλικού φορτίου.

- Μεταβολή του ρυθμού προχώρησης σ' ένα εφικτό στην πράξη εύρος, έδειξε ότι επίσης δεν επηρεάζει τη συνθήκες στράγγισης αλλά ούτε και τις επαγόμενες μετακινήσεις σε σημαντικό βαθμό.
- Αποδείχτηκε ότι η εξώθηση του μετώπου και η σύγκλιση της διατομής είναι δύο στενά συνδεδεμένοι και αλληλοεξαρτώμενοι μηχανισμοί παραμόρφωσης καθώς η προοδευτική εξώθηση που λαμβάνει χώρα μπροστά από το μέτωπο είναι αποτέλεσμα της προοδευτικής σύγκλισης της διατομής.
- Η επιρροή του υδραυλικού πεδίου στην ευστάθεια του μετώπου εκτιμήθηκε κυρίως μέσω της κατανομής των υπερ/υπό-πιέσεων του νερού των πόρων μπροστά από το μέτωπο. Βρέθηκε ότι μείωση της διαπερατότητας ή/και αύξηση του ρυθμού προχώρησης ακόμη και σε μη ευνοϊκές συνθήκες (χαμηλή εδαφική αντοχή – χαμηλή πίεση μετώπου) λειτουργεί υπέρ της ευστάθειας του μετώπου λόγω του περιορισμού της στράγγισης και της ανάπτυξης υπο-πιέσεων (μύζηση). Η συμβολή αυτή όμως είναι χρονικά εξαρτώμενη κάτι που υποδεικνύει πως μεγάλες παύσεις στον κύκλο εργασιών (σταλία μηχανήματος, συντηρήσεις κλπ) πρέπει να αποφεύγονται. Σημαντικές δυνάμεις ροής δεν αναμένονταν λόγω των αστράγγιστων συνθηκών, ωστόσο η αύξηση της υδραυλικής βαθμίδας λόγω πτώσης της συνοριακής πίεσης πόρων συντελεί στην περαιτέρω αύξηση της εξώθησης.
- Τέλος, προέκυψε ότι ακόμη και σημαντική αύξηση των ενεργών τάσεων στο εσωτερικό του θαλάμου εκσκαφής (πτώση της συνοριακή πίεσης των πόρων) λόγω στερεοποίησης του εκσκαπτόμενου υλικού δεν ήταν ικανή να επηρεάσει τόσο το υδραυλικό φορτίο όσο και τις επαγόμενες παραμορφώσεις.

# INTRODUCTION

As it is well known, when it comes for shallow tunnelling in urban areas and especially soft ground conditions, the EPB-Shield machine is probably the optimum option. This type of machine, best applicable in cohesive soils, turns the excavated material into a soil paste in order to use it as a support medium during the whole procedure. The latter, enables optimum control and distribution of the pressure exerted at the tunnel face, minimum settlements at the surface and last but not least, avoidance of uncontrolled inflow of soil and water into the machine. More frictional, e.g. sandy soils, are usually treated with Slurry machines; however considering: i) the undesirably large space that has to be occupied with the so-called separation plant on the work site, ii) the additional costs that arise compared to those of EPBs in case of considerable fine content presence and iii) the latest progress of the additive industry which extended the application range of EPBs, the use of Slurry Machines in urban tunnelling is nowadays limited.

One of the most important tasks that an EPB machine has to deal with is the demand for constant stability of the tunnel face, both during the excavation procedure and during the standstills. The term standstill refers to any pause of the boring process including the unavoidable ring construction phase. Besides, as Lunardi (2000) admitted, experience has shown that the most common type of failure in tunnelling process is the failure of the heading or its vicinity leading to serious delays and financial surcharges. Tunnel face stability can really be affected in case of tunnelling in saturated soils, very often encountered in urban areas. Any difference in the piezometric head between the excavation chamber and the underground table of a frictionless soil, may lead to considerable water seepage flow inwards the tunnel and as a result in serious face instabilities, unless suitable measures are predetermined. In other occasion, an unnecessary high rate of advance in cohesive soils, could lead to sudden pore pressure rise in the vicinity of the tunnel face. The latter will result in effective stresses' decrease and probably in collapse. Similar type of failure could also be caused by liquefaction of granular soils due to the excess pore pressure build up in the case of constrained drainage. To sum up, it is evident that many factors and parameters have to be taken into consideration when the face stability is under investigation in shallow tunnelling practice.

The main purpose of the present Thesis is to investigate through multi-parametric analyses, the hydraulic conditions' effect on tunnel face stability of EPB-bored tunnels, during the excavation procedure. In order to accomplish the latter, ninety three (93) 3D-coupled, numerical analyses were conducted using the finite element code "Abaqus v.11.1". The stability of the tunnel heading is interpreted in terms of face extrusion and radial wall convergence whereas the practical aim is to seek for any relationship between the previous two (2) instability moduli and the geotechnical properties of the soil, for given values of applied face pressure. Parallel investigation of the ground permeability and the applied advance rate will determine the drainage conditions of the tunnel face and consequently their effect on the problem.

Explicit presentation of the function of EPB-Shield TBMs and its parts is considered to be redundant since it has been extensively analyzed so far in the international literature and thus it has been omitted from the present contribution.

# ABSTRACT

The present Postgraduate Thesis deals with the subject of face stability demand in mechanically excavated tunnels below the water table. More specifically, the effect of hydraulic conditions on the stability of the excavation face was thoroughly investigated through multi-parametric analyses that refer to EPB-bored, shallow tunnels, in fully saturated, clayey soil, during the excavation procedure.

In order to achieve the aforementioned investigation, a set of ninety three (93) numerical, 3D-coupled analyses were carried out through the Finite Element code "Abaqus v.11.1". The EPB machine was modelled only as an equivalent pressure load on the working face without considering any other feature such as tail/annular voids, weight of the machine, geometry of the shield, grouting etc. because of their negligible effect on face stability. The aforementioned analyses concern specific geometrical characteristics (H/D) and hydrostatic initial stress field.

Face stability was interpreted in terms of extrusion and radial wall convergence of the investigated cross section. In each set of analyses, geotechnical properties of the soil (c, $\phi$, E, $\delta$) were modified according to the Mohr-Coulomb failure criterion. Regarding the hydraulic conditions, the effect of the applied face pressure, soil permeability and advance rate of the machine was particularly investigated. The applied face pressure was correlated with the hydrostatic pressure at the crown of the shield. One of the basic modelling assumptions that had to be made in order to define the hydraulic boundary conditions of the problem, concerns the muck's condition. The muck was assumed to act as a viscous fluid thanks to effective soil conditioning. The latter means, in terms of modelling, that the applied face pressure (total pressure values) coincides with pore pressure values at each node of the face. Resulting face extrusion and radial wall convergence were evaluated in association with developed hydraulic phenomena such as excess pore pressure build up, suction, unfavorable seepage forces etc.

Results are plotted versus the newly introduced stability factor $2C_u/\gamma'H$. The use of undrained shear strength parameter was verified as the results showed negligible variation of void ratio in all the investigated cases. To sum up, it was proved that the applied face

pressure is decisive regarding the stability of the face and thus pressure fluctuations have to be foreseen and avoided. Pore pressure values at the face (hydraulic boundaries) were found also to have a significant effect on face stability as they control the excavation-induced disturbance on the local hydraulic head field. Hydraulic boundaries at the working face depend on the condition of the muck indicating the major importance of soil conditioning. In parallel, decrease of the ground permeability or/and increase of the excavation advance rate up to feasible limits enhance the stability of the face due to negative excess pore pressure development as the drainage conditions are hindered and vice versa. However, the effect of advance rate variation found to be significantly lower compared to that of permeability. Finally, investigation of hydraulic head field disturbance and its impact on deformations caused by consolidation of the muck showed that even a significant rise of effective stresses into the muck is not adequate to affect neither the anticipated deformations nor the hydraulic head distribution for the assumed permeability.

# LIST OF FIGURES

# LIST OF TABLES

# LIST OF SYMBOLS/ABBREVIATIONS

A: face pressure parameter/Skempton's coefficient

AR, v: advance rate

c: soil cohesion

$C_u$: undrained shear strength

D: tunnel's diameter

E: Elasticity modulus

e: void ratio

EPBM: Earth Pressure Balance Machine

FEM: Finite Element Method

FIR: Foam Injection Ratio

$f_S$: seepage force

G': submerged self-weight of the wedge

H: overburden height, measured from z=0 (tunnel axis)

i: hydraulic gradient

$I_C$: consistency Index

$I_P$: plasticity Index

JV: Joint Venture

k: soil permeability

$K_0$: coefficient of lateral earth pressure "at rest"

MC: Mohr-Coulomb

MCC: Modified Cam-Clay

NATM: New Austrian Tunnelling Method

$P_0$: pressure value at the tunnel crown

$P_{m,eff}$: mean effective geostatic stress

R: tunnel's radius

s: coefficient of storativity

$S_r$: degree of saturation

TBM: Tunnel Boring Machine

u: pore water pressure

$U_h$: extrusion (or $U_2$)

$U_{R,\infty}$: maximum radial convergence (far, behind the face)

$U_R$: radial wall convergence

V′: submerged overburden weight

$V_{extr}$: average extruded volume of the face

x: distance from the investigated section (y=40m)

$\gamma'$: submerged unit weight

$\gamma_{sat}$: saturated unit weight

$\delta$: dilatancy angle

$\Delta u$: excess pore water pressure

$\lambda$: de-confinement ratio

$\nu$: Poisson's ratio

$\sigma_1$: vertical principal stress

$\sigma_3$: lateral principal stress

$\phi$: angle of inner friction

$\Omega_F$: dimensionless extrusion factor

$\Omega_R$: dimensionless radial convergence factor

# 1
# Review of the Theoretical Background

## 1.1. Face Stability in saturated media – A 3D problem

Even nowadays, the most common approach for tunnel design is the plane-strain state, due to its simplicity and saving in computational time. This approach may be adequate for support measures' design but when the stability of the face or the effect on the overlain structures has to be evaluated, especially in the presence of underground water, the problem is indisputably three-dimensional. On the other hand, the alternative type of two-dimensional analysis, i.e. the axisymmetric stress-strain state, can be properly applied only in the case of deep tunnels as the rotation of problem's boundaries is not a valid assumption when considering shallow tunnels.

A two-dimensional analysis, not only neglects the evaluation of the face stability but also overlooks the crucial matter of the **preconvergence**, i.e. the soil movement ahead of the tunnel face and towards it, induced as a response of the medium to the action of excavation (Figure 2). During the excavation, the soil tends to fill up the cavity created and moves towards its interior (convergence). The cause of this effect is well interpreted. While the excavation propagates, an incremental loss of confinement is induced in the vicinity of the tunnel. The extent of this area, known as the **plasticization zone** and the questions over the timing and the capability of reaching equilibrium (arching), are highly dependent to the in-situ stress state and soil characteristics. In cases where soil strength is too low or in-situ stresses too high, arching is insignificant near the tunnel and soil plasticization is triggered. In cases where soil strength is adequate to withstand loading elastically, arching of the face is significant and practically no deformation of the face is induced (Figure 1). Finally, in extreme cases, soil may be not able to respond to stress variations and failure is triggered quite instantly, in form of a chain effect, without being able to reach equilibrium. Arching of the face is sparsely encountered in common soil formations while chain-like failures is more probable in dry, soft, cohesionless soils or in heavily jointed rocks (Figure 2, Figure 3).

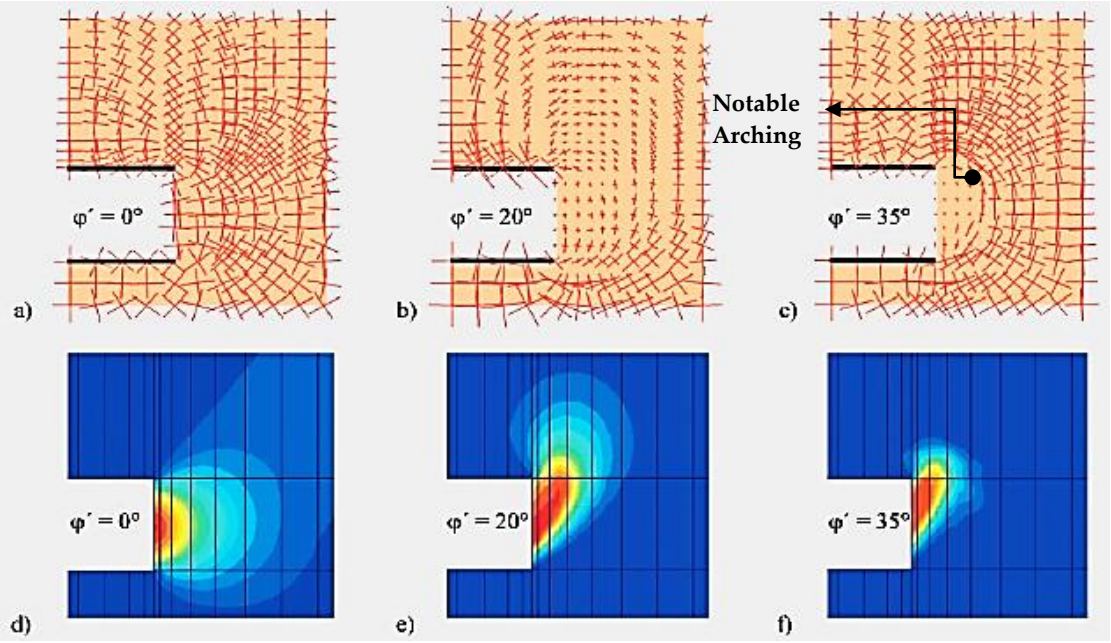


**Figure 1:** Course of principal stresses (a-c) and respective incremental displacements at failure in cohesionless soil with H/D=5 (d-f) (Vermeer P.A. et al, 2002)

The preconvergence is cumulatively encountered at the excavation face as **extrusion**. Supposing that no stabilization measure of the face is taken, the horizontal stress $\sigma_3$ (in direction of the tunnel axis) exerted on an elementary (infinitesimal) piece of soil in chainage advance, is constantly reduced as the excavation proceeds, to zero value when the face arrives, resulting in extrusion. According to Lunardi (2000), the term extrusion refers to the primary component of the deformation response of the medium to the action of excavation that develops largely inside the **advance core** and appears mostly as "bellying" of the face for common soil formations. Other usual forms of face extrusion, often encountered in rocky formations are the dislocation of unstable volumes due to the unfavorable joint network of the rock mass (structural failure, Figure 3). The aforementioned advance core consists of the soil volume that lies **ahead** of the face, virtually cylindrical in shape with height and diameter approximately equal to 1D. Preconvergence and face extrusion are found to be closely related and chronologically consistent as it can be reasonably argued that the soil volume intruded in the advance core is comparable to the soil volume intruded from the face (Figure 2). In order to verify the latter, thorough investigation was carried out and results are presented in chapter 4.

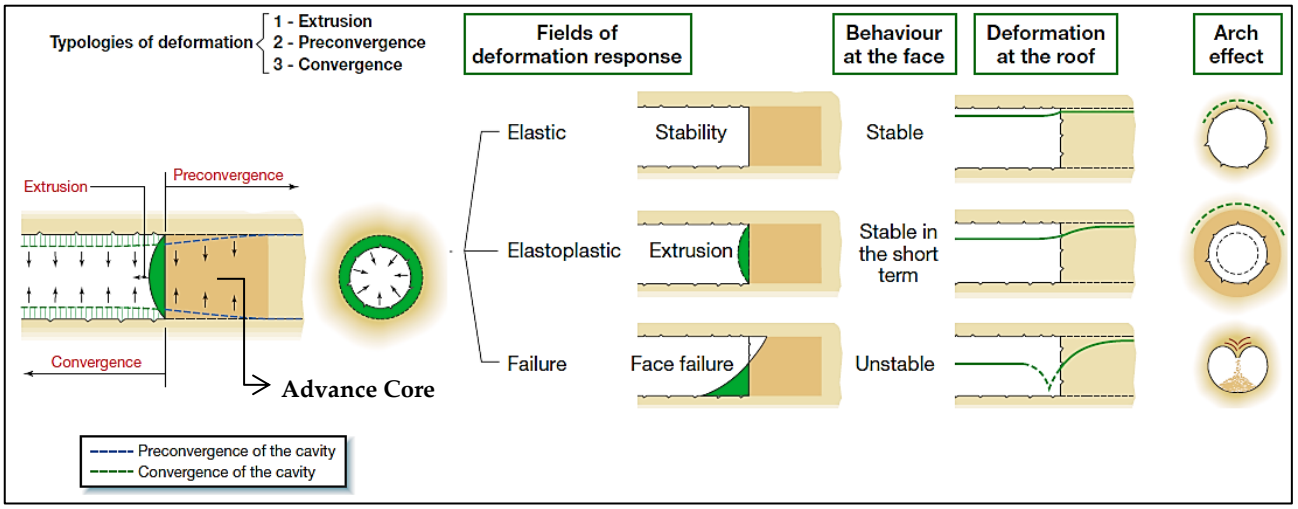


**Figure 2:** Illustration of soil "deformation response" to the excavation (Lunardi, 2000)

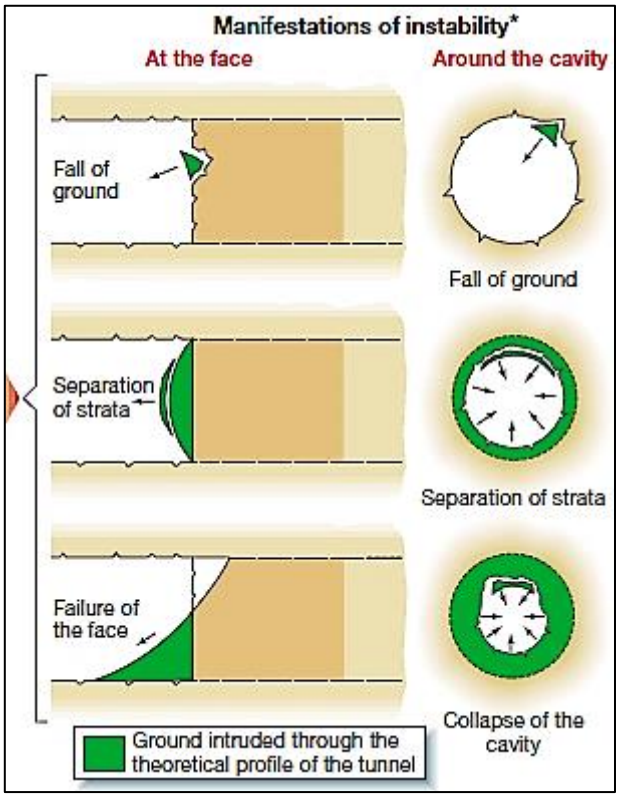


**Figure 3:** Schematic presentation of common face failure mechanisms; the first two refer to fractured/jointed rocks while the last to loose soils (Lunardi, 2000)

Many researchers have tried in the past, mainly through the use of the de-confinement ratio ($\lambda$), to implicitly include the phenomenon in common analytical solutions. The de-confinement ratio is defined as the ratio of the radial displacement ($U_R$) at the tunnel wall to the final radial displacement, supposed to be far away from the face ($U_{R,\infty}$), obtained from the

widely used convergence-confinement analysis (e.g. Panet M. , 1993, 1995 ; Chern et al, 1998). In other words, assuming a stress equilibrium analysis in an infinitesimal soil element, vertical stress ($\sigma_1$) is decreased to a certain extent (i.e. 1-$\lambda$) due to the preconvergence (Kavvadas, 2014). Therefore, for the desired deformation ($\lambda$), through an "equivalent" 2D analysis, it is possible to crudely calculate within tolerable limits the necessary support pressure ($\sigma_3$) for a stable working face either from the design stage or during the construction given the in-situ conditions (Figure 4). However, these lower bound solutions require an acceptable initial stress field which in most cases is thought to be isostatic ($K_0$=1); they are also based on dry conditions in rocky formations and therefore refer mostly to conventional excavation methods (NATM).

Analytical solutions can also be based on upper bound solutions considering a force limit-equilibrium analysis on a specific failure mechanism. Some of the most known methods, based on a wedge-like type of failure are presented in the next session.

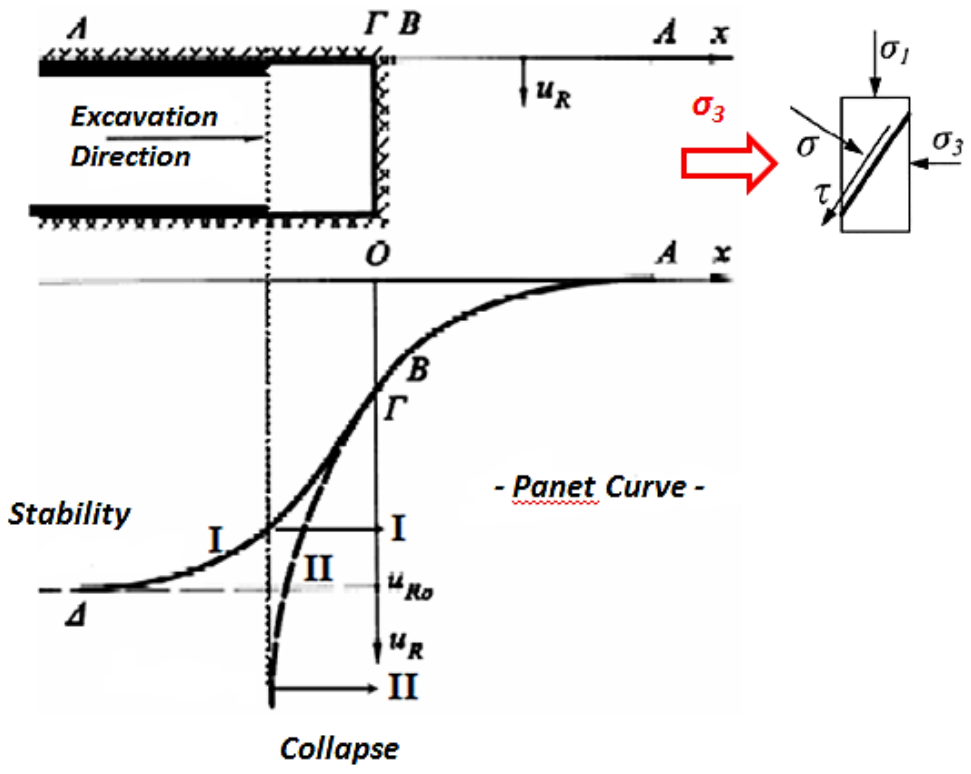


**Figure 4:** Longitudinal view of a 2D face stability analysis based on convergence-confinement theory; $\lambda$=(OΓ)/(OΔ) (Kavvadas, 2014).

## 1.2. Common methods of face stability evaluation

Several analytical methods have been developed in order to assess face stability and estimate the required support pressure in mechanized tunnelling. The vast majority of these methods are based on limit equilibrium analysis of specific 3D failure bodies in front of the excavation face (Krause, 1987; Leca & Panet, 1988; Leca & Dormieux, 1991; Anagnostou & Kovari, 1994 & 1996). Horn (1961) was one of the first to propose a model to assess the face stability under drained conditions considering the limit-equilibrium of a **sliding wedge** as a failure body. Jancsecz & Steiner (1994) applied this model to shield-tunnelling. The main idea consists of a 3D wedge, loaded by: i) its self-weight (submerged) and ii) the overburden soil or/and any superficial loads in shallow conditions (**Silo Theory**), counter-balanced by shear strength along its walls and a retaining face pressure as well (Figure 6).

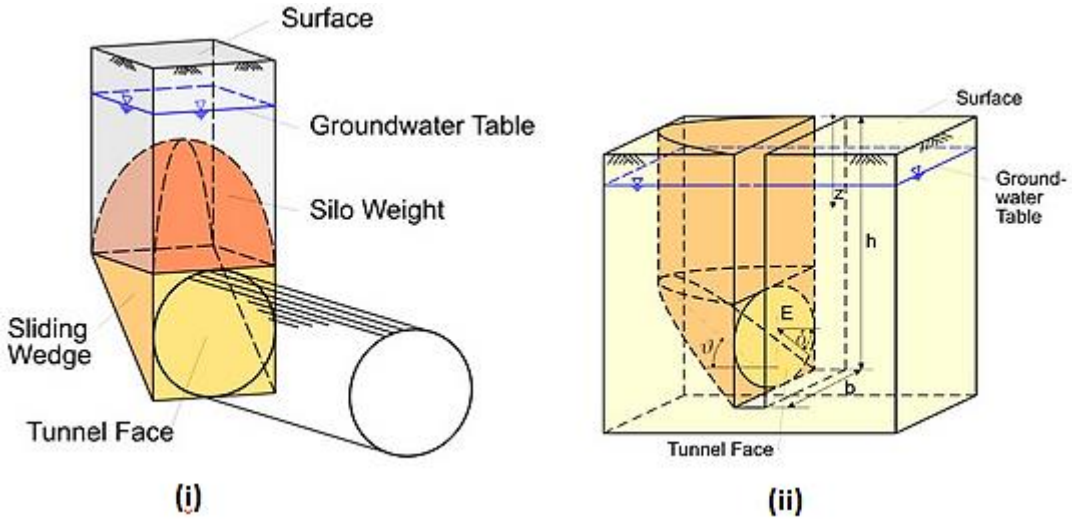


**Figure 5:** Examples of kinematic failure models; (i) Model proposed by Horn (1961), (ii) Model proposed by Piaskowski & Kowalewski (1965) (www.facesupport.org)

In a limit equilibrium analysis the deformation of the ground is disregarded, the soil is thought to be rigid-perfectly plastic, obeying probably the Mohr-Coulomb yield criterion, either using the effective shear strength parameters ($c'$, $\phi'$) or the undrained shear strength ($C_u$) depending on whether a drained or undrained type of analysis is carried out. As in other problems involving unloading of the ground (reduction of the first invariant of total stresses, $J_1$) undrained conditions are considered more favorable regarding the short-term stability of the face (Anagnostou G. , 2002). It is well-known that, the proper selection of analysis type lies mainly on the type of soil that is to be bored. In a commonly permeable,

coarse-grained soil, drained conditions should be considered whereas undrained analysis is proposed in a less permeable, fine-grained soil during the drilling phase. During a long standstill though, a drained analysis may be more appropriate, regardless of the soil type. In the case of open-shield tunnelling (see next section), the piezometric head difference between the tunnel and its vicinity results in water seepage towards the tunnel face. The latter creates an **extra destabilizing force** ($f_s$) exerted in the aforementioned wedge that has to be counter-balanced (Figure 6). The computation of the seepage force is often accomplished through steady seepage-flow analysis which is also an extra simplification, valid only under certain circumstances (see §1.4).

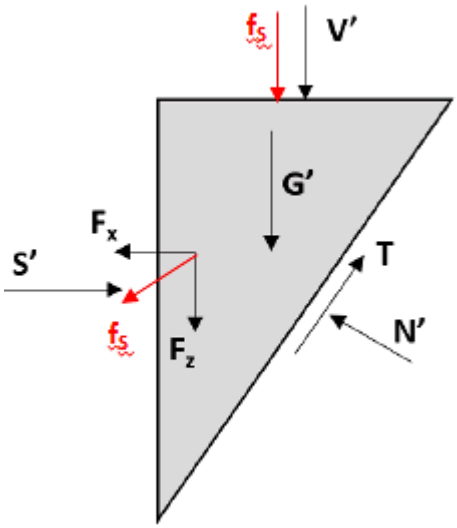


**Figure 6:** Forces acting on the sliding wedge in case of underground water seepage towards the tunnel face (Kavvadas M. et al, 2013)

Limit-equilibrium analysis cannot capture the interaction between tunnel - surrounding soil and overlying structures which is unarguably a 3D problem. Additionally, it is only valid for the two extreme drainage conditions as it is not adequate for the intermediate phase (partially drained) or the transition from undrained to drained behavior and vice versa because of its lack of time-dependency. Depending on certain characteristics such as the permeability of the soil, the rate of advance and of course the type of excavation method, conditions may vary between these two extreme cases leading to different results. Coupled-numerical analyses include time-dependent, hydro-mechanical phenomena (e.g. excess pore pressures, water seepage, suction, consolidation etc.) that affect the overall soil deformations in conjunction with stresses and provide the best approach so far to the problem. This type of analysis though, is time-consuming and demanding and thus it is not used in common

design practice while analytical solutions are extremely helpful especially for urgent situations or as a preliminary stage of a more complex analysis in order to reduce computational time. However, due to the fact that modern urban tunnelling design is focused mostly on serviceability criteria (i.e. tolerable settlements) and not only on demand for structural integrity of tunnel parts (face, lining etc.) the use of numerical methods has become a necessity.

## 1.3. EPB-Shield tunnelling under the water table – Closed VS Open mode

Tunnel boring in fully (or quasi) saturated soils is always a challenge even for experienced crews and engineers. The stabilization of the tunnel face can be mastered by application of TBMs working in **closed-mode**. In closed mode, the excavation chamber is filled up with the supporting medium (muck, compressed air, slurry suspension or combination of them). Open mode refers mostly to hard rock TBMs or EPB machines with partially filled excavation chamber.

Closed mode operation renders redundant, expensive and time-consuming precautions and countermeasures such as groundwater depletion, advance drainage, ground freezing etc. (Anagnostou & Kovari , 1994). As it is mentioned before, apart from limiting the surface settlements, EPB machines working in closed mode operation, eliminate the risk of heading failure through constant and controlled support. Face pressure control in an EPBM is achieved mainly through control of: i) the amount of the muck collected from the excavation chamber (e.g. through regulation of the screw conveyor's rotational speed, Figure 7) and ii) the advance rate (through control of the forward thrust). The upper area of the chamber is often filled with pressurized air as a safety measure so as to cope with pressure fluctuations due to possible heterogeneities of the soil (e.g. sand lenses) that could hamper the stability of the face. Air bubble enables the operator to monitor and control more efficiently such contingencies comparing to simply adjusting screw conveyor's rotational speed (Attiko Metro S.A., Line 3 Extension to Piraeus). Such machines are known as **mix-shields** (semi-closed mode). In slurry TBMs, air-cushion is an integral part of the machine as it determines the pressure regime in the excavation chamber that equalizes the in situ earth and water pressure. As a result, excavation chamber and pressure bulkhead are separated in a slurry machine by a submerged wall (Figure 8).

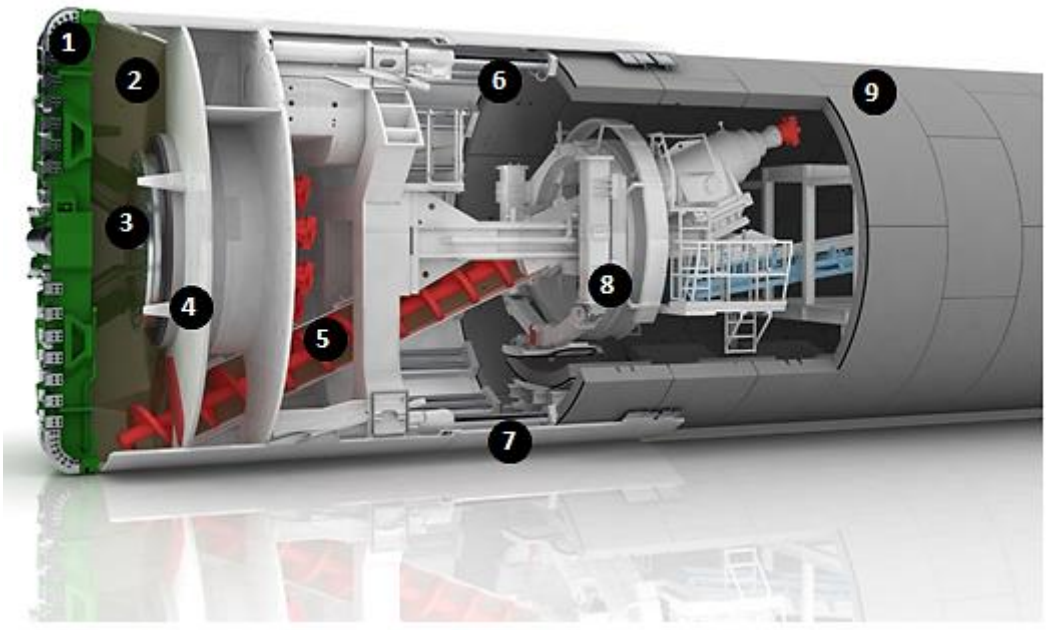


**Figure 7:** Illustration of a typical longitudinal section of an **EPB** machine: **1)** Cutter head; **2)** Excavation chamber; **3)** Rotor; **4)** Pressure bulkhead; **5)** Screw conveyor; **6)** Thrust cylinders; **7)** Shield skin; **8)** Erector; **9)** Segmental lining (www.herrenknecht.com)

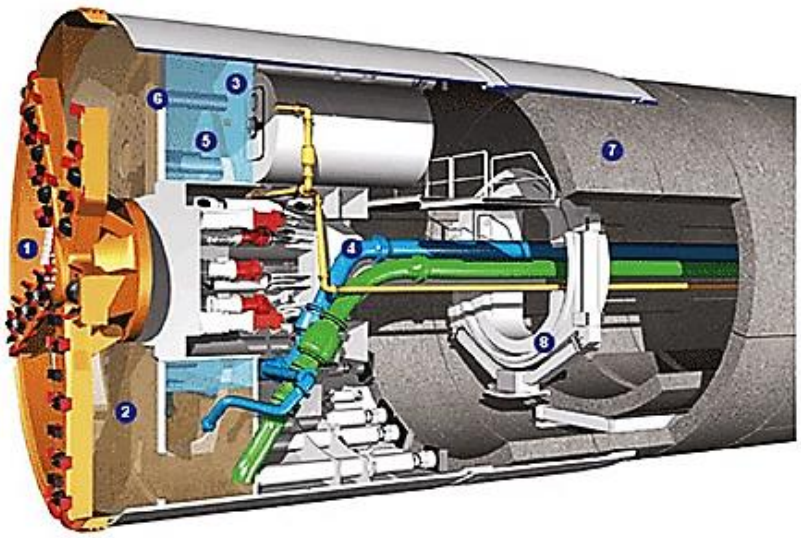


**Figure 8:** Illustrative sketch of a typical longitudinal section of a **Slurry** machine: **1)** Cutter head; **2)** Excavation chamber; **3)** Bulkhead; **4)** Slurry Feed line; **5)** Air-cushion; **6)** Submerged wall; **7)** Segmental lining; **8)** Erector (Kavvadas M. et al, 2013)

Lack of sufficient face support can lead from small scale tunnel face instability to extensive and global failure of the face and the soil above the tunnel crown, propagating under circumstances towards the surface (Anagnostou & Kovari, 1994). The latter is also known as "chimney" collapse. In such a case, the soil subsides, forming a crater (or in extreme cases, a sinkhole) on the surface while the machine excavates continuously more

material than the theoretical excavation volume without being able to advance. Such craters were created during the excavation works at "Athens Metro", probably due to the selection of unsuitable type of machine (Open-mode - large openings on the cutter head) as well as during the excavation works of "Metro do Porto", in Portugal, due to the overestimation of the highly heterogeneous granitic subsoil, leading unfortunately to fatal accidents (Figure 9).

**Figure 9:** Photos of "chimney" failures and the resulting craters ("Athens Metro", left; "Metro do Porto", right; P. Marinos Lecture, 2014)

On the contrary, an **overestimation** of face pressure may seriously delay tunneling operations due to excessive wear of the cutting tools, face "blow-out" incidents when pressurized air is used (Figure 10) or even uplift of "light-weighted" soil layers due to excessive pore pressure build up (Bezuijen A., Pruiksma P.J., van Meerten H.H., 2006).


**Figure 10:** Schematic presentation of face blow-out (left); Capture of the phenomenon from the surface (right) (www.facesupport.org; Redmond & Romero, 2011)

Moreover, closed mode operation renders the inflow of soil mixture into the working chamber highly controlled, especially with the assistance of ejected conditioning agents. From a geotechnical point of view, a "monophasic" muck containing low permeable, fine-grained, viscous soil supports the tunnel face in terms of total pressures, while it is relatively easy to be sustained. Soil conditioning is an extremely helpful operation and has been lately a standard engineering practice in EPB-projects. The whole concept will be explicitly presented in §1.6.

In case of **open mode** operation, the tunnel works as a conduit. The piezometric head inside the tunnel is zero (generally atmospheric pressure), resulting in water flow due to the piezometric head difference. If the permeability of the soil is relatively high, this may affect (decrease) the water table in the surrounding ground rather soon. Consequently, the effective stresses increase and the soil experiences compaction quite soon, leading initially to surface settlements and severe damages to any overlying structures or/and utilities and finally additional and unexpected loading on the tunnel lining (Figure 11). Needless to mention the environmental impact of lowering the underground water table elevation (see T3 Tunnel "Maliakos – Kleidi" Motorway Project). These time-dependent phenomena are not so crucial in case of less permeable soils (clayey) where the required time for the water to escape and the ground to consolidate theoretically exceeds the time span required for the machine to pass by. Nonetheless, clayey soils very often contain very permeable formations such as saturated sand lenses or enclosed water pockets that can not only threaten the face stability

but also the machine itself . In extreme cases, for example when drilling under open water (river bank or sea) or when opening intermediate access shafts when pipe jacking is implemented without waterproofing, water ingress may be sudden and ferocious resulting in flooding of the machine while the discharge volume is practically unlimited. Such incidents, primarily risk the personnel's safety and secondary induce serious delays and budget surcharges due to expensive countermeasures (e.g. installation of pumps) and restoration of damaged components.

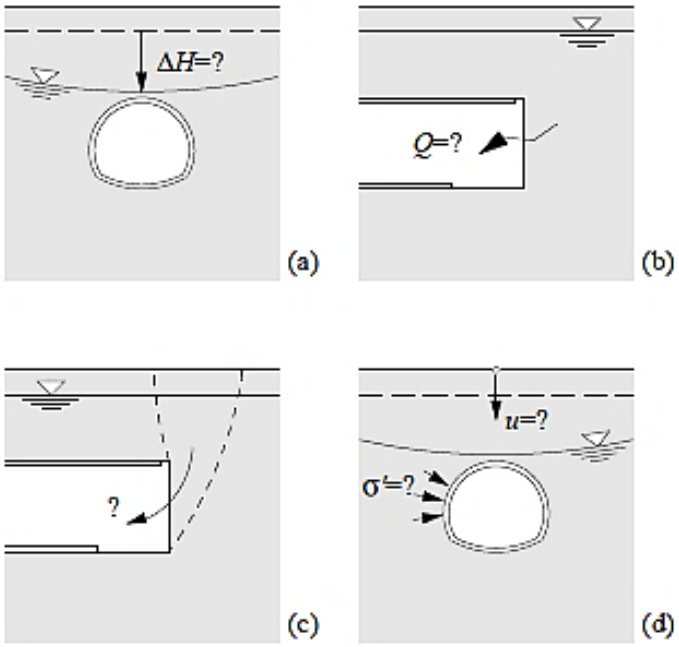


**Figure 11:** Problems of tunnelling in saturated ground: a) water table depletion, b) water inflows, c) tunnel face stability, d) surface settlements – additional load on the lining (Anagnostou G. , 2002)

In practice however, the soil is not homogeneous; the excavation process does not follow textbooks and it may be interrupted for many reasons whereas unforeseen incidents may always occur e.g. the machine runs into an ancient well consisting of unknown saturated fill with zero stand-up time. Thus, for safety reasons, closed mode is used in the vast majority of urban tunnelling practice. On the contrary, the open mode is advised only in special cases where the geotechnical properties of the excavated material (mostly E) in conjunction with the geometric characteristics of the project (mostly H/D) are adequate to provide self-support of the face. For instance, a layer of confined marl with commonly low permeability would allow the contractor to empty the excavation chamber, speed up and gain in time and money, accepting concurrently the risks that come along with such a choice.

## 1.4. Groundwater Flow Problem

Tunnel face stability can really be impaired in case of underwater flow. As explained before, tunnelling under the water table in open mode even in impermeable formations is prohibitive because of the contingencies involved. Driving in closed-mode, one may consider significant groundwater flow that could severely destabilize tunnel's face, in permeable, sandy soils with insufficient soil conditioning (drained conditions). In more impervious formations (clayey), underground water flow is not expected to threaten short term stability of the working face.

It is well-known that, when the water seeps through the soil, it exerts drag forces on the grains in the direction of the flow, known as seepage forces, due to the piezometric head difference. The size of these forces depends on the energy gradient, known as the hydraulic gradient (i), provided by the hydraulic head difference (Figure 12). In shallow tunnels, due to low depth of cover, this head difference has to be dissipated within a smaller distance and as a result, pressure gradients in tunnel's vicinity and subsequent destabilizing seepage forces are higher (Anagnostou G., 2014). Ground water flow problem may be dealt directly through e.g. a numerical seepage-flow analysis or implicitly as a part of a numerical coupled analysis. Because in the present work the groundwater flow problem was integrated in the coupled analyses, in this section we will discuss the former case.

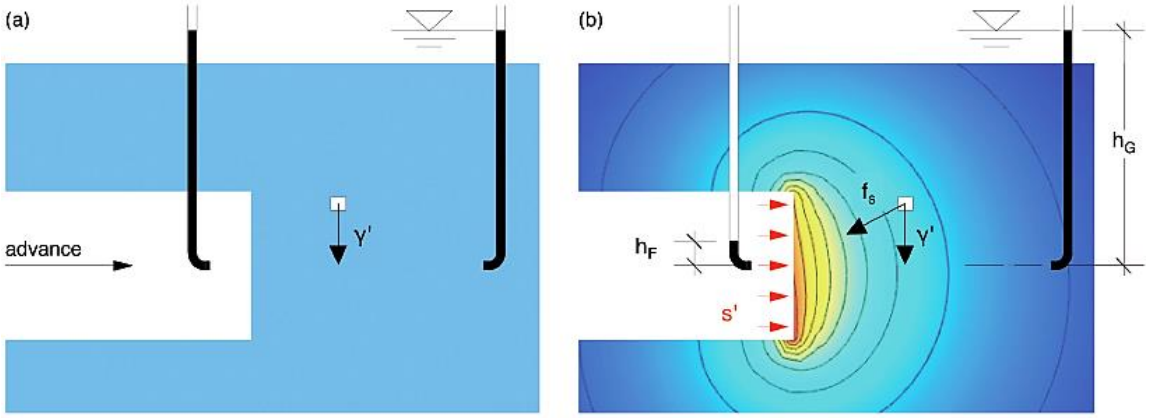


**Figure 12: (a)** Hydraulic balance between the excavation chamber and the field ($h_G$=$h_F$); gravity ($\gamma'$) is the only body force exerted as no seepage occurs; **(b)** atmospheric pore pressure conditions in the chamber resulting in seepage forces ($f_S$) and necessary effective support pressure ($s'$) to maintain stability (Anagnostou G., 2014)

For simplicity reasons, the problem of groundwater flow is usually dealt assuming **steady state** of flow. The steady state hydraulic head field depends solely on the **fixed** hydraulic boundary conditions. Since the hydraulic gradient (i) is constant, constant seepage force (fs) respectively can be introduced in a numerical stress analysis or added in the force equilibrium of analytical solutions depending on the drainage regime (Anagnostou & Kovari, 1994). For practical reasons, in de-coupled analyses, only the horizontal component of the resulting seepage force vector is utilized (In-Mo Lee, Seok-Woo Nam, 2004). This approach requires considerably less computing time and storage than solving simultaneously stress and seepage flow equations (coupled analysis) and can be really advantageous in parametric studies (Anagnostou G., 2002). Assuming a waterproof tunnel lining, a no-flow boundary condition applies to the tunnel walls.

However, steady flow state is valid only in high permeable soils, in very slow excavations or in major pauses where the loss of the hydraulic head takes place readily in the vicinity of the tunnel or when only the long term behavior of the ground (e.g. surface settlements) is of interest. In less permeable soils or/and rapid excavations, it takes significant amount of time to reach steady state conditions and usually this interval is smaller than the required for the machine to pass by (short term behavior). Therefore, in the vast majority of situations, the governing flow conditions refer to transient[5] flow of water depending on the propagation of the face. In this case, a 3D numerical seepage-flow analysis is suggested to calculate the varying gradient and seepage forces (head distribution). Finally, Anagnostou (1993) proposed an analytical method of computing the hydraulic head field distribution taking into account the face propagation in open-mode (**semi-fixed** boundaries), by inserting the advance rate as an additional parameter to its diffusion equations (**quasi-steady** state of flow).

Groundwater flow is highly determined by the properties of the mixture (FIR, permeability, porosity, pore pressure) in the working chamber illustrating the crucial role of soil conditioning. In case of optimum soil conditioning, porosity of the mixture exceeds the maximum porosity and thus effective stresses will be zero (**fluid behavior**). This practically means that any variation of pressure into the chamber will be a variation of pore pressures altering the hydraulic boundary conditions of the problem (Bezuijen, 2006). The latter will be

[5] Transient flow analysis: varying water flow velocity; the alteration of the hydraulic head field takes place simultaneously with the process of excavation (Anagnostou G. , 2002)

discussed more explicitly in §2.5 while the procedure of soil conditioning is described in more detail in §1.6.

Indisputably, presence as well as movement of water in low permeable soils is a major cause of time-dependent effects in tunnelling. Depending on the amount of time available, soil is subjected to consolidation phenomena along with the spatial stress redistribution in the vicinity of the advancing face. Although in most cases, water seepage effects are not expected to directly jeopardize short term frontal stability, the pore pressures build up during drilling and their consequences proven by various monitoring campaigns, have to be carefully considered. The latter will be discussed in the next section.

## 1.5. Excess Pore Pressures Effect

Tunnel excavation, in general, generates excess pore pressures in front of the face that can be either positive or negative depending on whether the soil experiences swelling or consolidation respectively (Anagnostou G., 2008). Positive excess pore pressure will result in reduction of effective stresses and consequently soil's shear strength, leading eventually to deformation and pore pressure relief. Negative excess pore pressures (suction) refer either to cohesive, dense materials tending to dilate when experiencing an abrupt alteration of its stress regime or to very permeable ground enabling extensive groundwater flow towards the excavation face. The latter can be encountered when tunnelling in loose, permeable sand beneath open water where the danger of hydraulic connection with a practically unlimited recharge leading to flooding of the tunnel is imminent. In order to evaluate the effect of the induced pore pressures on the stability of the tunnel face one should initially distinguish the **type of soil** (fine or coarse grained), the **type of retaining pressure** (muck or bentonite suspension) and the **process phase** (boring or standstill). The present work focuses on EPB machines (muck) in cohesive material (fine-grained) during the excavation phase (boring).

Positive pore pressures are primarily developed if the resulting support pressure obtained by the thrust cylinders is greater than the lateral total earth pressure. If so, the soil in front of the TBM experiences compression leading consequently to excess pore pressure build up (Broere, 2001). The amount of time required for the pressures to be relieved depends on the permeability and the available drainage paths.

Excess pore pressures can be alternatively be developed by infiltration. Broere & van Tol (2000) studied the effect of pore pressure build up in front of the tunnel face on its stability

due to slurry penetration in frictional soil (medium sand). They claimed that excess pore pressures are likely to develop in heterogeneous, stratified soils with confined drainage paths (e.g. tunnelling in sand lenses). They tried to quantify their influence by developing an analytical solution to calculate minimal required support pressure based on the wedge model of Jancsecz & Steiner (1994) and assuming stationary flow, including also soil stratification. The solution appeared to be in good accordance with field measurements (Figure 13).

It is true that in **coarse-grained** materials, bentonite filter-cake cannot be formed during the excavation as it is continuously removed before plastering occurs, thus membrane model is not valid. The latter will result in infiltration of slurry or conditioning agents (in case of EPBM) which in turn may lead to excess pore pressures build up, as large amounts of filtrate water will continuously flow into the soil. The penetration distance is primarily dependent on the piezometric head between the slurry (or the pump) and the soil. During standstill or any pause and unless the permeability is too high to cause loss of the bentonite, plastering is permitted and a filter-cake is formed to seal the face and in the case of slurry TBMs, transfer the slurry pressure onto the soil. In the case of EPBMs, this may lead to serious degradation of muck properties (dry mixture) and as a result in face instability risk (Bezuijen, 2006). Permeability values as well as the process phase (excavation) studied herein are not considered capable to permit such infiltration to affect the hydraulic field and consequently the face stability.

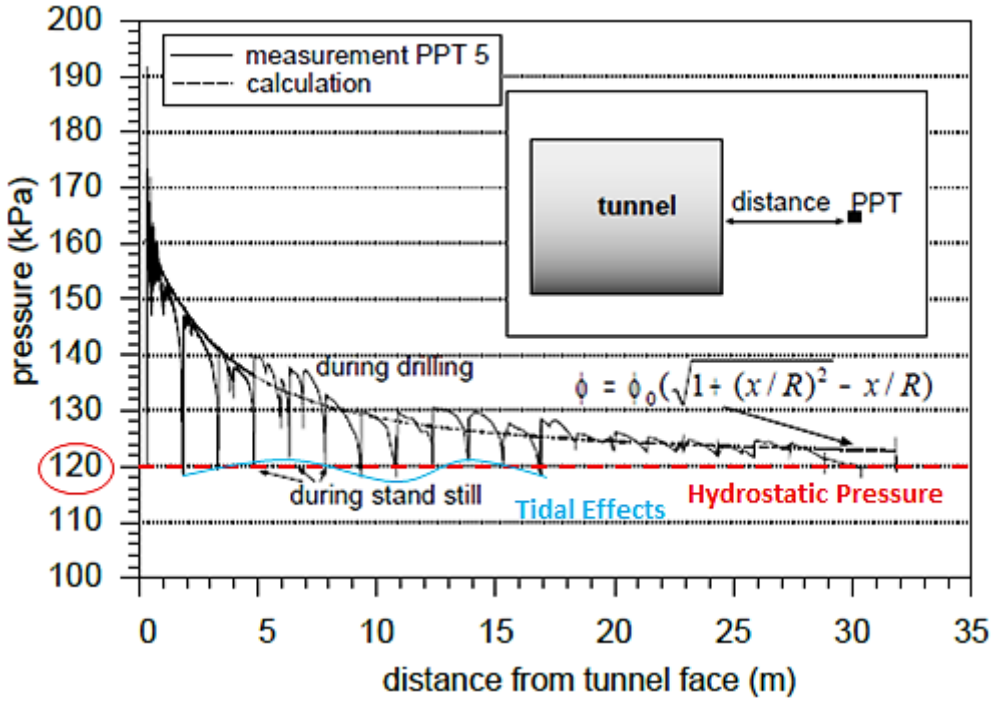


**Figure 13:** Excess pore pressures measured in front of a **Slurry shield** (2nd Heinenoord Rail Tunnel, Netherlands) and the fitted equation: $\phi_0$ is the piezometric head at the tunnel face, $\phi$ is the piezometric head at distance x in front of the tunnel face and R is the radius of the tunnel section (Broere W., van Tol A.F., 2000)

In an EPB Shield the excavated soil used to retain the working face is almost always treated with additives in order to meet certain requirements (see §1.6). Based on the aforementioned points, these additives are injected into the excavation chamber or directly into the soil at pressures greater than the pore water pressure. The pressure difference will lead to infiltration, the extent of which is dependent on the soil permeability. As a result, positive excess pore pressures are developed. During excavation in low permeable formations (clayey) and for common values of applied pressure the latter infiltration is not expected to be significant. Even in such situations, excess pore pressure may be observed, which have been linked to excessive grouting of the tail gap and not to the excavation process (Broere, 2001). During standstills, someone can assume that a certain infiltration may occur when applied face pressure remains high and should the medium's permeability permits it. Broere & van Tol (2001) studied the effect of EPBs' additive infiltration into silty sands assuming transient state of flow and proved that in low-permeable formations, the typical amount of time available during the ring erection[6] is not adequate for the pore pressures to dissipate and also a certain percentage (e.g. about 20%) remains for the next

[6] Usually 30-60min

boring cycle. In what extent the decrease in effective stresses (due to pore pressure build up) can be compensated by the seepage forces acting on the soil skeleton in front of the face (due to infiltration) requires a closer view, especially when face stability is evaluated via analytical methods.

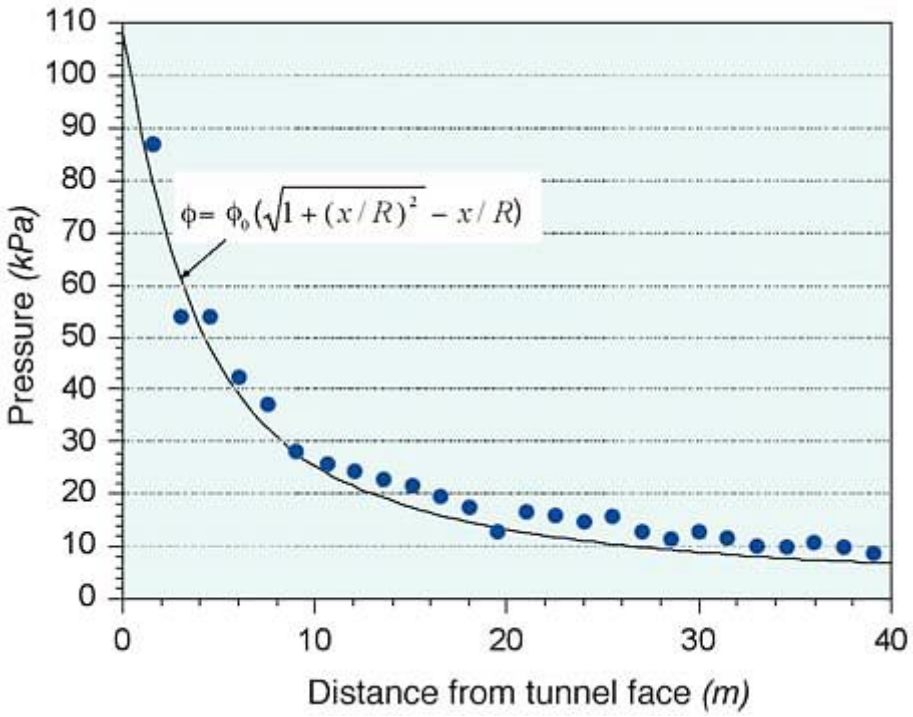


**Figure 14:** Excess pore pressures measured **during drilling** in front of an **EPB-Shield** (●) and the fitted equation; Botlek Rail Tunnel, Netherlands (Bezuijen A., Talmon A.M., 2008)

Finally, another issue not yet thoroughly studied is the influence of tidal variations when tunnelling below open water. Although is not an excavation-induced phenomenon, it has to be mentioned as not only results in variation of hydrostatic pore pressure (Figure 13) but also in overburden stress especially when overburden depth is limited (Broere, 2001). Such phenomena should be seriously taken into consideration when driving tunnels under straits where strong currents prevail (e.g. Bosporus, Gibraltar etc).

## 1.6. Soil Conditioning

Driving an EPBM can be rather challenging even for an experienced operator as he must ensure stable face pressure support, prevention of uncontrollable water inflow and as low as possible torque requirements through uncertain and varying soil conditions. In order to cope with the aforementioned challenges effectively, soil must ideally have certain characteristics.

These include: i) **good plastic behavior**, ii) **minimum permeability**, iii) **minimum inner friction** and iv) **pulp to soft consistency** (Feng, 2004). As it is quite impossible in common practice to encounter such a formation, soil in front of the cutterhead, into the excavation chamber and into the screw conveyor has to be treated with additives to improve its rheological properties. The most common types of additives used are **water**, **foam**, **polymers** and **bentonite**, all serving different requirements. In general terms, for fine-grained soils, water, polymer or bentonite are used as conditioning agents while foam is more effective to reduce possible adhesiveness. On the contrary, in coarse or mixed grained soils foam is more or less prerequisite, usually in conjunction with bentonite. Recent foam conditioning technologies enable dealing with various soil types and conditions extending the application field of an EPBM towards the range of slurry (or hydro) machines (Figure 15). The usual requirements for support media are summarized in Table 1, based on former investigations (Thewes M., Budach C., 2010):

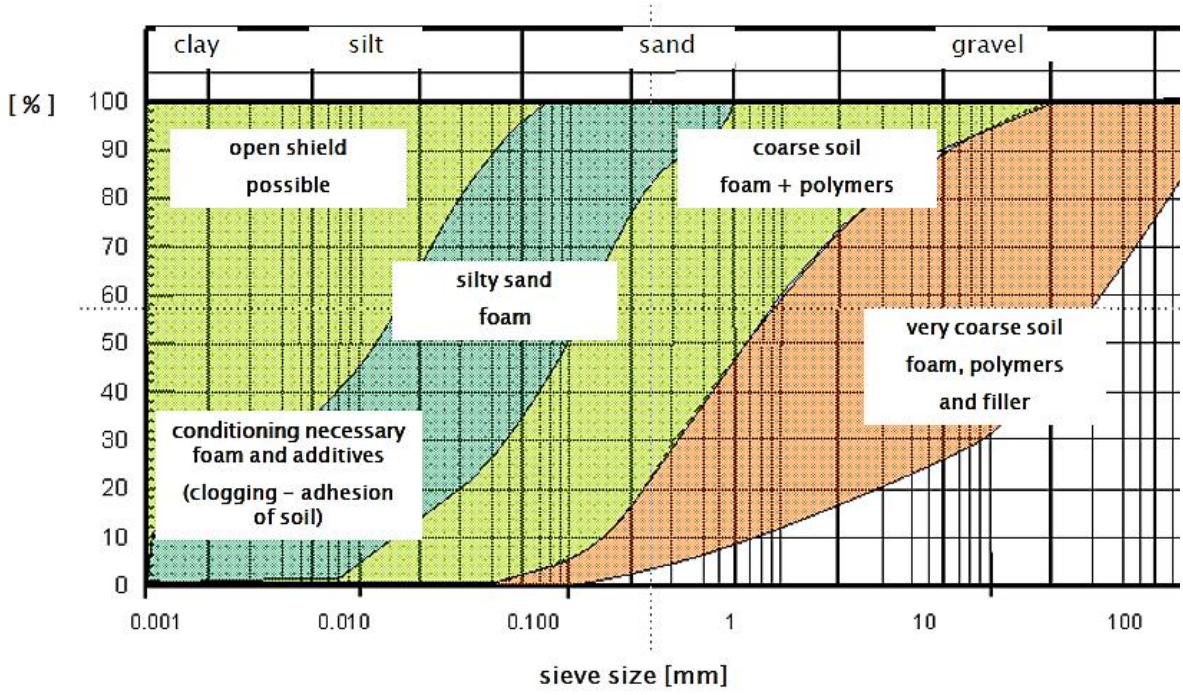


**Figure 15:** Suggested application limits of EPB machines regarding the type of soil conditioning (D. Peila, L. Borio, 2010)

**Table 1:** Overview of desired properties of support media in EPBMs (Thewes M., Budach C., 2010)

| **Parameter** | **Properties of the support medium** |
|---|---|
| permeability | $k < 10^{-5}$ m/s |
| consistency for workability | $0.4 < I_C < 0.75$ |
| supportable pressure in the screw conveyor | $0.6 < I_C < 0.70$ |
| compressibility | depending on the geological conditions of the ground and geometrical dimensions of the shield machine |
| tendency to stick | $I_C < 0.5$ or $I_P < 20\%$ |
| wear effect | $I_C < 0.8$ |

**Foam** is the most widely used additive because it is cheap, environmental friendly and extremely beneficial. It was firstly introduced as a conditioning agent, in Japan 1974. It consists of water (5-10%), air (90-95%) and a surfactant substance (0.5-1%) created by tensides and polymers, in specific proportions. When the surfactant is mixed with water, a foaming solution is produced. Foam is created when compressed air is mixed with the foaming solution by foam generators on the backup of a TBM and is injected into the soil by nozzles mounted on the cutter head (Figure 16). Because of foam's short lifetime[7], the length of the conveying system should be small enough to maintain its properties. The required amount of foam to be added (FIR[8]) is based on experience or laboratory tests on soil specimens when available, or on "trial & error" when no information is provided (Bezuijen, 2006).

Foam is used to improve soil conditions especially in granular materials and up to now constitutes an integral part of EPBMs. Its main functions are (Bezuijen, 2006):

- Increases the porosity between the grains: Measurements from the excavation chamber showed that sometimes the porosity exceeds the maximum porosity necessary for inter-grain forces to be developed. The latter results in minimum effective stresses (minimum inner friction angle) in the mixture and thus reduction

[7] Foam's typical stability (half-life): 1 hour after its generation (Babendererde et al, 2005)

[8] FIR (Foam Injection Ratio) is the ratio of foam volume injected to a certain volume of excavated soil and can be calculated depending on the advance rate and the face area (Thewes M., Budach C., 2010). Common values of FIR lie between 30-40% (EFNARC, 2005).

of the torque required to rotate the rotor and the screw conveyor resulting in lower energy consumption and wear of its mechanical components (Figure 7).

- Reduces the permeability of the mixture by increasing its air content of the mixture (creation of bubbles). A less permeable mixture renders the inflow of excavated material fully controllable. In case of less permeable formations, the difference in permeability is negligible, for the usual amount of foam (FIR), as foam's infiltration is restricted and the water content of the mixture is determined to a large extent by the water content of the soil in front of the face.
- Increases compressibility & plasticity of the mixture; A compressible mixture with plastic properties leads to better control of the exerted pressure, avoiding fluctuations and consequently serious instabilities of the face. Granular materials (e.g. medium to coarse sands) which are generally highly permeable and lack plasticity are turned into a consistent earth paste. The lower the fine content the lower would be the effectiveness of the foam. In such cases, polymers are additionally used as a binding substance (Feng, 2004).
- Lubricates and cools the cutting tools delaying the unavoidable wear and consequently decreasing total costs and necessary maintenance pauses.

**Figure 16:** Testing of foam injection in an EPBM cutterhead (Kavvadas M. et al., 2013)

The basic benefit of foam conditioning, apart from the fact that it is the most economic additive, is its passive activation when pressure fluctuations occur in the excavation chamber (Kavvadas M. et al, 2013):

- When the pressure in the excavation chamber abruptly drops, the air bubbles in the grain skeleton expand controlling the drop of the pressure.
- When the pressure in the excavation chamber abruptly increases, the air voids in the soil skeleton contract, making this abrupt pressure increase more gradual.

However, foam requires special attention regarding the advance rate because it mainly consists of air bubbles (~93%). During an undesirable downtime, air bubbles will diffuse within a few hours, they will move upwards and accumulate in the crown. When air will escape the working chamber, the volume of the support medium will be reduced causing pressure fluctuations (both effective and pore) and consequently instability issues (Babendererde, 2003). Furthermore, more attention should be drawn on the methods used to pre-determine the amount of foam injected into the soil and its properties (i.e. stability & density). As mentioned before, previous experience is the most common solution and when laboratory tests are carried out, these are conducted under atmospheric conditions. The latter

is an unrealistic assumption if someone considers that foam is actually produced under hyperbaric conditions.

Last but not least, foam is used to deal with the sticky behavior of certain types of soils. Cohesive soils generally consist of highly plastic clay, characterized by a high plasticity index. These types of soils tend to become very adhesive in metal surfaces when mixed with water, due to the swelling effect of the clay particles. Tunnelling in such soils can be a really hard task as the risk of **clogging** of the cutting wheel as well as of the screw conveyor is high. The latter may cause serious delays or even complete halt of the machine (Figure 17) unless countermeasures are taken. Usually, anti-clay polymers and highly dispersing foams are a preferred solution to provide the desired workability. Cleaning the cutter head is also a demanding task as it requires time, very often in hyperbaric conditions[9] in order to maintain face stability (Feng, 2004). Clogging initially occurs at the central parts of the cutterhead due to their reduced linear velocity. The main concept is to keep the soil active by constantly mixing it as lack of movement permits the soil to stick. Therefore, additional configurations are installed such as the central, independent cutter head of the machine depicted in Figure 17.

**Figure 17:** Clogged cutter head (left); central, active cutter head installed in an EPB to prevent clogging (right; Michalakopoulos, 2014)

Concluding, someone can now consider the importance of the investigation stage and the following laboratory tests (e.g. Atterberg limits, grading curve etc.) in order to avoid

[9] In typical values of applied pressure, the maximum time allowed for a worker into the plenum is two (2) hours. Further human presence may cause health problems (Athens Metro, Extension to Piraeus Project, Contractor JV).

unpredicted and unacceptable incidents and provide optimum conditioning operations. Such tests provide vital information to both the Designer and the Contractor regarding the feasibility of conditioning, the estimated costs and the management of risks and time (Peila, 2014). Therefore, focus should be drawn on enhancing the reliability of the aforementioned tests and investigations.

# 2
# Presentation of the numerical model

## 2.1. Introduction

It is widely known that the results of numerical analyses are as valid as the assumptions in a simulation process. A basic assumption of the present Thesis is that the EPB machine was modelled only as an equivalent pressure load on the working face without considering any other components of the machine, such as tail/annular voids, weight of the machine, geometry of the shield, grouting, shield-soil interface simulation etc. Detailed modelling of the process was omitted because previous sensitivity analyses (Kavvadas M. et al, 2015) in more explicit models proved that such parameters, associated with conditions far behind the excavation face, have negligible effect on phenomena occurring at the front of the machine (preconvergence, extrusion, pore pressure development etc). Therefore, the use of a simplified model that would require less computational time and facilitate parametric analyses thought to be the most efficient choice. In order to properly simulate the applied face pressure in fully saturated conditions, a crucial assumption concerning muck's condition had to be made. The latter is based on the condition of the muck and it will be described explicitly in the following sections.

The coupled hydro-mechanical analyses were conducted through the 3D finite element code "Abaqus v.11.1". In this chapter, focus will be drawn only on the model created and studied and no further reference will be made on the software used due to its widespread academic use in the field of research. The effect of different geometrical conditions was not addressed and thus the presented work focuses on a single model representing the tunnelling process of a circular-shaped section in shallow conditions (H/D=1.5), where H is the overburden height measured from the tunnel axis and D is the diameter of the cutter head. Primary focus on model's development was the "monitoring" section. In order to be desirably i) unaffected from the boundary condition effect and ii) accurate in the areas of interest (tunnel's vicinity), the model's dimensions and meshing respectively were carefully chosen and remained constant during the parametric analyses. Finally, due to the assumed

symmetry of the problem (geotechnical conditions vary only with depth) only the left half of the entire domain is modelled resulting in reduced computational time.

## 2.2. Geometrical Features

The aforementioned choice of the model's geometrical features was based on previous sensitivity analyses (Prountzopoulos, 2012) conducted in order to optimize the geometrical characteristics in relation to the:

i. Boundary effects: In need of adequate distance between the tunnel section and the front-back boundaries so as to stabilize face extrusion at later stages and in need of adequate distance from the side and bottom boundaries in order for the geostatic and hydrostatic conditions to be reestablished within the model's boundaries, even in case of large deformations.
ii. Desired accuracy of the results (concerning the level of discretization/meshing of the tunnel section and its vicinity and the number of simulation steps)
iii. Calculation time of the analyses (the model's meshing and dimensions had to meet the minimum requirements to achieve the previous two (2) demands)
iv. Nature of the analyses (consolidation phenomena developed in coupled analyses influence the soil movements extensively behind the face even when pressure on the face is applied)

Based on the above, the model's geometrical features are presented in the next two figures (Figure 18, Figure 19). Tunnel's diameter selection was consistent to commonly constructed tunnels in urban environment as well as the length of the excavation step and the overburden height (Table 2). In order to ensure that invert uplifts, often observed in FEM when the Mohr-Coulomb criterion is used, will not affect the results it is assumed for practical reasons that the soil under the tunnel bed has a 10-fold Elastic modulus, hereinafter referred as stiff layer (Figure 19). Upheavals are caused by unrealistic soil de-confinement due to the fact that the Mohr-Coulomb criterion stipulates the same elasticity modulus both for loading and unloading of the soil. Moreover, the density of the mesh was properly rarefied in order to limit the computational time as we stray from the tunnel. Last but not least, the elevation of the underground water is assumed to coincide with the free surface.

The element type used to model the medium (soil) is the 8-noded, brick, **porous** element **C3D8P** whereas the element type used to model the segmental lining, which is deliberately

described in a following section, is the 4-noded shell element **S4** (see Abaqus Documentation).

**Table 2:** Model's basic geometrical features

| **Model's Geometry** | |
|---|---|
| Excavation Length | 40m(=5D) |
| Excavation Step | 1.0m |
| Tunnel Depth (H) | 12m |
| Tunnel Diameter (D) | 8.0m |
| Overburden Height ($H_1$) | 8.0m |
| Water table elevation ($H_1$) | 8.0m |
| Overall Length | 90m |
| Overall Width | 50m |
| Stiff Layer height | ~30m |
| No of Elements | 58938 |

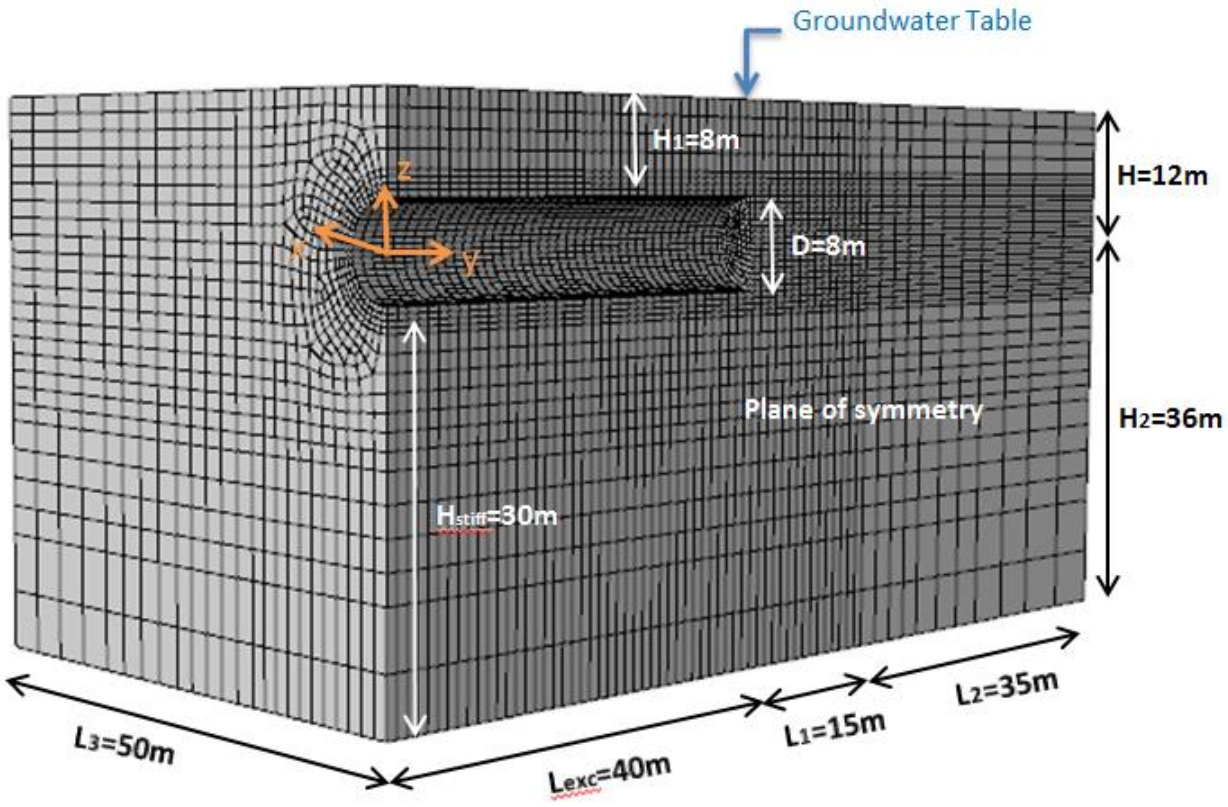


**Figure 18:** Basic geometrical features of the numerical model (H/D=1.5)

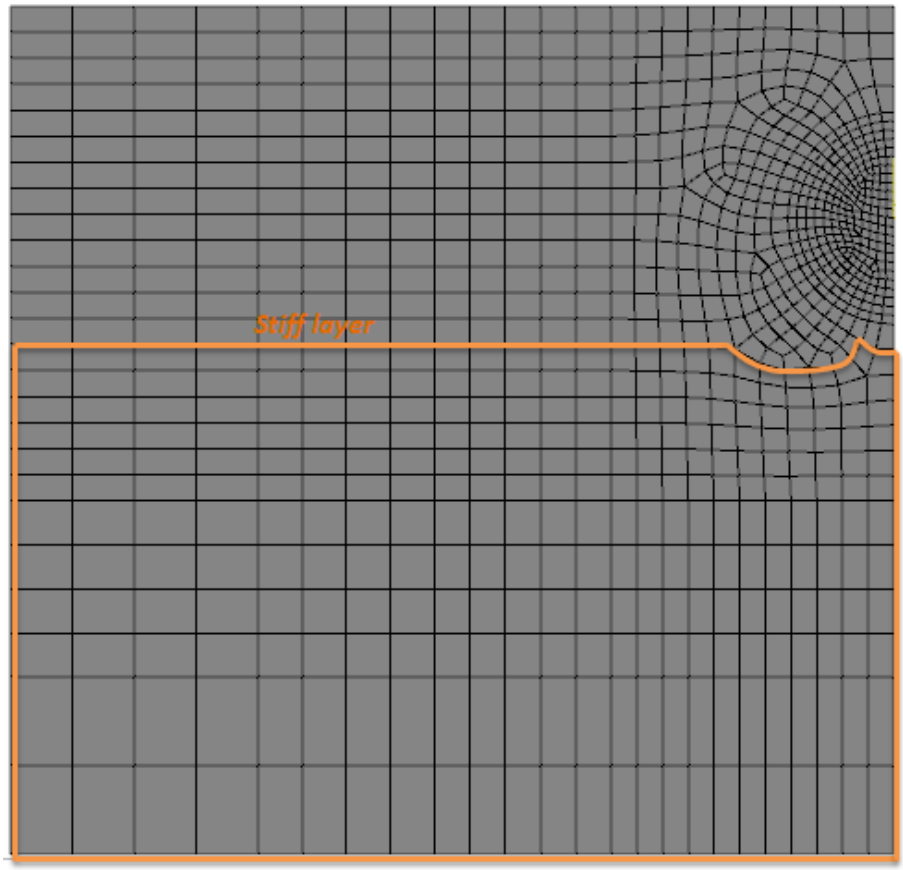


**Figure 19:** X-Z view of the model's mesh

## 2.3. Final Lining Simulation

Typical shield TBM tunnels are supported using precast concrete segmental linings often connected together with steel bolts and dowels. A usual segmental lining ring consists of five (5) to seven (7) segments and one smaller key-element installed last in order to complete and stabilize the ring. The main characteristic of a segmental lining is the high degree of jointing. The joints are distinguished to (i) ring joints between the rings and (ii) longitudinal joints between the segments of a ring (see Figure 20, **i**; Kavvadas et al, 2015).

As in most tunnelling simulations, the final lining was modelled as an elastic, continuous tube with shell elements (S4) and therefore, for simplicity reasons, no interaction between the segments or the rings was taken into account (Figure 20, **ii**). The aforementioned assumption, hardly deviates from the reality as in case of longitudinally distributed loads exerted on the lining, staggered configuration of its joints produces the activation of force interaction mechanisms between adjacent rings, originating the so called coupling effects (Arnau O., Molins C., 2012). Finally, tunnel lining represent an impervious boundary at tunnel's walls,

so as to direct water flow only towards the face. The properties of tunnel's lining are presented in the following table.

**Table 3:** Properties of tunnel lining

| **Tunnel Lining** | |
|---|---|
| Outer diameter | 8.0m |
| Thickness | 0.35m |
| Ringth length | 1.0m |
| Young Modulus | 30GPa |
| Bulk density | 2.5kg/m$^3$ |
| Poisson's ratio | 0.2 |

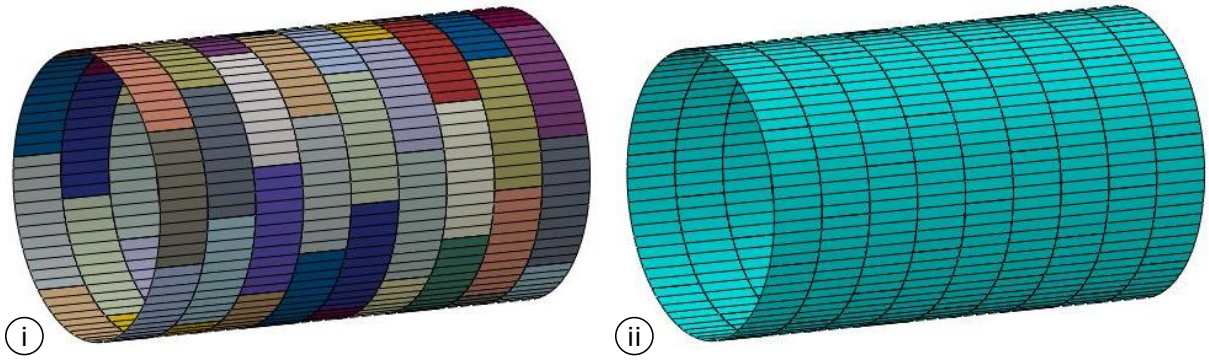


**Figure 20:** Indicative illustration of (i) segmental lining simulation and (ii) continuous shell lining. Herein, case **ii** was adopted (Kavvadas M. et al, 2015)

## 2.4. Face Pressure features

It is well known that an EPB machine retains the excavated material (muck) into the excavation chamber and "treats" it with the assistance of additives in order to apply a stabilization pressure on the face through its self-weight. The muck is controllably collected from the chamber by a screw conveyor placed at the bottom. As mentioned in §1.3, the upper area of the working chamber is often filled with pressurized air as a safety measure so as to cope with pressure fluctuations due to expected and unexpected heterogeneities of the soil (e.g. sand lenses) that could hamper the stability of the face (mix-shield). However, in our case, such an air cushion was ignored and the whole chamber is assumed to be filled up with muck leading to trapezoidal pressure distribution (constant pressure gradient equal with

muck's unit weight). Figure 21 shows an indicative sketch of pressures applied from and against the EPB machine during the excavation procedure.

Having an absolute pressure ($P_0$) at the shield crown due to thrust forces or air bubble pressure, the applied pressure in the excavation chamber was assumed to vary linearly over the tunnel height according to the regarded bulk density of the muck. In our case, $P_0$ was totally correlated with the hydrostatic pressure at the tunnel crown through a dimensionless coefficient **A** whereas the bulk density of the muck was assumed to be **15kN/m³**. Indicatively, value of A equal to 1.0 means that $P_0$ coincides with the hydrostatic pressure at the tunnel crown. The absolute pressure $P_0$ is given by the following equation:

$$P_0 = A * \gamma_w * H_1 = A * \gamma_w * (H - D/2) \quad \text{Eq. 2.1}$$

Equilibrium of stress at the tunnel face yields equation 2.2 that defines the relationship between applied face pressure (FP) with respect to that exerted on the cutter head ($\sigma_H$) which is presented below:

$$\frac{FP}{\sigma_H} = \frac{\boldsymbol{A} * \gamma_w * \left(H - \frac{D}{2}\right) + \gamma_m * \frac{D}{2}}{\gamma_{eff} * H * K_0 + \gamma_w * H} \quad \text{Eq. 2. 2}$$

With: FP, the applied Face Pressure (KPa)

$\sigma_H$, the horizontal earth pressure (KPa)

$\gamma_w$, the unit weight of water (~10 KN/m³)

$\gamma_{eff}$, the submerged unit weight of the soil (KN/m³)

$\gamma_m$, the unit weight of the muck (KN/m³)

$K_0$, the geostatic stress ratio

Three (3) typical values of applied face pressure were investigated corresponding to **A** values of **0.5, 1.0** and **1.5.**

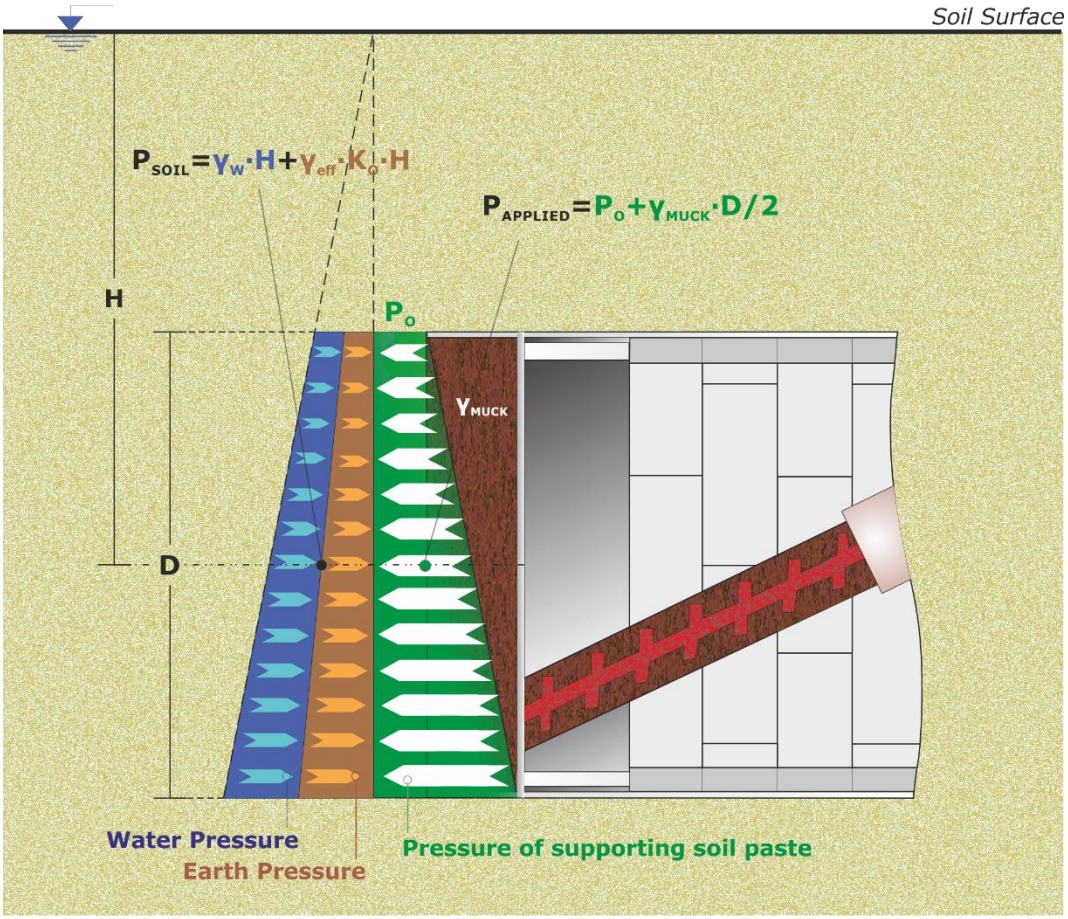


**Figure 21:** Indicative sketch of the pressures exerted on and against the tunnel face during the excavation process of an EPB machine (Sitarienos P. et al, 2015)

Actual pressure measurements in the excavation chamber (bulkhead) of an EPB, presented by (Bezuijen A. et al, 2005a), taken from the Botlek Rail Tunnel are plotted below (Figure 22). The unexpected pressure drop close to the bottom (E5) is due to instrument's position that is close to the screw conveyor where the muck is attracted. The maximum and the minimum pressure gradient is indicatively highlighted by the author, as well as the corresponding muck densities just to show that the assumed muck density (15kN/m$^3$) is considered to be a reasonable value. Although, such measurements clearly show that, at least for the case of an EPB, pressure gradients into the chamber can be highly variable because, as it is mentioned, additional mechanisms to the muck's density affect the gradients. In case of slurries, the vertical gradient found into the chamber is equal to the density that corresponds to the density of the slurry (Bakker K. et al, 2003).

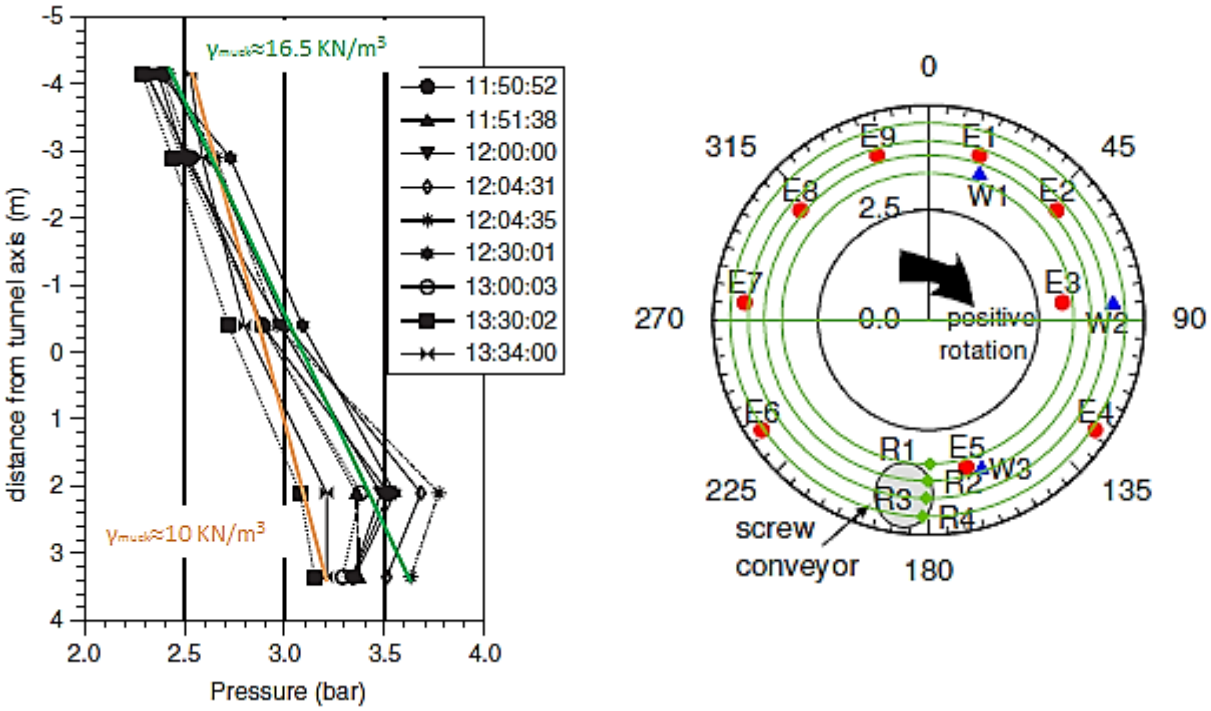


(i) (ii)

**Figure 22:** (i) Pressure distribution along tunnel height (z axis) for various time steps, (ii) Instruments' configuration (Bezuijen A. et al, 2005b; Bezuijen A., Talmon A.M., 2014a,b)

## 2.5. Hydraulic Simulation of Face Pressure

In case of modelling an EPB-bored tunnel in **dry** conditions, face pressure is modelled only as a distributed, mechanical loading exerted on the face surface. When it comes for coupled hydro-mechanical analyses though, things are far more complicated as also hydraulic boundary conditions have to be determined. In order to accomplish the latter, someone can either determine directly the drainage conditions (e.g. impermeable boundary) or to do so indirectly by assigning pore boundary value at each node of the excavation face (Sitarienos et al, 2015). Drainage ability is not a parameter that can be controlled directly as it is determined by a combination of the drilling process (e.g. EPB's rate of advance, soil conditioning) and material properties (e.g. soil permeability). It is often accepted though, that especially in case of Slurry machines, a bentonite "filter-cake" can be formed in front of the cutterhead, acting as an impervious membrane, due to infiltration of the bentonite to the soil. In case of EPBs, where foam is mostly used as a conditioning agent, this cannot be assumed as the absence of solid fraction in the foam hinders the formation of a membrane (Maidl, 1995). However, apart from the fact that this phenomenon refers primarily to "Slurry" operations, previous research has shown that it should not be considered as valid in

face stability evaluations during boring. Plastering of the bentonite suspension can only be assumed during the standstills or in very low advance rates and should the medium's permeability permits the infiltration (Broere W., van Tol A.F., 2000). During advancement, bentonite's infiltration rate is much smaller than cutting tools' penetration rate and consequently the "filter-cake" is subtracted before it starts to plaster (Bezuijen A. et al, 2006). Thus, we selected to assign hydraulic pressure values at each face node.

The reasonable question raised afterwards is what values should be assigned. To answer that question the usual condition of the mixture had to be considered. In slurry shields, is much more evident that the mixture approaches the behavior of a continuous, homogeneous fluid. Indeed, measurements into the excavation chamber indicate that the applied face pressure is governed by the density of the mixture (Bezuijen A. et al, 2005a). In the case of EPB shields, as mentioned in previous chapters, the excavated soil is turned to a pliable earth paste owing to additives (water, foam, polymers etc.) injected by nozzles placed on the cutter head. It is proved from previous works (see Bezuijen et al, 2005a, b) that the aforementioned paste acts more as a viscous fluid rather than a solid mixture (zero shear resistance). Pressure measurements inside the excavation chamber (Figure 23) from the aforementioned monitoring campaign as well as muck sampling and density measurements (Figure 24) clearly show that effective stresses in the mixture were negligible. When the porosity of the mixture is larger than the minimum required for the inter-grain forces to be developed then hardly any effective stresses will be measured. The aforementioned view was further enhanced after visiting the worksite of Athens Metro Line 3 Project: "Extension to Piraeus" and observing the fluid state of the muck during its transportation (Figure 70; Figure 71), it was concluded that it is a fairly accepted assumption.

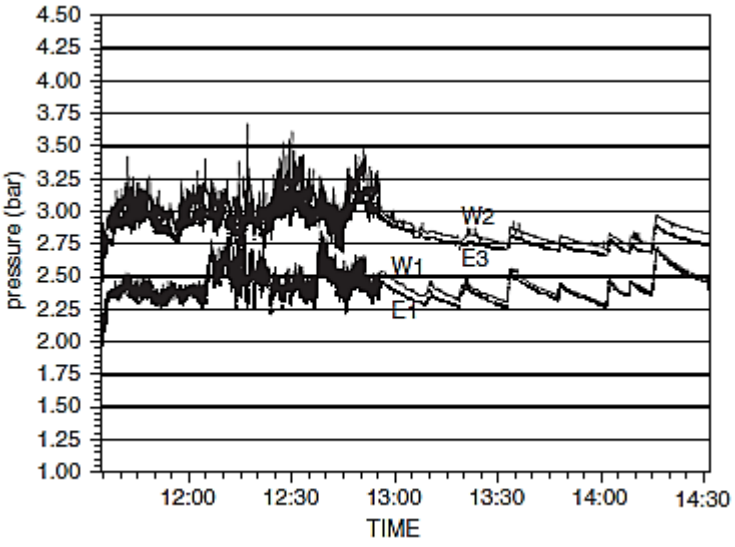


**Figure 23:** Measurements' comparison of total (E) and pore (W) pressure cells at various time lapses (Bezuijen et al, 2005a, b)

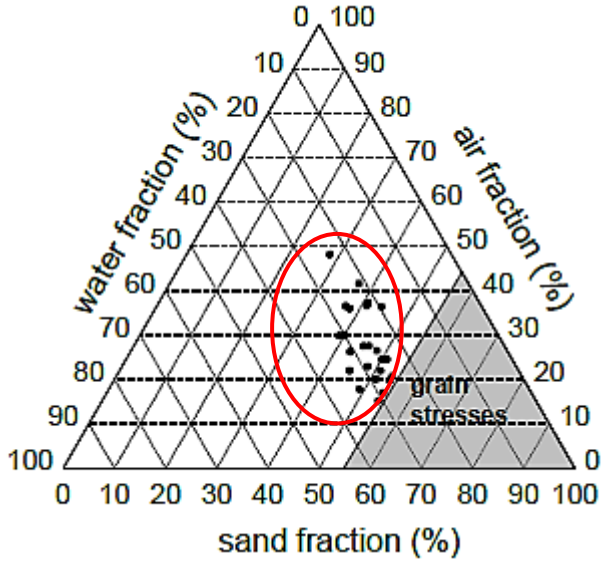


**Figure 24:** Measured water, solid and air fractions of muck samples from the EPB-bored Botlek Rail Tunnel, in Netherlands (Bezuijen A., Talmon A., 2006)

In order to model effectively this behavior, it has been selected to apply **identical** pore and mechanical (total) pressures at the face nodes. To do so, a further assumption was inserted to gain in modelling and computational time. Instead of assigning at each node of the face a unique pore pressure value, the face surface was divided in four (4) node-sets, each having a constant pore pressure (Figure 25). Figure 26 is an indicative sketch of the simplification made for the case of absolute pressure $P_0$ at the crown equal to the hydrostatic one (A=1). In order to validate the aforementioned simplification, a verification analysis was carried out in which unique pore pressure value was assigned at each face node. The results

of this analysis are presented in §4.6. Pressure values were not assigned at the peripheral nodes as false hydraulic boundary conditions would remain after the passage of the face.

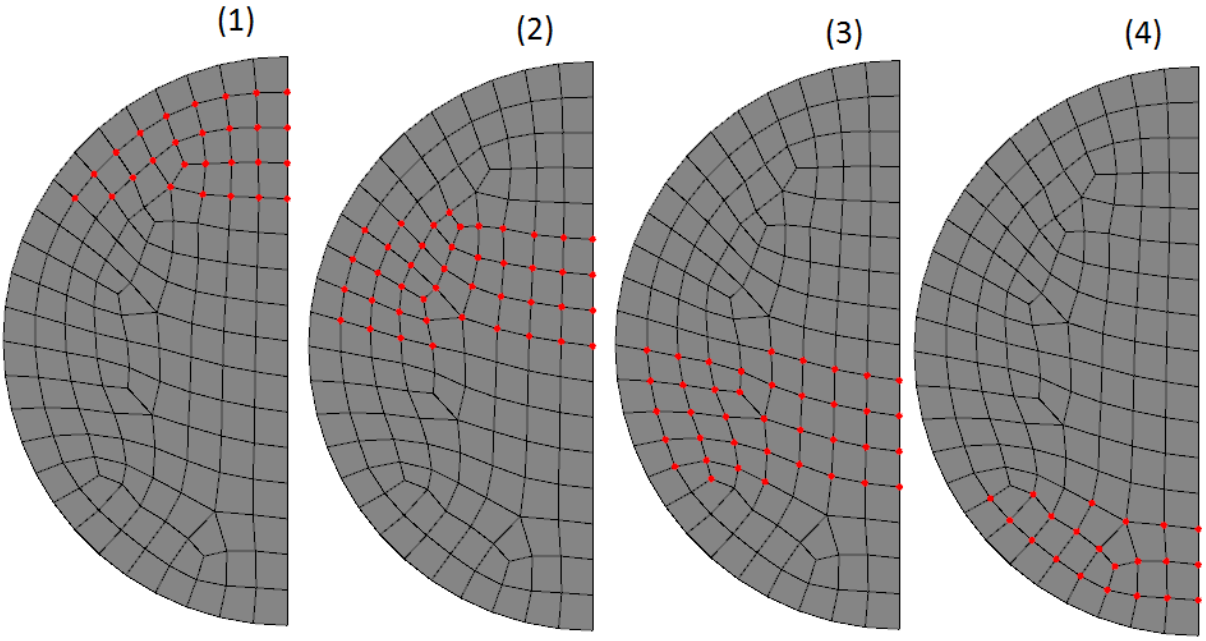


**Figure 25:** Illustration of the four (4) node areas assumed to have constant pore pressure values.

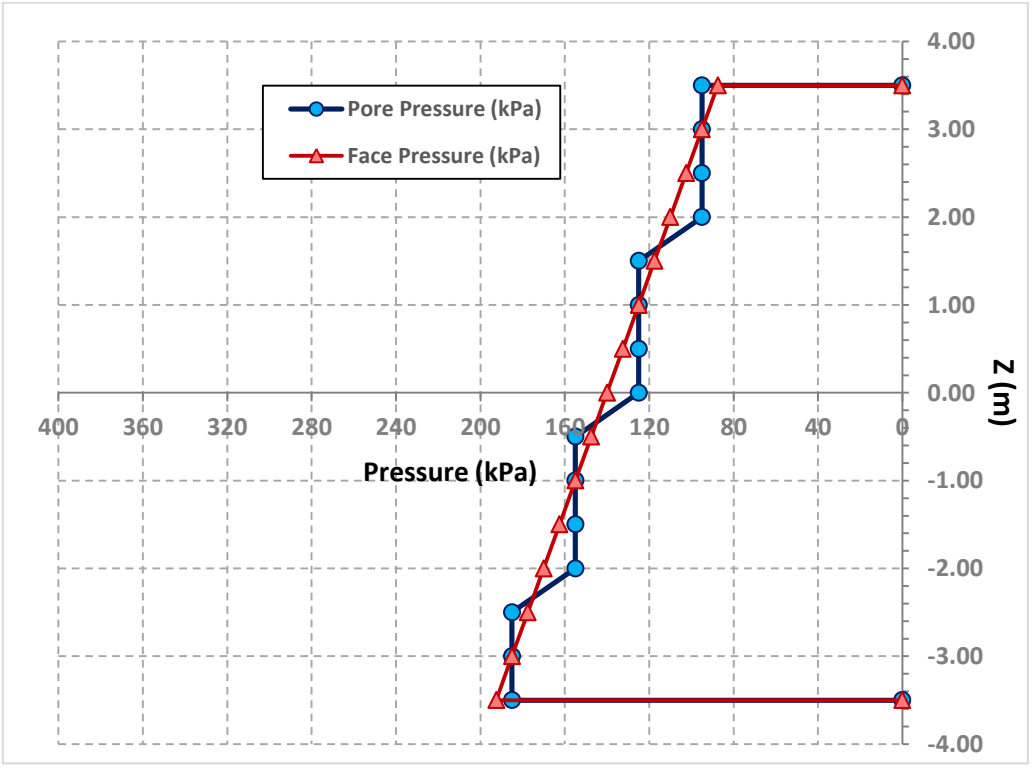


**Figure 26:** Indicative sketch of the simplification introduced regarding the hydraulic pressure assignment.

## 2.6. Description of simulation steps

Since the necessary features of the model have been presented, it is essential to describe the simulation steps of the excavation. Excavation is simulated by the successive de-activation of specific, finite elements. The analyses carried out included the following simulation steps:

- **Geostatic step:** During the geostatic step, the initial stress field is established.
- **Step 1:** Since the initial geostatic conditions are successfully established, the first five (5) meters (slices N0 1-5) are excavated (subtracted) and supported simultaneously in order to avoid boundary effects. At the end of the step, face pressure at slice N0 6 is applied.
- **Step 2:** Actual start of the simulation process. Slice N0 6 is subtracted but no support is placed. Face pressure at slice N0 7 is applied. 1m is left unsupported to counterbalance the modelling absence of EPB's components such as tail/annular gaps, shield's tapering, cutter wheel's overcut that would allow the de-confinement of the surrounding soil. In this way, an equivalent de-confinement is assumed to take place and more realistic deformation values are anticipated.
- **Step 3-36:** From Step 3 until the end of the analysis (Step 36) the same sequence is followed. Each slice is excavated in 1.5 hours, thus corresponding to the assumed excavation rate. Afterwards, the previous, unsupported section is supported. Finally, the stabilization pressure (both mechanical and hydraulic) is applied at the next section (new excavation face).

# 3
# Characteristics of the parametric analyses

## 3.1. Introduction

The basic structure of the parametric analyses consists of three (3) investigated fields. In each set, the effect of one (1) basic parameter is investigated. Given that the scope of the present Thesis is to study and evaluate the prevailing **hydraulic conditions** during the excavation process of a common EPB-bored tunnel with respect to their influence on the face stability, the three (3) parameters selected to be modified in each set, are the following:

- applied Face Pressure, A
- soil Permeability, k
- Advance Rate, AR

Each set constitutes of 8-12 analyses where the geotechnical properties of the soil are modified accordingly from poor to favorable conditions. The selected values are listed in Table 4.

## 3.2. Soil type – Constitutive Law

Given that EPB-shields are preferably used in fine-grained materials, typically found in shallow tunnels, the type of soil is assumed to be cohesive, fully homogeneous and isotropic. Consequently, face failure mechanisms that require modelling of micro-zonation and discontinuities, such as micro-instabilities, wedge-like failures caused by insufficient support or fracturing of the soil due to excessive support pressure were neglected and thus not investigated. The constitutive law adopted was the elastic-perfectly plastic **Mohr-Coulomb** yield criterion. Indisputably, Mohr-Coulomb criterion is by far the most practical constitutive law used in the scientific field, but one should respect its application limits. In tunnelling applications, where the state of failure is resulted due to gradual loss of confinement (unloading), a failure criterion which includes separate elasticity modulus of loading and un-loading is perhaps more consistent. Further interesting results of analyses in the same model, implemented using the Modified Cam-Clay criterion can be found in Sitarienos et al (2015).

Comparison of the results yielded by the two constitutive laws and its effect will be presented in the future.

**Table 4:** Properties and parameters of the analyses

| **Soil Parameters** | | **TBM Parameters** | |
|---|---|---|---|
| Friction Angle, $\phi$ | 20 - 35 (deg) | Advance Rate (m/h) | 0.5, **0.67**, 1.0 |
| Dilatancy angle, $\delta$ | 0 - 30 (deg) | Face Pressure (A) | 0.5, 1.0, 1.5 |
| Cohesion, c | 5 - 40 (KPa) | H/D | 1.5 |
| Undrained Shear Strength, Cu | 36.2 - 97.2 (KPa) | $\gamma_{muck}$ | 15 (KN/m$^3$) |
| Young Modulus, E | 18.1 - 48.6 (MPa) | Eff./Total Stresses at the bottom | 30% (A=1)<br>37.5% (A=0.5) |
| Permeability, k | $5*10^{-6}$, $\mathbf{5*10^{-7}}$, $5*10^{-8}$ (m/s) | | |
| **Soil Properties** | | | |
| Poisson's Ratio, $\nu$ | 0.3 | | |
| Saturated Unit Weight, $\gamma_{sat}$ | 20 (KN/m$^3$) | | |
| Void Ratio, e | 0.7 | | |
| Coefficient of Lateral stress, $K_0$ | 0.5 | | |
| Degree of Saturation, Sr | 100 (%) | | |
| Unit weight of pore water | 10 (KN/m$^3$) | | |

**Table 5:** Soil Profiles investigated and its properties

| **Soil Profiles** | | | | | | | |
|---|---|---|---|---|---|---|---|
| **Code** | **$\gamma$ (KN/m$^3$)** | **$\phi$ (deg)** | **c (kPa)** | **E (MPa)** | **$\delta$ (deg)** | **$C_u$ (KPa)** | **v** |
| ***a*** | 20 | 20 | 5 | 18.09 | 3.33 | 36.19 | 0.3 |
| ***b*** | 20 | 20 | 10 | 20.74 | 3.33 | 41.49 | 0.3 |
| ***c*** | 20 | 20 | 15 | 23.40 | 3.33 | 46.79 | 0.3 |
| ***d*** | 20 | 20 | 20 | 26.05 | 3.33 | 52.09 | 0.3 |
| ***e*** | 20 | 25 | 25 | 32.86 | 4.17 | 65.73 | 0.3 |
| ***f*** | 20 | 30 | 25 | 36.99 | 5.00 | 73.98 | 0.3 |
| ***g*** | 20 | 30 | 30 | 39.59 | 5.00 | 79.18 | 0.3 |
| ***h*** | 20 | 35 | 40 | 48.62 | 5.83 | 97.24 | 0.3 |

## 3.3. Soil permeability

Indisputably, tunnelling in saturated formations is directly correlated with time-dependent, coupled phenomena. Loading or unloading the working face will result in disturbance of the hydraulic head field by increasing or decreasing hydrostatic pore pressures. Excess pore pressure build up (negative or positive) is likely to trigger water

seepage towards (or from[10]) the tunnel face. Consequently, pore pressures will start to dissipate over the course of time, effective stresses will be increased accordingly leading eventually to deformation and volume change. The decisive factor for the chronical evolution of the above statement is the permeability of the soil i.e. the velocity of the water flow via the soil voids. Anagnostou (2008) stated that "*where the permeability is an order of magnitude higher, effective stresses and deformation will develop 10 times faster*". Estimation of permeability includes high level of uncertainty mostly due to anisotropy. It is a fact that practically impermeable formations often contain thin, highly permeable layers or lenses that may shorten the drainage path and accelerate consolidation. However, the latter will not be examined herein as the soil is assumed to be homogeneous.

The reference value of soil permeability corresponds to a moderate permeable clayey soil, that is $k=5*10^{-7}$ m/s. In order to modify the drainage conditions and investigate its effect on the heading stability, a higher and a lower order of magnitude respectively were selected for investigation (Table 4).

## 3.4. Retaining Pressure

Whenever tunnel face stability in mechanized tunnelling is under investigation, the effect of support pressure exerted on the face is a standard parameter of the problem. Any pressure exerted during advancement on the tunnel face of a saturated formation is instantly transferred to the pore water and as a result, an excess pore pressure in front of the face is developed. As time passes, they tend to dissipate and gradually be transferred to the soil skeleton (effective stresses increase) leading eventually to deformation (pre-convergence). The dissipation rate depends on the prevailing drainage conditions which are determined by the properties of the soil (i.e. permeability) and the loading rate or in case of tunnelling, **unloading rate** (i.e. the advance rate).

Furthermore, in the present case it happens to be additionally crucial as any modification of the support pressure (total pressures in the muck) is directly interpreted as pore pressure change at the face (pore pressure boundaries) due to the assumption made regarding the

[10] The case of water flow **from** the tunnel face refers to either infiltration of water-additives mixture into the soil either due to higher pore pressures in the chamber or excess injection pressure by the pump directly to the soil. As a result, the in-situ pore water is expelled. This can lead to significant excess pore pressure build-up in case of permeable soils or during a long standstill of the machine and severe reduction of the water content in the mixture (Broere, 2001).

condition of the muck. The latter practically means that, in each of the three (3) sets of analyses a different hydraulic state is established where the pore pressures at the free surface are zero whereas those at the face are determined by the coefficient A. Consequently, seepage direction and rate are varying (also in z axis) affecting the overall stability of the face.

Three (3) typical values of the applied face pressure were investigated corresponding to A values of **0.5, 1.0** and **1.5** and assuming a typical muck density ($\gamma_{muck}$) of 15KN/m$^3$ (see Table 6 below).

**Table 6:** Face Pressure value correspondence

| A | FP/$\sigma_H$ | $P_0$ (KPa) |
|---|---|---|
| 1.00 | 0.78 | 80 |
| 0.50 | 0.56 | 40 |
| 1.50 | 1.00 | 120 |

## 3.5. Rate of Advance

Before analyzing the role of the advance rate on the problem, it is essential to define it. The advance rate of an underground project is the ratio of the distance bored to a specific time scale. This time scale includes the drilling procedure (penetration rate) and any pauses of the excavation, scheduled (e.g. ring erection, services) or not (contingencies). Usually, it is measured in m/day or m/h whereas typical values reached in practice range from 14 to 24m/day.

Rate of advance is not a recent subject of research and as many researchers have proved in the past, it is highly correlated with the permeability of the soil. However, the advance rate is an operational parameter and thus it can be pre-estimated in the design phase more safely or it can be measured precisely during the excavation. Moreover, although they both affect in a broader sense the same mechanism, their effect is not of the same magnitude. The evaluation of their effect on the problem is a subject of the present work.

The drainage ability and consequently the average degree of consolidation is not only dependent on the **soil type** (mainly permeability) but also is regulated from the **advance rate** of the tunnel (AR). The former parameter cannot be controlled in large scale and practically modified as it refers to in-situ conditions while the latter lies primarily on human factors

such as the thrust forces exerted, tunnel's diameter and alignment curvature etc. Vermeer et al (2002) referring to analytical solutions, noted that "*the question whether a drained or undrained stability analysis should be carried out can be answered by considering the type of ground and its properties and the advance rate of the tunnel face*". Anagnostou (2002) claimed that the hydraulic head field distribution is governed mainly[11] by the ratio of advance rate to soil permeability (v/k). Given that an impervious lining is installed, the higher the ratio, the smaller the excavation-induced disturbance on the hydraulic head field. Lee & Nam (2004) studied the effects of advance rate on seepage forces and on tunnel face stability as well and concluded that the advance rate must be carefully controlled in less permeable soils (i.e. $k<10^{-6}$ m/s) that is in higher v/k ratios. This is a valid conclusion, if someone considers that time-dependent effects are irrelevant when tunnelling in highly permeable formations (Anagnostou G. , 2002).

To sum up, a high rate of advance implies, in full accordance with low permeability that there is not practically sufficient time for the water to escape and the pore pressures to dissipate, leading to undrained behavior of the soil (deformation under constant volume). On the contrary, a slow excavation or a long standstill may be sufficient for the water to escape, pore pressures to be relieved and the soil to deform volumetrically (consolidate) thus tending to drained conditions.

To be consistent with the realistic tunneling practice, a common rate of advance was selected as a basic value, i.e. 0.67m/h (1.5 h/m). To further investigate its effect on the hydraulic head field and therefore on tunnel's face stability, one higher and one lower rate of advance were selected (Table 4).

## 3.6. Effective stresses' development in the muck

The assumption made regarding muck's condition was elaborated in §2.5. However, this case is practically valid only in case of optimum soil conditioning. In the vast majority of tunnelling projects, the porosity of the mixture is lower than the maximum and thus effective stresses are developed into the excavation chamber due to varying FIR, air bubble escape, drilling speed, screw conveyor's rotational speed etc. In other words, if the incoming quantity (excavated) is greater than the outgoing quantity (extracted), then the average soil

[11] Compressibility of the ground mass, translated into hydraulic storativity (s) was found also to have some influence on the hydraulic head distribution (sv/k).

porosity of the mixture decreases causing the effective stresses to increase, supposing that conditioning process is unable to regulate this difference. On the contrary, if too much material is extracted (high rotational speed of the screw conveyor – low rate of advance) then the porosity will increase leading to effective stress decrease (Anagnostou & Kovari, 1994). The lower the plasticity of the muck the higher will be the fluctuation of support pressure.

Bezuijen & Talmon (2014b) presented measurements of soil pressure on both sides of the cutter head and afterwards in comparison to those obtained at the pressure bulkhead (2014a), during tunnelling in saturated, Pleistocene sand with an EPBM (Figure 27). Instruments' exact position can also be seen in Figure 27. Gauges E1-9 measured **total** pressures while W1-3 measured **pore** pressures, both at the bulkhead. Gauges R1-4 measured total pressures on both sides of the cutter wheel (overall 8). The course of instruments during the rotation of the rotor is indicated by the authors with green circles.

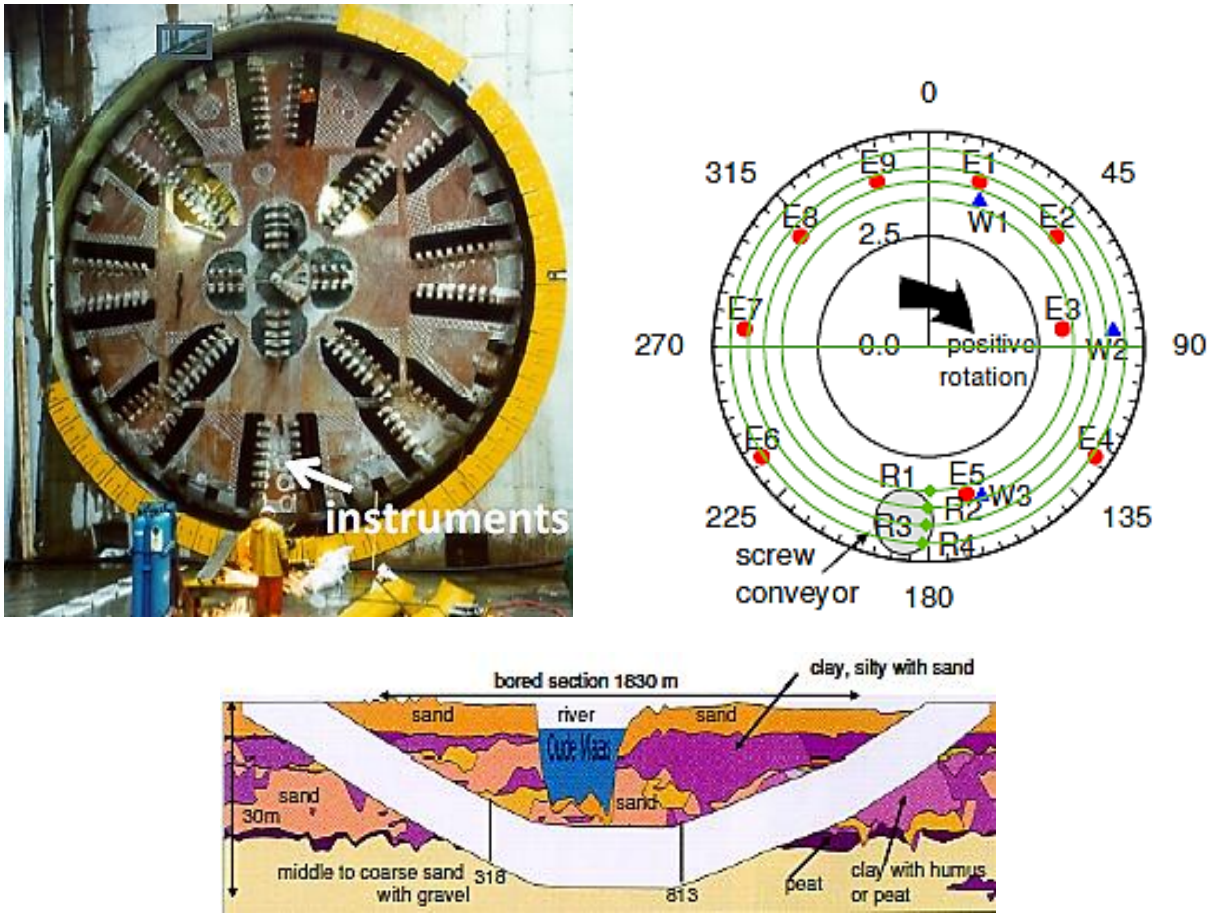


**Figure 27:** Cutter wheel of the Botlek Rail Tunnel EPB (above left); Instruments' configuration (above right); Geotechnical profile of the project (below) (Bezuijen A., Talmon A.M., 2014a,b)

Results such as these presented in Figure 28, referring to a specific location, indicate that effective stresses are developed at the back of the cutter head (i.e. into the muck) leading to sharp increases of total stresses (Bezuijen A., Talmon A.M., 2014a). The latter practically means that the muck does not behave as a liquid (total ≠ pore pressures) because inter-grain forces are developed.

The pressure fluctuation noted is caused by the rotation direction; when the rotor moves upwards pressure increases and respectively decreases at the opposite direction. The latter is attributed to the viscous and yield forces of the muck because when the rotor has to move upwards, more pressure has to be applied to overcome these forces (Bezuijen A., Talmon A.M., 2014b). Consequently, as diameter increases (from R1 to R4), fluctuation increases.

Figure 29 depicts total pressure distribution with respect to the tunnel height at four (4) consecutive moments. It is clearly depicted that at the bottom half of the section, an increase in total pressures is recorded at the bulkhead between evenly elevated stress gauges E6 & E4[12]. This observation supports measurements at the cutter wheel which denote that effective stresses may be present in the muck (Figure 28). The mixture is probably compressed at the lower parts of the section leading to densification and air bubble concentration at the top and thus effective stresses to be developed. Presumably some of the causes could be the drainage at the screw conveyor's entrance, the self-weight of the muck or ineffective conditioning. The small pressure decrease measured by E5 is due to pressure release during the discharge by the screw conveyor. Indisputably, also these observations do not form the rule and more measurements need to be evaluated in order to reach a safe conclusion regarding the condition of the muck.

[12] The pressure difference between E6 & E4 was explained earlier and has to do with the position and rotation of the cutter head (Figure 27).

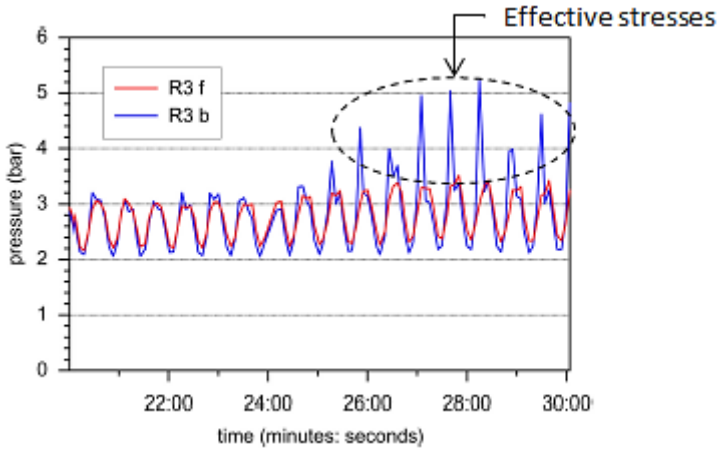


**Figure 28:** Total pressures measured with R3 at the front (f) and back (b) of the cutter wheel (Bezuijen A., Talmon A.M., 2014b)

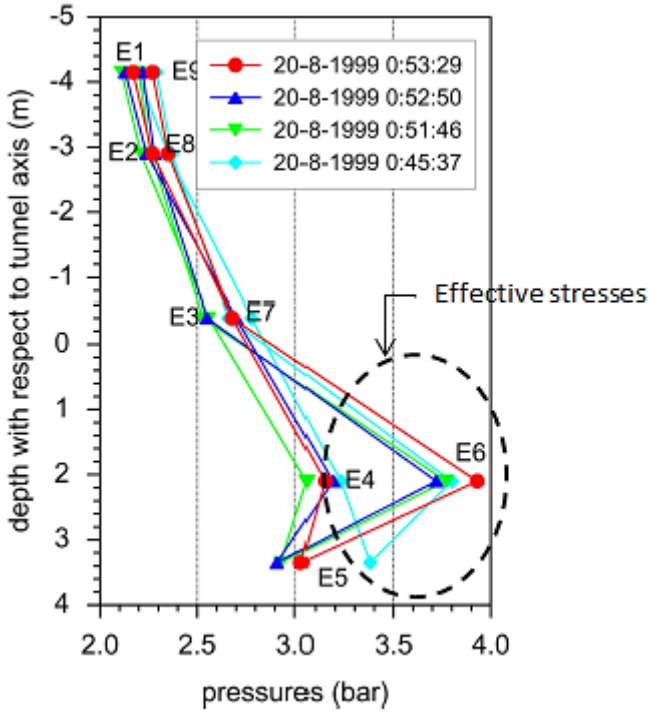


**Figure 29:** Total pressures measured at the bulkhead with respect to the tunnel height; (Bezuijen A., Talmon A.M., 2014b)

Nonetheless, in order to investigate the possible effects of this phenomenon, an ensemble of twelve (12) analyses was created and carried out. The first six (1-6) analyses were conducted assuming face pressure coefficient A=1 and the last six (6-12) assuming A=0.5. To model effective stress development into the chamber, bottom half pore pressure values applied at the face were decreased to the pressure value at the center of the tunnel (Figure 30). Mechanical **F**ace **P**ressure (total stresses) are depicted with brown color, $U_m$ stands for

the pore pressure in the **m**uck (dark blue color) and $U_{m,m}$ for the **m**odelled pressures (dashed line). Results and conclusions are presented in the following chapter.

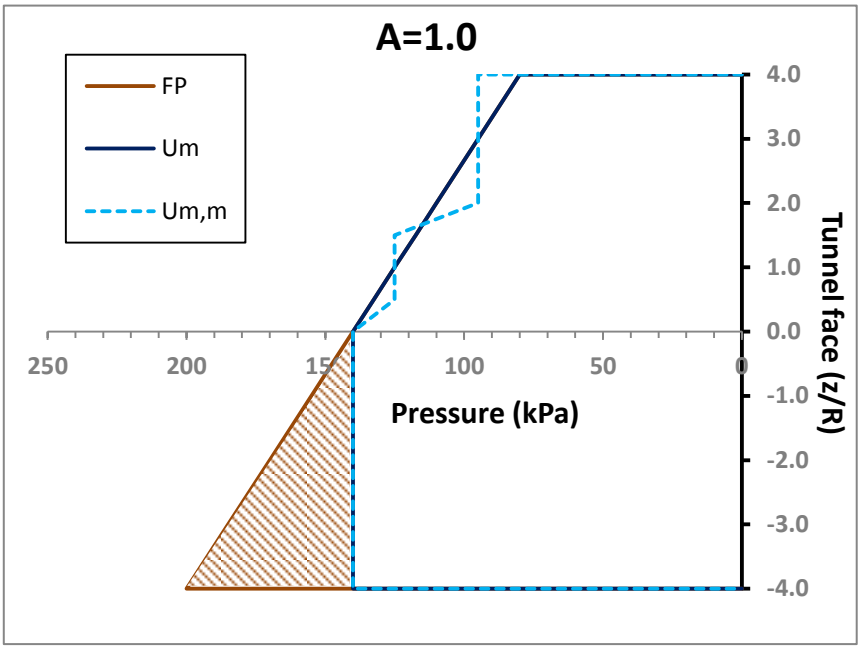


**Figure 30:** Illustrative sketch of the applied pressure when effective stresses in the muck are present for the case of **A=1.0**.

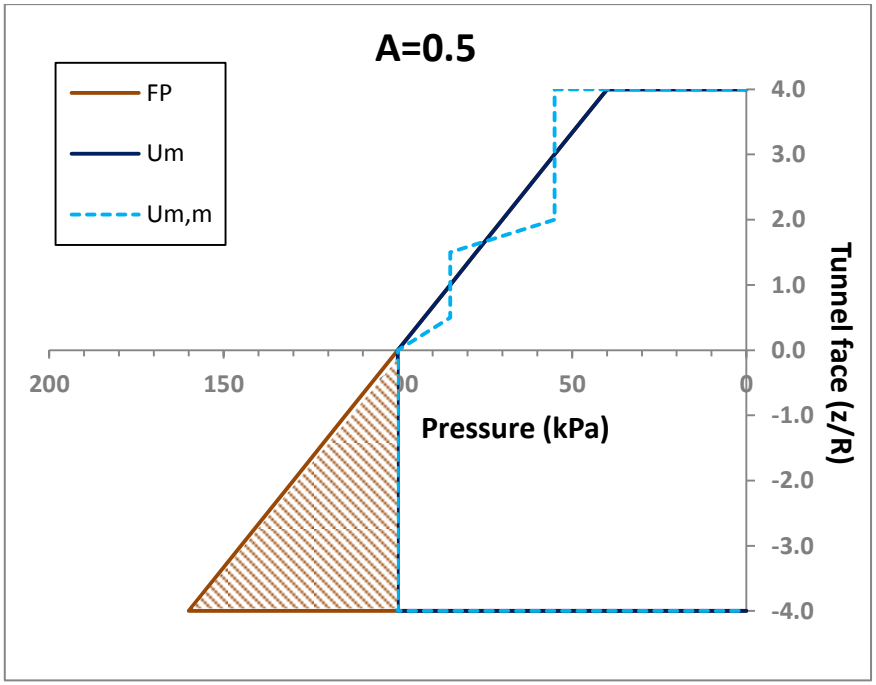


**Figure 31:** Illustrative sketch of the applied pressure when effective stresses in the muck are present for the case of **A=0.5**.

## 3.7. The calculation of Undrained Shear Strength

Calculation of soil's undrained shear strength ($C_u$) was necessary both for the input and for the output phase of the analyses. During the **input** stage, Young's modulus used was correlated with the undrained shear strength through the following empirical equation:

$$E = K_c * C_u = 500 * C_u \quad \text{Eq. 3.1}$$

, where $\mathbf{K_c}$ is a correlation factor based on laboratory/field tests in undisturbed soil specimens. The value of $K_c$ selected, indicatively corresponds to medium-stiff clay (Bowles et al, 1997). As for undrained shear strength, stiffness modulus was considered constant with depth as the overburden height is relatively small in shallow (urban) tunnelling. During the **output** stage, undrained shear strength was selected as a characteristic parameter to support the interpretation of the results (see §4.2).

Undrained shear strength could be indirectly calculated combining the Mohr-Coulomb yield criterion and Skempton's formula (Eq. 3. 7) for pore pressures build up in a triaxial undrained test assuming that such a test is executed in an elementary piece of soil at the tunnel axis. It may be calculated either for compression, calculating the additional total vertical stress $\Delta\sigma_1$, or for extension, calculating the additional total horizontal stress $\Delta\sigma_3$ in order to satisfy the Mohr-Coulomb criterion. Despite the fact that face extrusion is induced by the incremental decrease of $\sigma_3$, in order to be consistent with Prountzopoulos (2012) and enable future comparisons, the undrained shear strength was calculated for the compression case ($\Delta\sigma_3$=0).

$$\Delta u = B * [\Delta\sigma_3 + A * (\Delta\sigma_1 - \Delta\sigma_3)] \quad \text{Eq. 3. 2}$$

Skempton's parameter **A** was selected to be equal to **1/3** (basic value). B parameter is equal to unity when the pore fluid is water. In terms of total stresses and assuming compressive loading, Mohr-Coulomb criterion is written as:

$$\sigma_1 = 2 * c * \sqrt{N_\varphi} + \sigma_3 * N_\varphi \quad \text{Eq. 3. 3}$$

and:

$$N_\varphi = tan(45 + \varphi/2)^2 \quad \text{Eq. 3. 4}$$

$$\sigma_1 + \Delta\sigma_1 = \sigma_1' + u + \Delta u \quad \text{Eq. 3. 5}$$

$$C_u = \frac{(\sigma_1 + \Delta\sigma_1) - \sigma_3}{2} \quad \text{Eq. 3. 6}$$

After considerable algebra, the undrained shear strength is given by the following equation:

$$C_u = \frac{1}{2}\left\{\sigma_1' + \frac{\sigma_3' * N_\varphi + 2c\sqrt{N_\varphi} - \sigma_1'}{1 + A(N_\varphi - 1)} - \sigma_3'\right\} \quad \text{Eq. 3. 7}$$

# 4
# Results

## 4.1. Introduction

In the present chapter, the results of the ninety three (93) aforementioned 3D-coupled analyses are presented. The face stability is quantified mainly by the two (2) following deformation parameters:

- The magnitude of axial face **extrusion,** i.e. the axial displacement of the excavation face towards tunnel's interior, known also as "face-take".
- The magnitude of radial wall **convergence**, i.e. the radial displacement of the surrounding soil at the rim of the excavation face as well as the pre-convergence, that is the evolution of the radial convergence of the soil ahead of the tunnel face (advance core) until the face arrival.

The aforementioned parameters are expected to be correlated since the resulting overexcavation is strongly connected with the face stability. However, any soil movement or convergence induced at the rear part of the machine hardly affects the soil displacement occurring at the face and since the demanding grouting simulation is neglected herein, it will not be discussed further. The scope of the present Thesis is to evaluate the effect of prevailing hydraulic conditions around the tunnel on the stability of the working face and not the calculation of its deformation as an absolute value. As a result, excess pore pressures and/or water seepage issues will be discussed accordingly with respect to time-dependency. At this point it should be noted that a small number of analyses did not succeed to terminate due to severe numerical instabilities of the method caused by excessive deformation. Despite that fact, deformation values are also plotted at the last successfully completed calculation step.

Finally, in order to evaluate the results as a whole, dimensionless factors and suitable indexes had to be selected to filter out the effect of parameters such as the geotechnical conditions and to obtain the best possible correlation for a broader use. The origins and consecutively the evolution of the above mentioned are presented in the following section.

## 4.2. Results' Interpretation

Coming to the results' interpretation we should focus on the proper selection of suitable factors and deformation indexes. To do so, we will examine the basis of the present work. Prountzopoulos (2012) quantified face stability conditions for **unsupported** tunnel face through an assembly of approximately 400 3D numerical analyses for different geometrical (H/D), geotechnical (c, $\phi$, $\delta$, E) and initial stress field ($K_0$). To accomplish the latter, he plotted results of a normalized extrusion factor ($\boldsymbol{\Omega_F}$) versus a dimensionless face stability factor ($\boldsymbol{\Lambda_F}$). The aforementioned work was extended to account for i) **reinforced** tunnel faces under **conventional** excavation in (Prountzopoulos G. & Kavvadas M., 2014) and ii) **critical state plasticity** (MCC model) in Sitarenios et al (2014). However, crucial difference between the aforementioned contributions and the present one is the presence of water, as **dry** conditions were assumed at the previous ones.

To begin with, it is essential to define the extrusion and convergence moduli that will be used to quantify the stability of the tunnel face. Prountzopoulos (2012) suggested three (3) different expressions regarding the resulting extrusion $\mathbf{U_h}$, varying from simple to more sophisticated:

- Extrusion may be the horizontal deformation of the tunnel center inwards. It is the simplest way to express face extrusion and is defined as the horizontal deformation of the central node of the face ($U_{h,\,center}$).
- Extrusion may be the average horizontal deformation of the vertical diameter of the tunnel ($U_{h,diameter}$). It is a more reliable measure of extrusion than the previous, given that the maximum extrusion is mostly observed at the central parts of the section due to excavation boundaries effect. It can be calculated via division of the area of the central extrusion profile with the diameter.
- Extrusion may be the average horizontal deformation of the whole face area ($U_{h,area}$). It is the most reliable measure as it approaches the phenomenon in an optimum way. It can be calculated by dividing the total extruded volume ($V_{extr}$) with the face area. The total extruded volume is the sum of all individual extruded volumes ($V_i$) of each element of the face. The latter can be obtained if someone multiplies the area of a single face element ($A_i$) with the mean deformation of its four (4) nodes upon the face ($U_{h,i}$). Each area $A_i$ is calculated by the half sum of the

four triangular areas defined by the four nodes. As the coordinates of each node are known, all side lengths ($L_k$) can be found easily. Afterwards, each triangular area is calculated through Heron's formula (Figure 32).

- Finally, another possible way of expressing face extrusion could be the use of the maximum value of horizontal deformation of all face nodes ($U_{h,max}$) or of the vertical diameter's nodes ($U_{h,dmax}$). The latter introduce an important level of conservatism to the results and thus they were not selected for use.

In the present Thesis, extrusion is expressed and presented via the $\mathbf{U_{h,area}}$ which constitutes the most representative expression despite its increased output time.

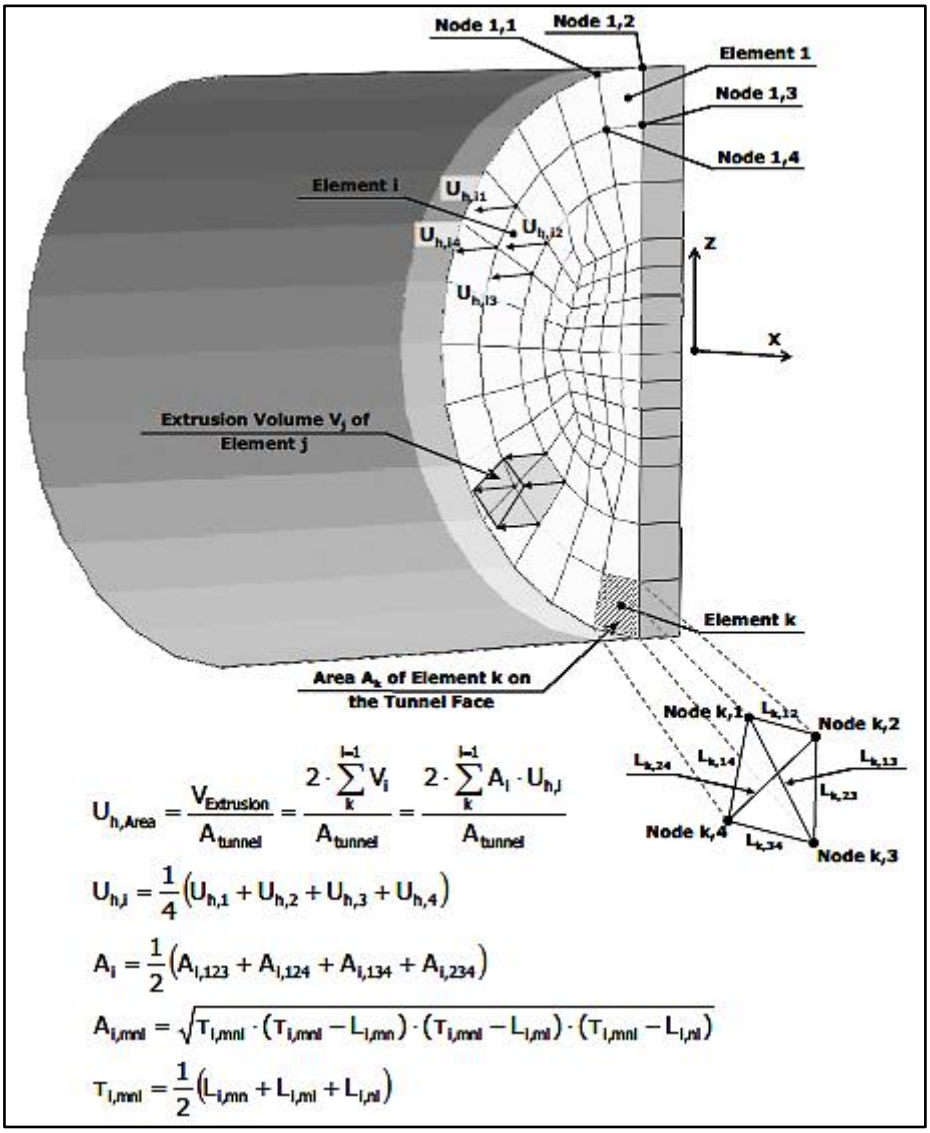


**Figure 32:** Illustrative sketch and calculation procedure of $U_{h,area}$ (Prountzopoulos, 2012)

Similarly, radial wall convergence at face chainage (x=0) could be expressed as:

- the average radial convergence of all circumferential nodes ($U_{R,avg}$)
- the maximum radial convergence of all circumferential nodes ($U_{R,max}$)

In the present Thesis, in order to avoid conservatism and to be consistent with extrusion (i.e. average value), also average radial convergence is used.

Radial convergence of each node, in each position of the face (x) is a function of transversal deformation ($U_1$ or $U_x$) and vertical ($U_3$ or $U_z$) and is simply expressed as follows:

$$U_{R,i} = \sqrt{U_{x,i}^2 + U_{z,i}^2} \quad \text{Eq. 4.1.}$$

Due to the fact that face extrusion as an absolute value does not have a practical meaning, a normalized expression that would accommodate crucial parameters such as the in-situ stress conditions should be adopted. For this reason, normalized extrusion factor $\Omega_F$ (Prountzopoulos, 2012) was used herein for a unified interpretation of results. $\Omega_F$ is defined as follows:

$$\Omega_F = \frac{U_{h,area}}{D} * \frac{E}{P_{m,eff}} \quad \text{Eq. 4.2.}$$

, where $P_{m,eff}$ is the **mean effective** stress in **geostatic** conditions at the tunnel axis level given by the following relationship:

$$P_{m,eff} = \frac{\sigma_v' + \sigma_h'}{2} = \frac{1 + K_0}{2} * \boldsymbol{\gamma}' * H \quad \text{Eq. 4.3.}$$

Similarly, normalized radial **convergence** factor $\Omega_R$ was also used and it is defined as follows:

$$\Omega_R = \frac{U_{R,avg}}{D} * \frac{E}{P_{m,eff}} \quad \text{Eq. 4.4.}$$

Since the deformation factors are defined, it is prudent at this moment to present the stability factors. The most common stability factor used, especially when deep tunnels in rocky formations are studied is the ratio of medium's uniaxial compression strength ($\sigma_{cs}$ or

$q_u$)[13] to the overburden load ($\gamma$*H). In our case, due to the presence of water, soil's compression strength is a function of its undrained shear strength, that is:

$$q_u = 2 * C_u \quad \text{Eq. 4.5.}$$

, where $C_u$ is calculated as described in §3.7. As overburden load, only the **effective vertical stress ($\gamma'$*H)** is used in order to be consistent with the definition of factor $\Omega_F$.

The use of $C_u$ implies undrained conditions. Indeed, by closely examining the resulting void ratio (e) of each analysis, it was proved that hardly any variation from its initial value ($e_0$=0.7) occurred. The latter means that any anticipated deformation is sustained under practically constant volume (undrained behavior) which is reasonable for a low-permeable soil subjected to cyclic loading. Figure 33 shows the void ratio variation at the last step, in very unfavorable conditions (**A=0.5**/soil profile: **a**[14]). It is shown that a slight but negligible increase of voids is mostly expected near the perimeter indicating a dilatant behavior. Moreover, undrained behavior leads to practically negligible water seepage. Consequently, face stability is not expected to be considerably affected from seepage forces.

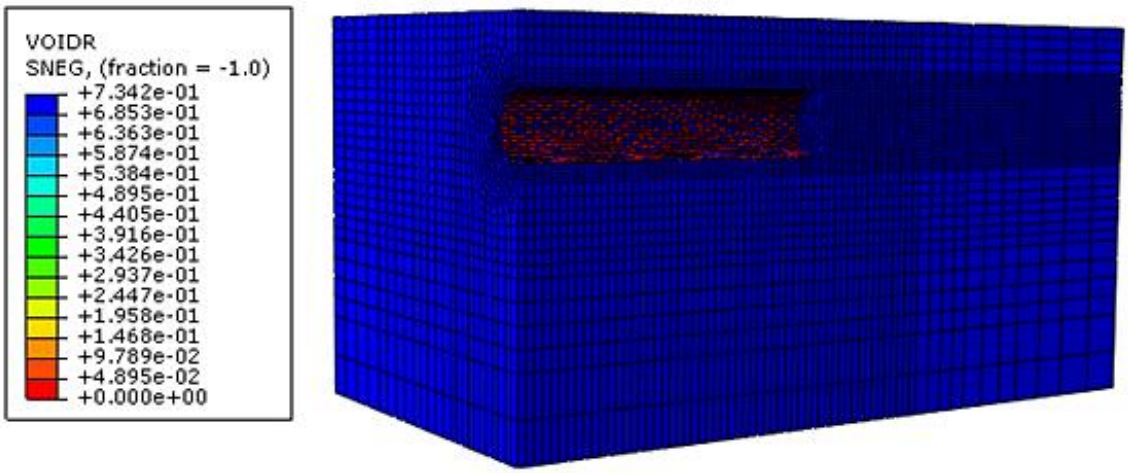


**Figure 33:** Indicative **void ratio** (e) variation resulted from Abaqus v.11.1 (A=0.5, soil profile a, k=5E-07m/s & AR=0.67m/h).

## 4.3. Support pressure effect on face stability

Results from parametric analyses will be presented separately for each of the three (3) investigated parameters (A, k, AR) which are considered to affect the hydraulic conditions of

[13] The former expression ($\sigma_{cs}$) is used mostly in rock mechanics while the latter ($q_u$) in soil mechanics.

[14] see Table 5

the problem and consequently the demand for face stability. In the present paragraph, results from the three (3) different support pressure cases studied (A=0.5, 1.0 & 1.5) are presented for both the specific ground conditions and all the examined soil profiles. Soil profile **c** which is considered as a moderate clayey ground was selected as a reference soil profile (Table 5). Reference values of permeability (i.e. k=5E-07m/s) and advance rate (i.e. AR=0.67m/h) correspond to a common clayey ground and typical advance rate for normal EPB operations respectively.

### 4.3.1. Face Extrusion

To begin with, magnitude of extrusion values and its distribution (contours) along the face surface are depicted in Figure 34. As it was found, lower values of support pressure applied on the face resulted in higher extrusion values of the face. The latter constitutes a general deduction noticed in all soil profiles (see Figure 36). No extrusion is observed for excess applied pressure (A=1.5), negligible extrusion is expected for common values of applied pressure values (A=1.0) and finally up to 4.4cm extrusion is calculated for low support pressure values (A=0.5). Regarding its distribution on the tunnel face, someone can reasonably support that higher extrusion values are expected in the central and higher parts of the section where boundary effect and face support are respectively lower. The sign of axial deformation (see legend) describes the direction of movement. Tunnel's advance direction is positively signed (negative extrusion) while negative axial deformation ($U_2$) denotes node movement inwards (positive extrusion).

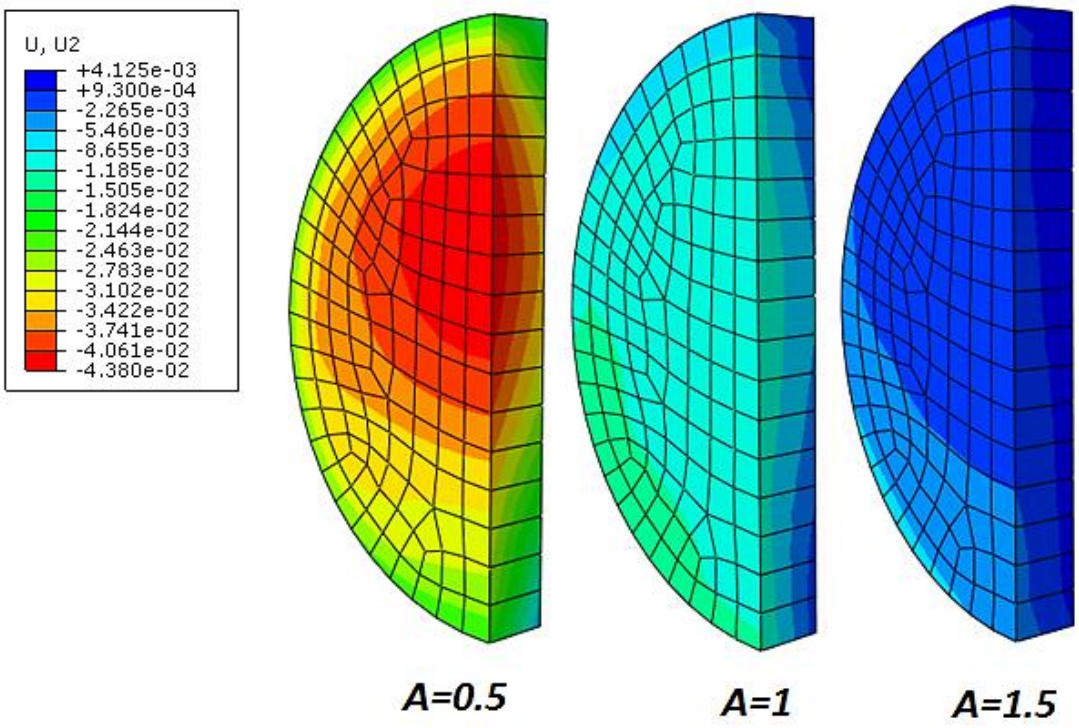


**Figure 34:** Resulted extrusion contours (in m) of the investigated section (x=0), for the three (3) pressure cases investigated, **k=5E-07**m/s, **AR=0.67**m/h and soil profile **c**. Minus sign indicate opposite direction in relation to that of tunnel advance.

Figure 35 shows the deformed profile of the face for the three (3) investigated support pressure values. Extrusion values for pressure cases A=1.0 & 1.5 seem to be constant irrespective of the face elevation implying a uniform dilatant tendency whereas the extrusion pattern for low face pressure values (=low pore pressure values) are localized at the upper part of the section. The latter is possibly attributed to the piezometric head and therefore development of minimal seepage forces towards the tunnel face. At this point, it should be mentioned that the aforementioned profile of the face is a **theoretical** deformed state and it is never observed in situ because extrusive deformation is triggered in a certain distance ahead of the working face the extent of which depends on geometrical and geotechnical characteristics. In every boring circle, part of this "extra" material is excavated (normal overexcavation) and thus it cannot be observed. It is helpful though to get a general idea of the magnitude of cumulative deformation.

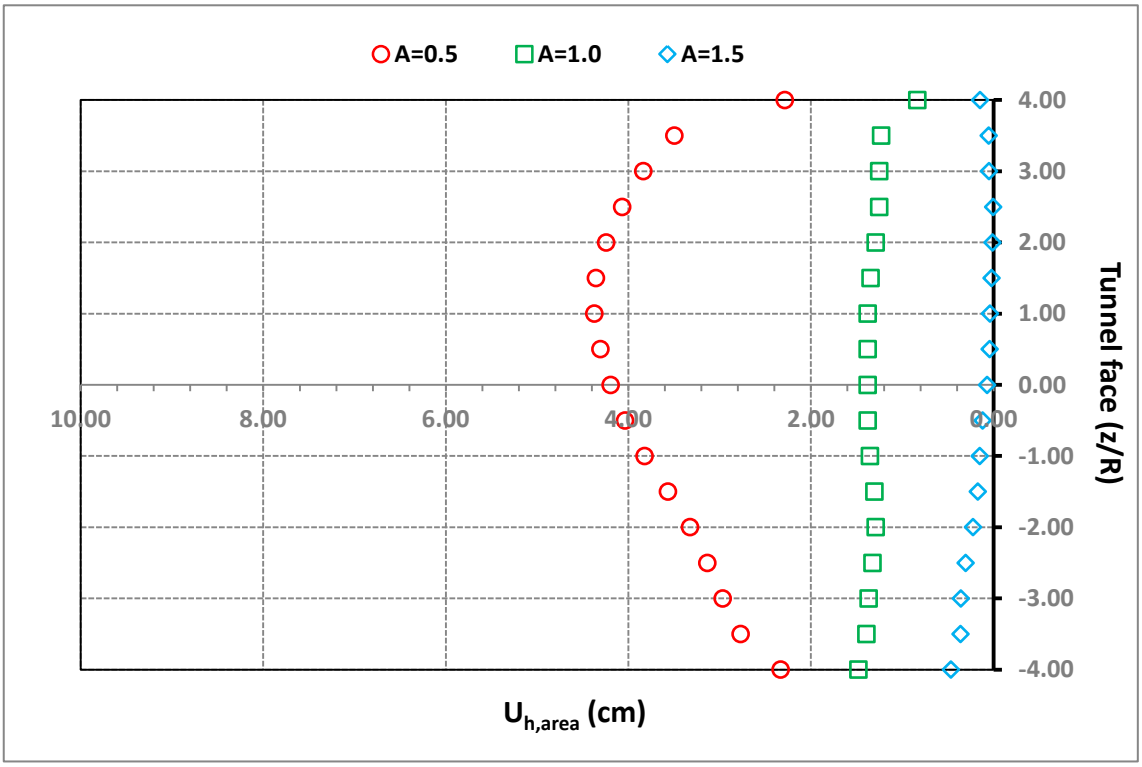


**Figure 35:** Indicative face extrusion profile along tunnel's diameter, for the three (3) investigated face pressure cases, **k=5E-07**m/s, **AR=0.67**m/h and soil profile **c**.

In order to filter out the effect of varying soil conditions, extrusion results are presented unified in Figure 36 with respect to the stability factor described in §4.2. Results show that for support pressure cases A=1.0 & 1.5, even in poor soil conditions (i.e. $C_u/\gamma'H<1.0$), working face retains a stable behavior. However, an unfavorable combination of poor in-situ conditions and loss of support pressure (A=0.5) could lead to significant face instabilities. Unity seems to be a marginal value separating unstable from stable state. Unstable region is recognized by an abrupt increase of deformations when a small decrease of soil's shear strength occurs (i.e. 1-2 kPa decrease in cohesion). The transition from stable to unstable conditions is not always abrupt and therefore limit state is not always clear and obvious. Previous works have shown that as the overburden ratio H/D increases, transition gets smoother leading to plastic deformations or creeping phenomena in deep tunnels (H/D>5). In shallow tunnels though, such as the one investigated herein, the overburden height is not sufficient to provide stress redistribution because of the boundary of the free surface. Consequently, face support is almost mandatory.

It seems that the selected ratio of the undrained compression strength over the vertical effective stress at the tunnel axis ($2C_u/\gamma'H$) can satisfactorily represent the varying geotechnical conditions and moreover to allow a more unified representation of the results.

Negative values resulted from support pressure ratio A=1.5, indicate that the thrust force exerted by the machine along with muck's self-weight is greater than the passive earth pressure and thus soil is locally squeezed by the cutterhead. The latter is considered unrealistic and no further attention will be drawn on.

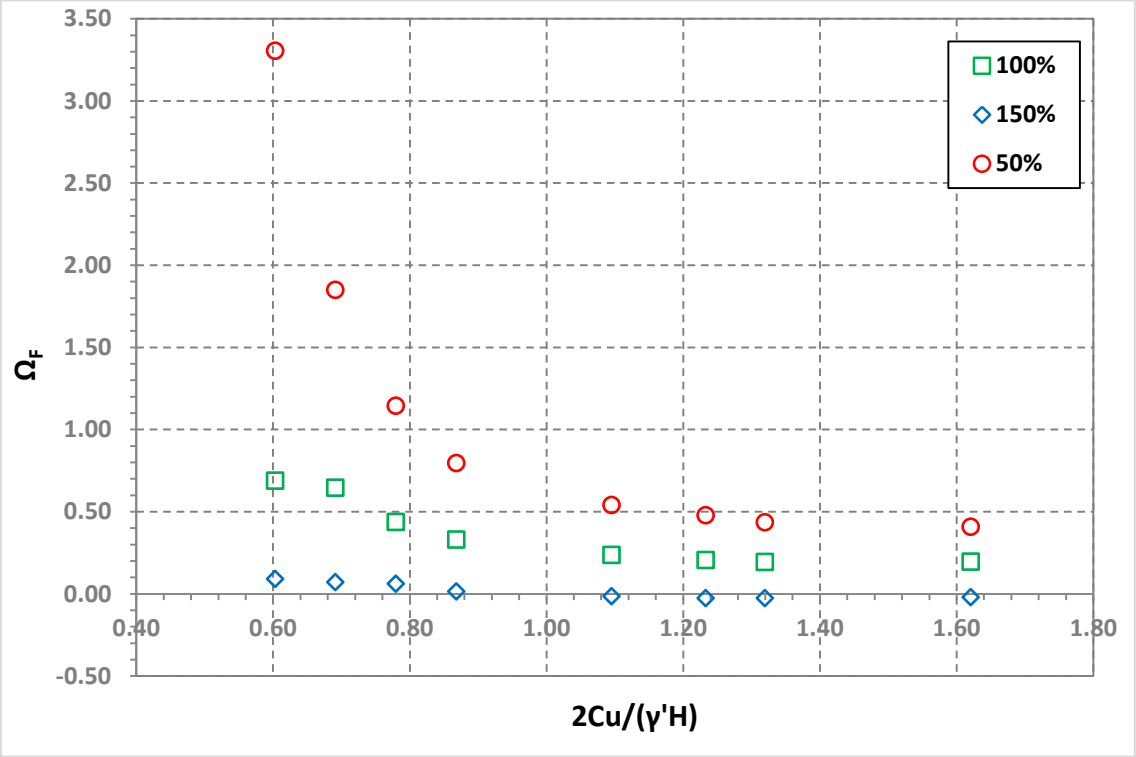


**Figure 36:** Average face extrusion versus the stability ratio $2Cu/\gamma'H$ for the three (3) face pressure cases investigated, **k=5E-07**m/s & **AR=0.67**m/h.

### 4.3.2. Face Convergence – Preconvergence

The second deformation modulus investigated is the "final"[15] radial convergence (i.e. at the investigated section, x=0) as well as its evolution, that is the convergence profile ahead of the face, along the tunnel axis (y). Initially, transversal cross-section (z-x) of its deformed state for each support pressure case is presented in Figure 37. Radial convergence values of the deformed section are presented 10-fold because its original scale did not facilitate parametric comparison. It is shown that convergence results come in perfect agreement with

[15] Convergence value is characterized herein as final because neither yielding lining nor void/tail grouting are simulated due their negligible effect on face stability.

those of extrusion validating that they constitute two strongly correlated deformation mechanisms, as the lower the face support pressure the higher will be the deformation of tunnel face resulting in greater overexcavation. Furthermore, the magnitude of convergence is reasonably higher near the crown comparing to the invert thanks to increasing face pressure towards the bottom.

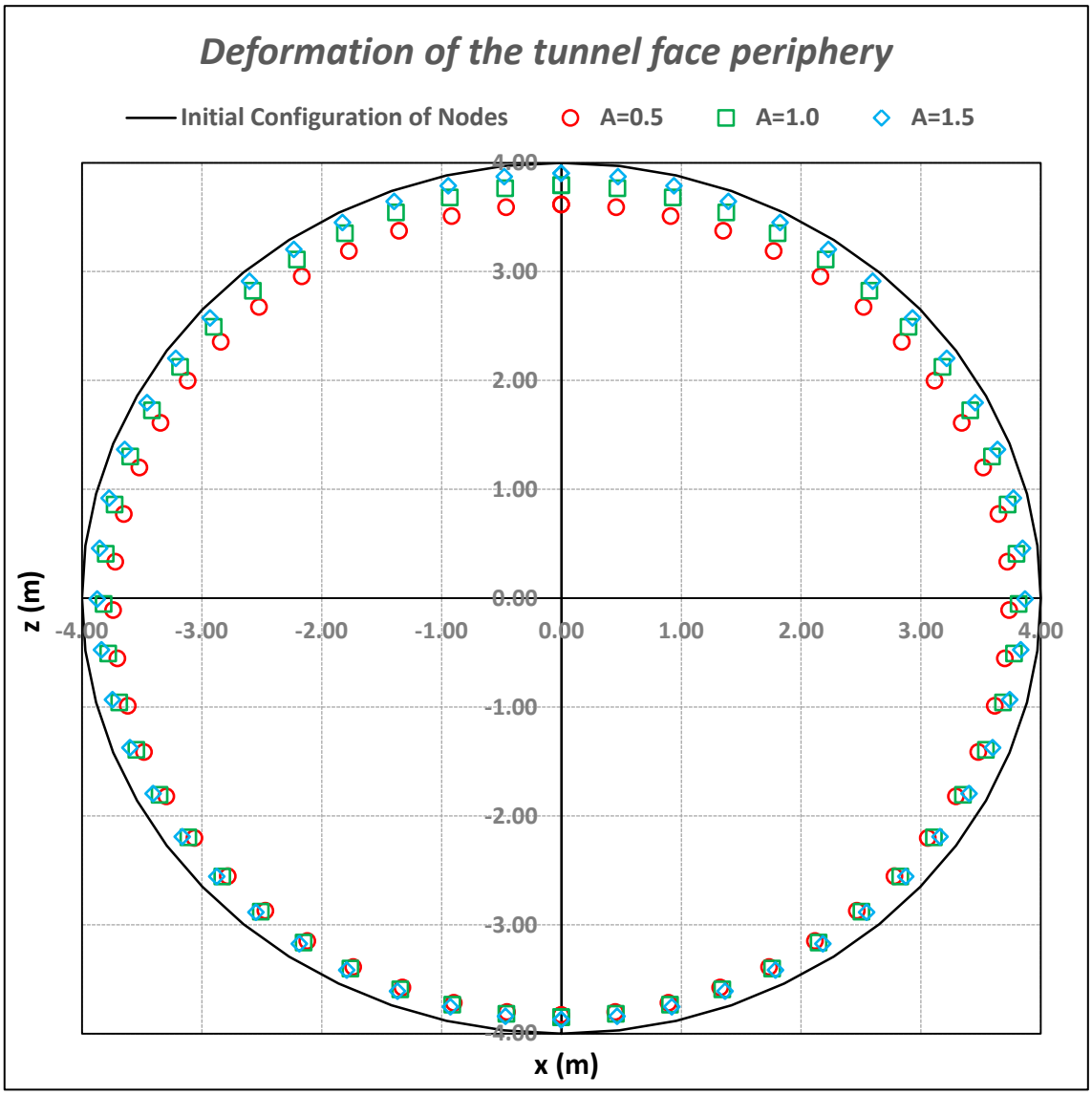


**Figure 37:** Illustration of 10-fold radial convergence at face chainage x=0 for the three investigated face pressure cases and assuming soil profile **c**, **k=5E-07**m/s, **AR=0.67**m/h.

In Figure 38 average radial convergence of the tunnel is depicted versus normalized distance from the face (x/R) in a longitudinal cross-section. The abrupt increase of $U_{R,avg}$ value noticed at face chainage x=0 is attributed to the modelling of the excavation procedure. As mentioned in §2.6, segmental lining (shell elements) is modelled in full contact with the surrounding soil disregarding the voids between the lining and the surrounding soil as well

as the geometry of the shield because of their minimal effect on face stability. As a result, no de-confinement of the soil will occur after the passage of the cutterhead. In order to get more realistic final deformation values it was selected to leave 1m unsupported which results in the different convergence noticed in the investigated section (x/R=0). The disadvantage of this modelling technique is that the deformation evolution **behind** the face is unrealistic. However, our attention is focused ahead of the face (x≤0) from where the following can be derived:

- Practically no preconvergence is expected in the case of A=1.5 which justifies the negligible final radial convergence.
- Convergence is triggered in 1D distance from the face of common support pressure values (A=1.0) and in approximately 2D in case of low support pressure (A=0.5).
- Support pressure effect is clear near the face (x≥-0.4D) where convergence tends to be stabilized (controllable).
- Fluctuation observed in high pressure case (A=1.5) is most probably attributed to the former noticed negative values of extrusion. Soil inside the advance core subjected to excessive loading tends to dilate and push the surrounding one, leading to decrease of convergence. The latter will not be further analyzed as it is considered unrealistic.

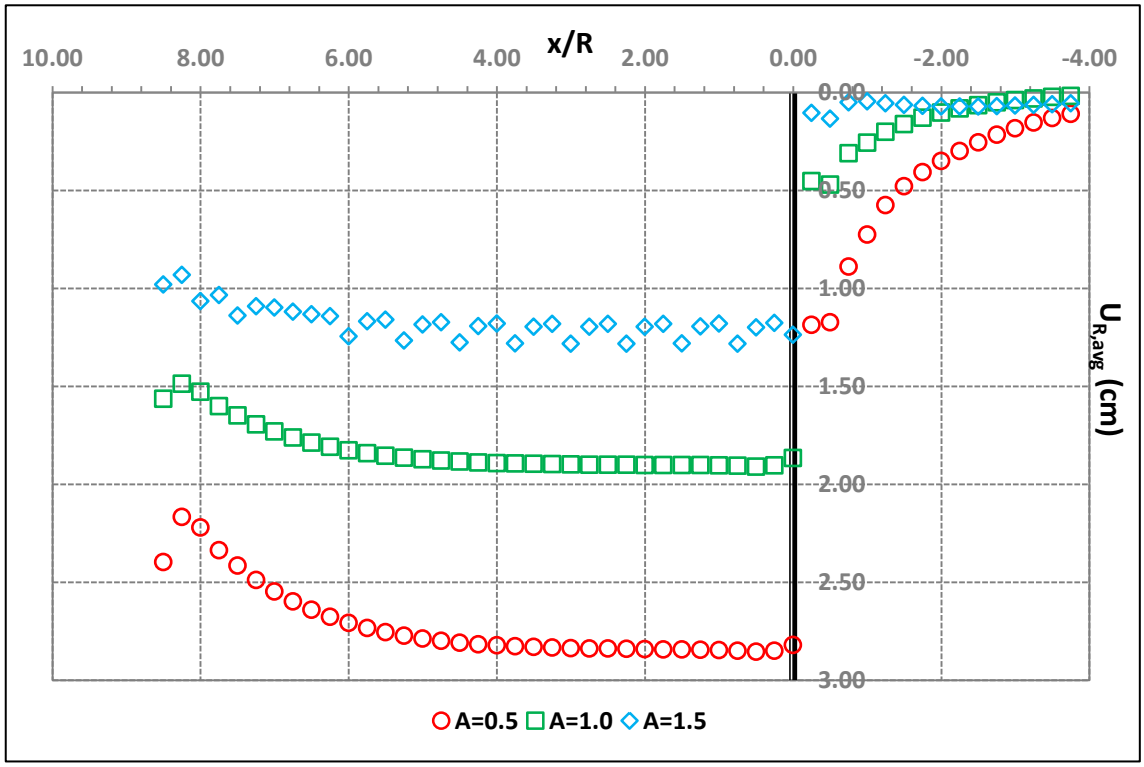


**Figure 38:** Indicative longitudinal profile of average radial convergence, ahead and behind the face for the three (3) investigated face pressure cases, **k=5E-07**m/s, **AR=0.67**m/h and soil profile **c**.

As mentioned in §1.1, face extrusion and preconvergence during tunnelling in soils are strongly correlated, as one may rationally claim that any soil movement inwards the tunnel advance core is translated into tunnel face extrusion. Therefore, the cumulative soil volume due to convergence ahead of the tunnel face is approximately equal to the soil volume extruded at the tunnel face. The main soil disturbance ahead of the face is assumed to occur inside the advance core which is a theoretical cylinder of the same size as the tunnel. The length of the advance core, i.e. the extent of the excavation-induced deformation depends on many factors, yet it can be assumed generally equal to 1D (Lunardi, 2000). Prountzopoulos (2012) also adopted that theory. In order to investigate the aforementioned volume correlation occurring inside the advance core, the same assumption was used. Consequently, radial convergence values were extracted for an equivalent length of 8m (=1D) ahead of the face. The intruded volume calculation procedure is described below:

- Each section is assumed to have a uniform radial convergence ($U_{R,avg}$) in order to be circular-shaped with minimum error inserted (less than 0.3%)

- The evolution of radial convergence within an excavation length (1m) is assumed to be linear with minimum error inserted mainly after the 1st excavation slice (x>-1 m).
- Frustum's volume is calculated via the following geometrical relationship:

$$V_{deformed,i} = \frac{1}{3} * \pi * L * (r_i^2 + r_i * r_{i+1} * r_{i+1}^2) \quad \text{Eq. 4.6.}$$

, where $r_i$ & $r_{i+1}$ are the radii of the circular areas that define each frustum (see Figure 40) calculated as follows:

$$r_i = R - U_i^{r,avg} \quad \text{Eq. 4.7.}$$

- Total volume **intruded** is calculated easily by subtraction of the total deformed volume ($\Sigma V_{deformed,i}$) from the initial cylindrical one.
- Total volume **extruded** is calculated via the methodology proposed by Prountzopoulos (2012) which is described explicitly in §4.2.

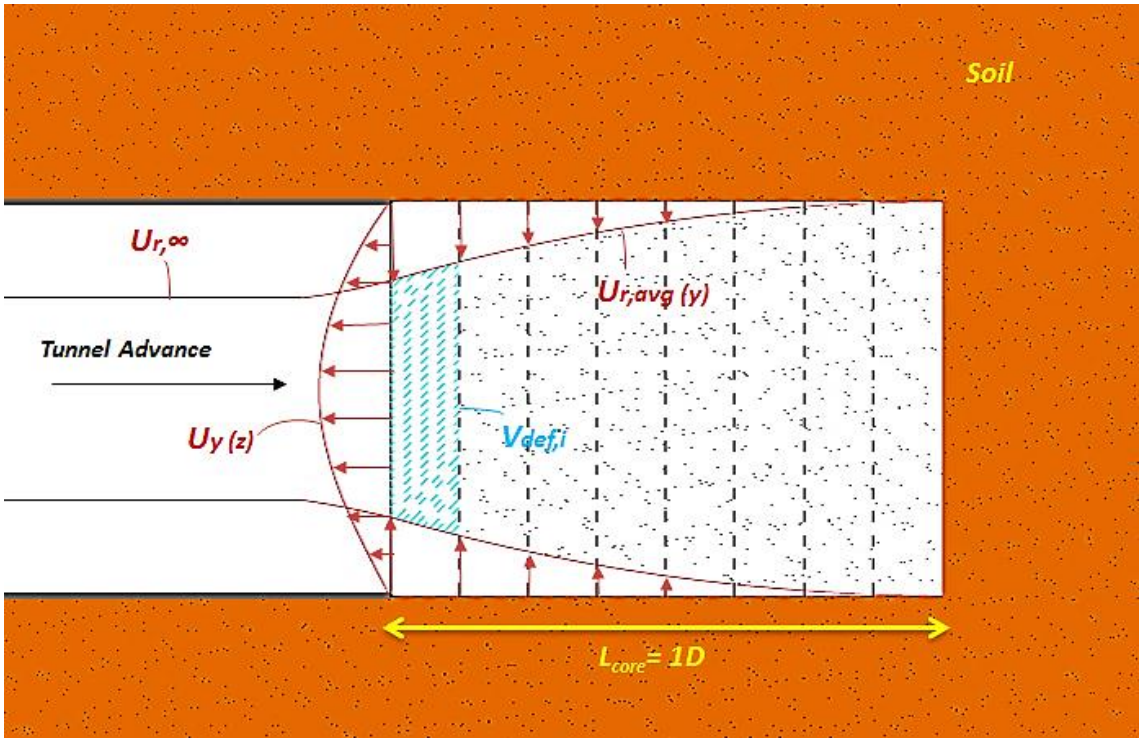


**Figure 39:** Schematic illustration of magnified deformation parameters controlling the stability of tunnel's face.

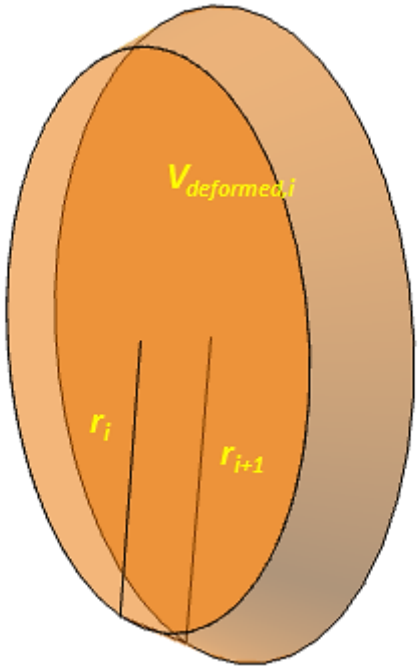


**Figure 40:** Illustrative sketch of the $i^{th}$ deformed volume assumed for the calculation of the total intruded volume.

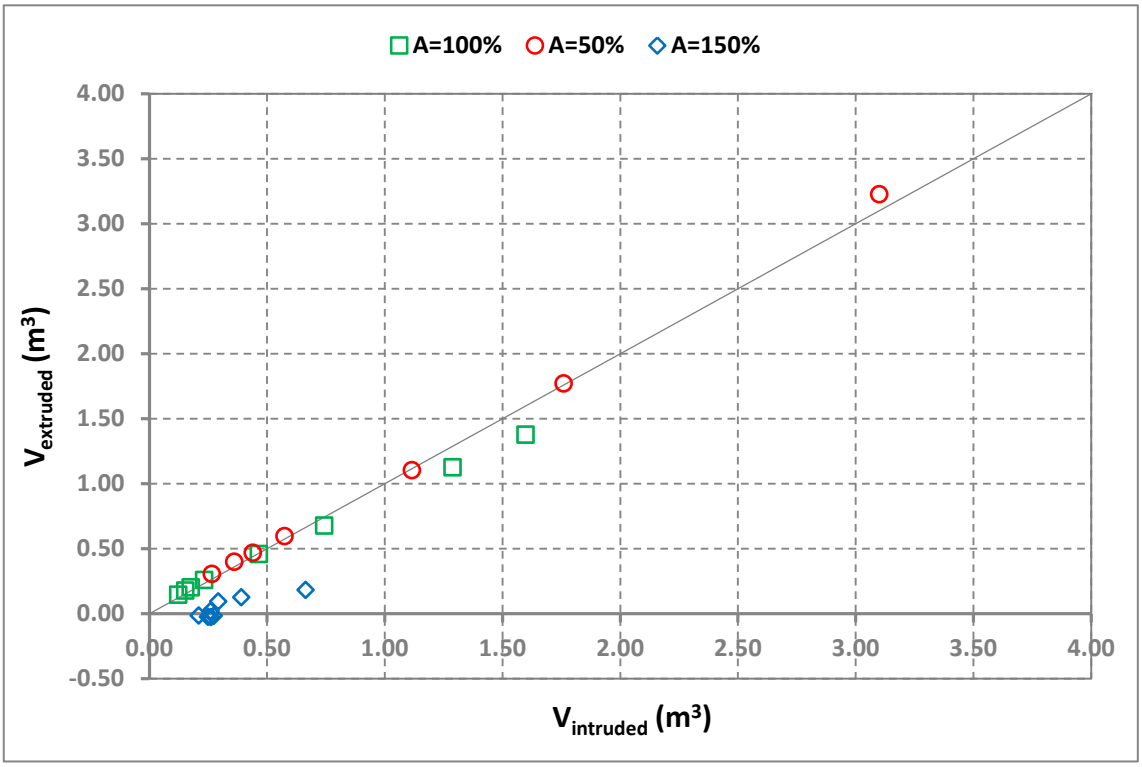


**Figure 41:** Correlation between **extruded** and **intruded** soil volumes, assuming 1D length of advance core, for the three (3) investigated pressure cases and **k=5E-07**m/s, **AR=0.67**m/h.

It is clearly shown from Figure 41 that there is indeed a strong correlation between the intruded and the extruded soil volume during excavation. In case of excess face pressure applied (A=1.5), a deviation from the previous theory seems to occur which cannot be attributed to consolidation phenomena (volume loss) as negligible deformation is expected (Figure 36). The latter is most likely caused by the unrealistic face extrusion values (negative) especially in competent soil profiles which imply that there is less soil volume intruded in the advance core leading to minimum overexcavations. Consequently, they cannot be considered reliable for conclusions.

Similarly to the final normalized extrusion ($\Omega_F$), normalized average radial convergence ($\Omega_R$) is presented in the next figure with respect to the stability ratio for all the examined soil profiles.

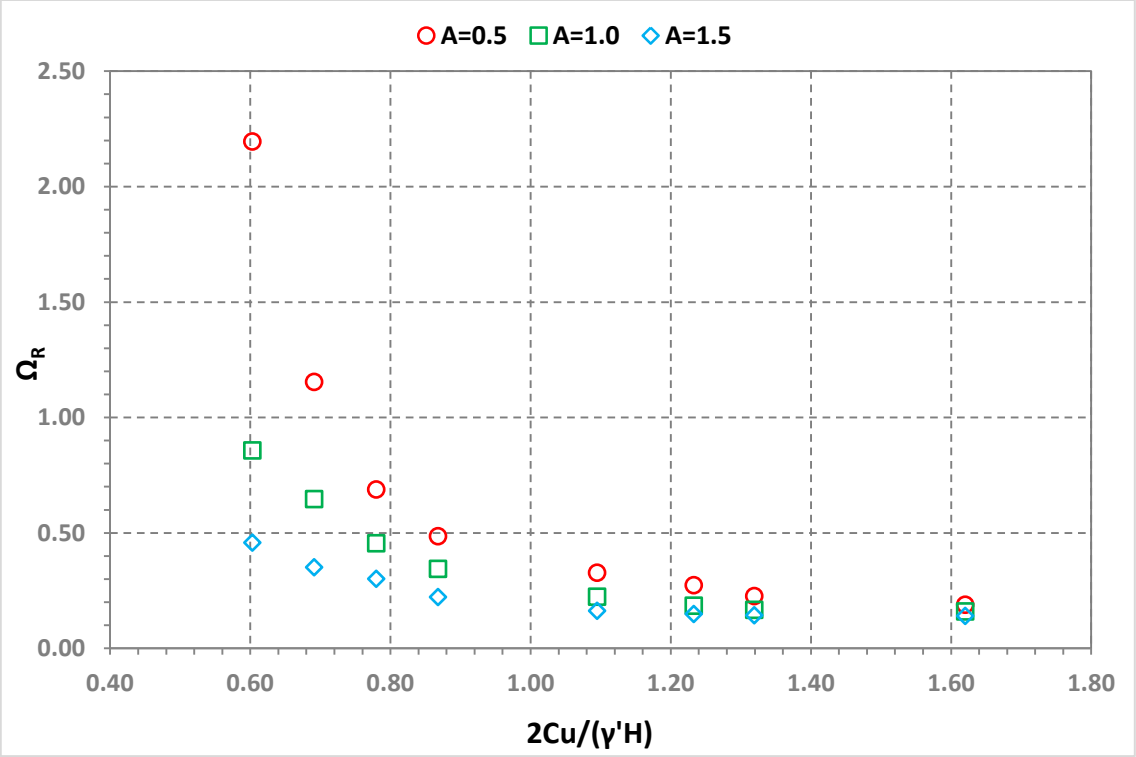


**Figure 42:** Average radial convergence at face chainage x=0 versus the stability ratio 2Cu/γ'H, for the three (3) investigated face pressure cases, **k=5E-07**m/s & **AR=0.67**m/h.

Comparison of extrusion ($\Omega_F$) and convergence ($\Omega_R$) results yields that support pressure variation affects face extrusion in greater degree than the convergence of the section. As stated again, face extrusion is clearly attributed to the incremental loss of the horizontal geostatic stress ($\sigma'_h$) as the excavation propagates and since the support pressure is applied in the same direction they are obviously highly correlated. Radial convergence of the section

depends on the total redistribution of stresses (both vertical and horizontal) complicating further the development mechanism.

Finally, radial convergence seems to have an incremental trend as the stability ratio decreases even for excessive support pressure while extrusion values seem to deviate from the parabolic form and stabilize indicating a "safe" state. The latter is probably attributed to suction phenomena developed even under small deformations which enhance the short-term behavior of the face. Suction will be analyzed further in the next paragraph.

### 4.3.3. Excess Pore Pressures ahead of the face

Excavation in saturated soils and application of face support affect the initial hydraulic head field (hydrostatic). The magnitude of this disturbance is pretty clear if someone draws his attention on the induced excess pore pressures, positive or negative. Since the stability of the face is the scope of the present Thesis, resulting excess pore pressures **ahead** of the excavation face will be presented and correlated with the deformation results in order to comprehend their effect on tunnel face stability.

Figure 43 shows the excess pore pressure distribution ahead of the tunnel face, on the tunnel axis until its dissipation. Lower pore pressure values in each set of analyses correspond to weaker soils while higher to competent soil profiles. Each curve in each set of analysis starts from the same pore pressure value at x=0 (face chainage) due to the imposed hydraulic boundary conditions at the center of the section (total pressure values).

Reasonably analyses with higher support pressure values result in higher pore pressure values. The latter is both attributed to the assumption made regarding the condition of the muck (see §1.5 & 2.4) and the prevailing undrained conditions (Figure 33). High value of applied support pressure, limits the deformation of the face even in unfavorable soil conditions yet it generates positive excess pore pressures which tend to dissipate in a relatively short distance from the face. Excess pore pressures (+) can be developed in the case of competent soil profiles which do not sustain considerable deformation (e-h). The dissipation distance seems to increase as face support decreases. In case of poor soil conditions where larger deformations are anticipated, suction phenomena are observed due to the prevailing undrained conditions. Suction acts in favor of the stability (in short term) as pore pressure decrease results in increase of effective stresses and therefore reduced deformation (see Figure 36, A=1.0 and $2C_u/\gamma'H<0.8$). However, after the passage of a certain

amount of time (depending on permeability), negative excess pore pressures dissipate leading to the opposite results.

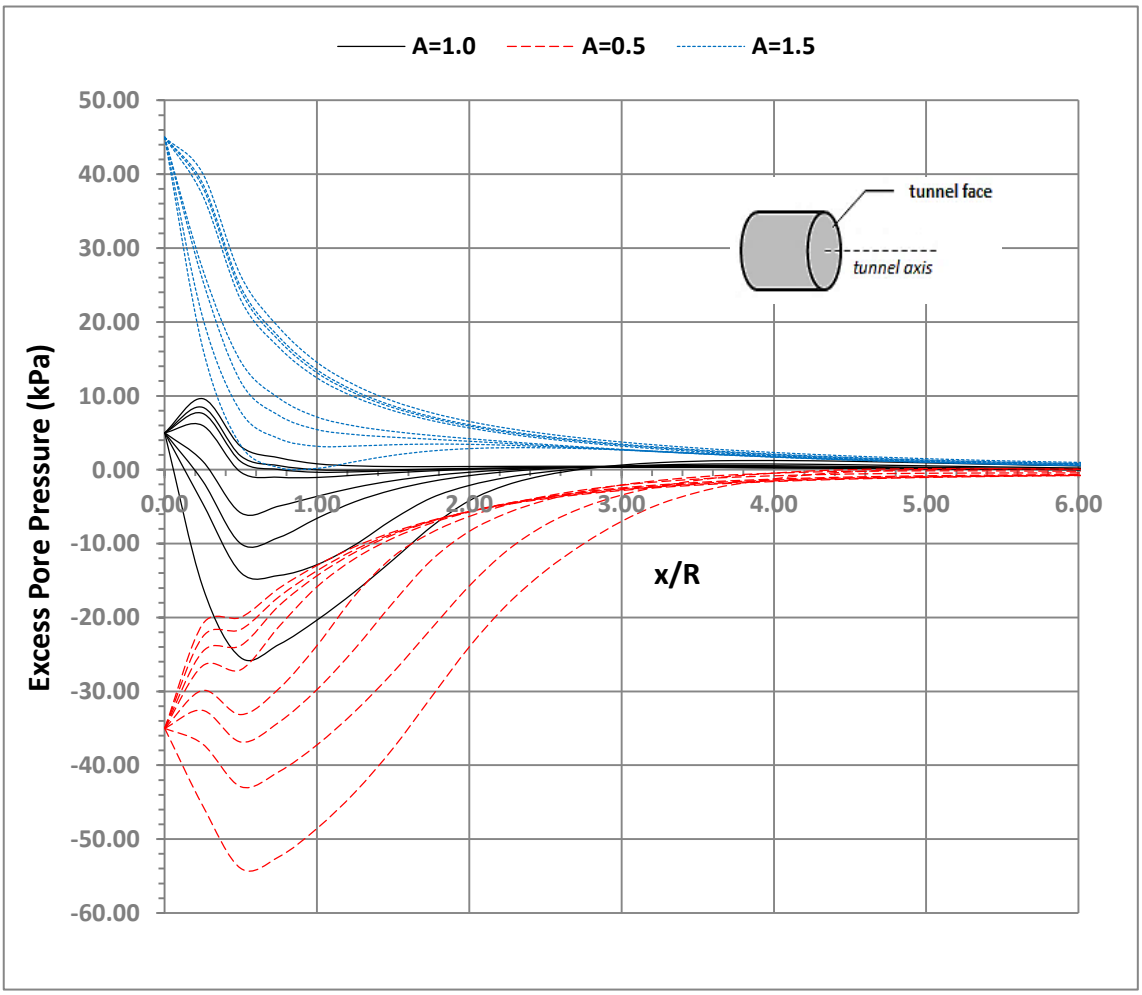


**Figure 43:** Excess pore pressures ahead of the tunnel face, calculated on the horizontal tunnel axis versus the distance (x/R), for various geotechnical conditions (**a-h**), **k=5E-07m/s, AR=0.67m/h** and three (3) different cases of support pressure (**A=0.5, 1.0 & 1.5**).

### 4.3.4. Investigation of varying condition of the muck

One of the basic assumptions of the present study refers to a homogenous muck with fluid behavior thanks to ideal soil conditioning. The latter, from a geotechnical point of view, means that hardly any effective stresses are developed in the excavation chamber and therefore total pressures are equal to pore water pressures. Although this is verified by previous monitoring campaigns, it is not the rule. In the majority of EPB applications, muck's condition deviates from the original concept and limited effective stress can be observed due to several operational irregularities (see §3.6).

Driven by recently published works[16], an ensemble of twelve (12) analyses including the development of effective stresses in the working chamber were executed to assess the impact on the expected deformations and hydro-mechanical phenomena. Consolidation of the muck is assumed to be developed partially at the bottom half of the tunnel section, so total stress reduction, as described in §3.6, was assigned at this part.

In Figure 44, variation of extrusion factor $\Omega_F$ with respect to the stability factor $2C_u/\gamma'H$ is depicted for two (2) different support pressure cases (A=0.5 & A=1.0). In similar way, Figure 45 presents the respective variation of radial convergence factor $\Omega_R$ while in Figure 46 the excess pore pressure distribution ahead of the tunnel face is depicted for the two (2) investigated muck conditions.

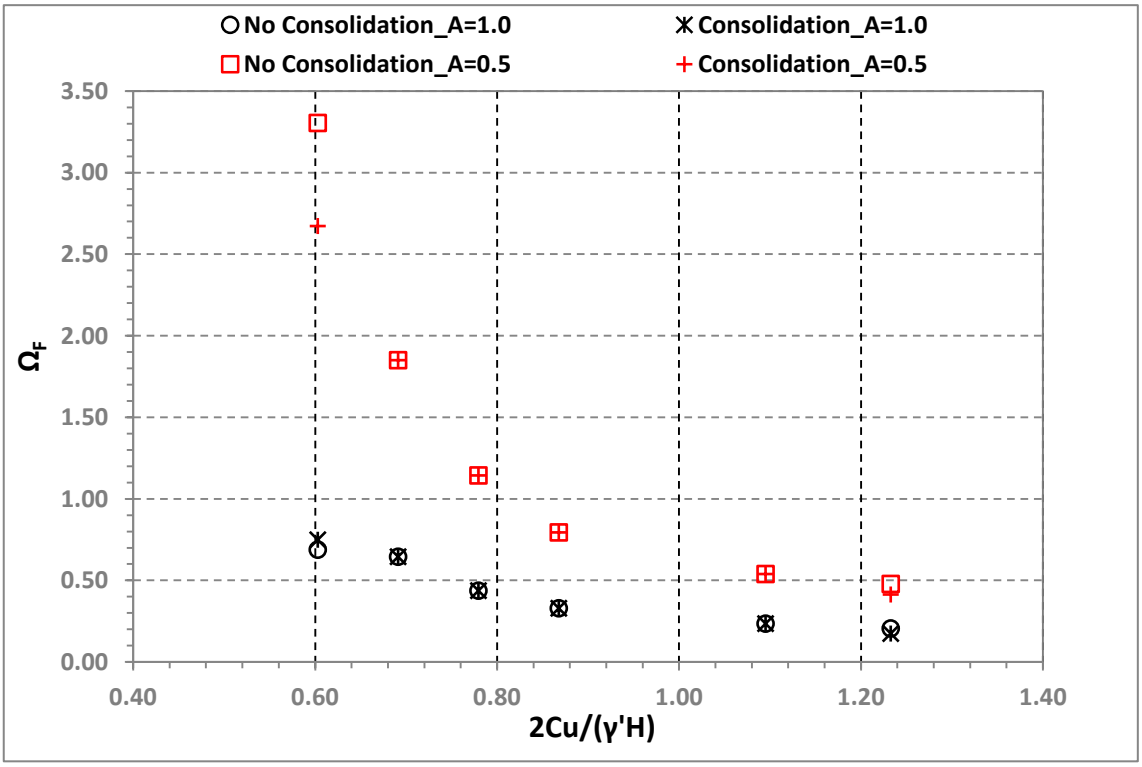


**Figure 44:** Average face extrusion versus the stability ratio 2Cu/γ'H for the two (2) assumed muck conditions, support pressure **A=0.5 & 1.0**, **k=5E-07**m/s, **AR=0.67**m/h and various geotechnical conditions (**a-f**).

All figures show that even a considerable development of effective stress in the working chamber (i.e. 30-40% of total stresses at the tunnel bed) is not capable neither to affect the induced deformation nor the hydraulic head field. Deformation seems to deviate only for the worst case scenario (low support pressure – poor geotechnical conditions) where

[16] see Bezuijen & Talmon (2014)

consolidation of the muck seems to act in favor of face stability. The latter may have a double impact. At first, increase of effective stresses in the working chamber means higher support pressure is exerted on the face and consequently lower extrusion values. However, reduced hydraulic pressure values at the face may lead to water flow towards it, i.e. increase of seepage forces and finally increase of extrusion values. Since practically undrained conditions are prevailing, the first mechanism seems to dominate. As far as pore pressures ahead of the tunnel face are concerned, those were found to be identical.

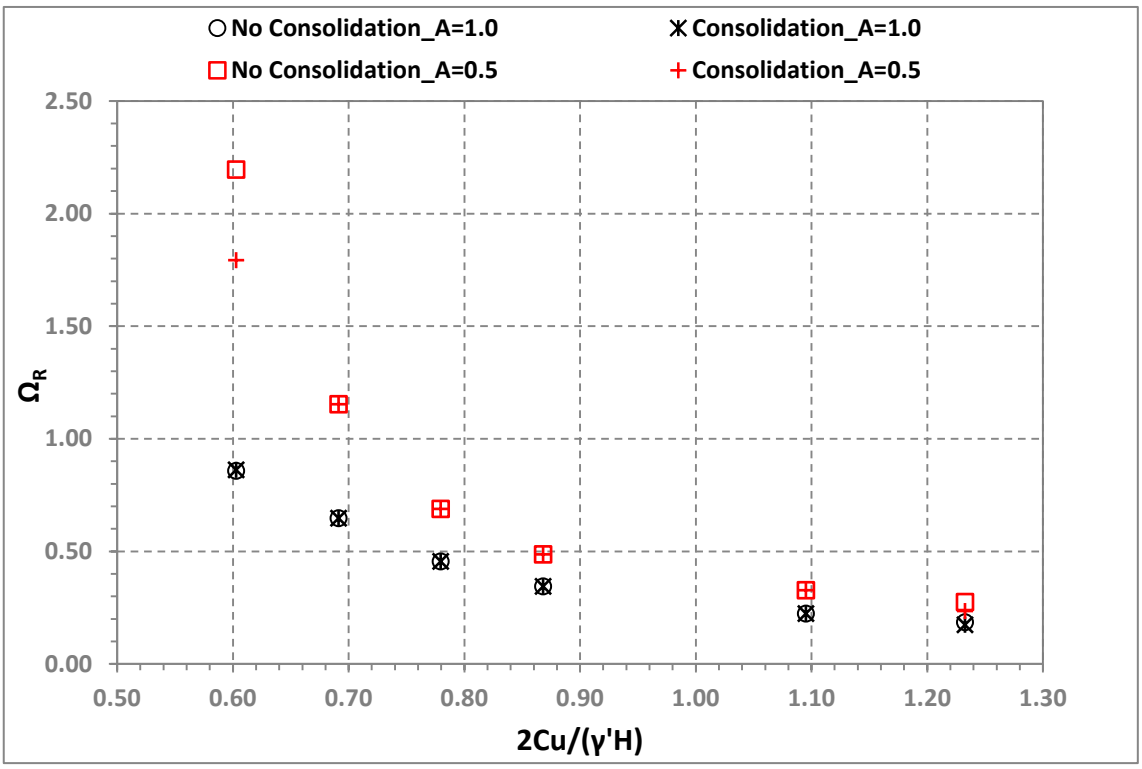


**Figure 45:** Average radial convergence at face chainage x=0 versus the stability ratio 2Cu/γ'H, for the two (2) assumed muck conditions, support pressure ratios **A=0.5 & 1.0**, **k=5E-07**m/s, **AR=0.67**m/h and various geotechnical conditions (**a-f**).

Although results for partial effective stress development do not seem to influence the face stability, conclusions need to be cautious because parameters such as the permeability or the initial support pressure (i.e. at the tunnel crown) seem to be decisive and for this reason further investigation with additional analyses must be carried out.

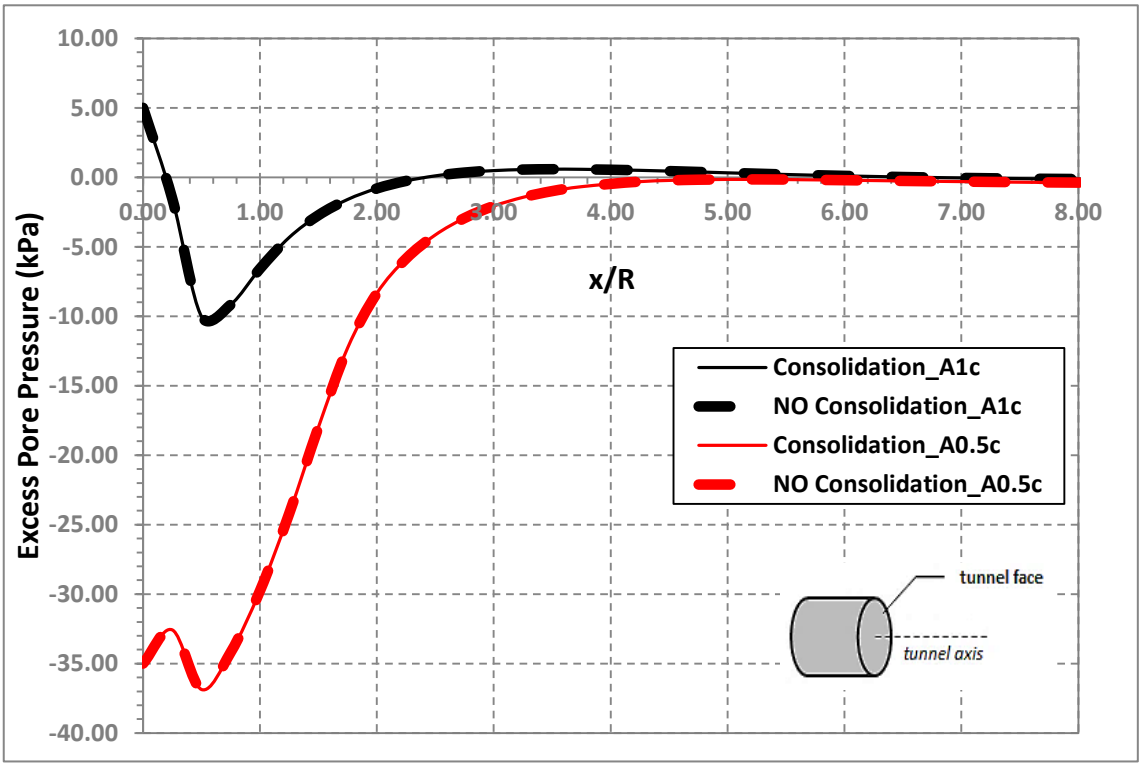


**Figure 46:** Excess pore pressure build up ahead of the face, along the tunnel axis, for the two (2) assumed muck conditions and support pressure cases **A=0.5 & 1.0**, soil profile **c**, **k=5E-07m/s** and **AR=0.67m/s**.

## 4.4. Permeability effect on face stability

In the present section, results from parametric analyses of ground permeability are given. The results correspond to analyses for various geotechnical conditions (a-f) and for two (2) different applied face pressures (A=0.5 & A=1.0). Three (3) different values of permeability were investigated, one order of magnitude increased and decreased compared to the basic value of 5E-07m/s. The selection was based on demand for compatibility with a clayey ground as higher values of permeability would deviate from the initial concept.

### 4.4.1. Face extrusion

To begin with, extrusion contours of the investigated section are presented in figures 47 & 48 for both support pressure cases and for reference soil profile c. Results clearly indicate that increase of soil permeability leads to increase of face extrusion. However, it is also clear that the magnitude of its effect depends highly on the applied face pressure which defines concurrently the imposed hydraulic boundary conditions. In more detail, in case of A=1.0 its effect on face stability is negligible (e.g. two order of magnitude increase leads only to twofold extrusion). On the contrary, in the case of A=0.5, its effect becomes quite significant denoting unstable face conditions which is localized mostly at the lower supported - upper part of the section.

In Figure 49 extrusion profiles of the investigated cases are shown. Initially, it is evident that permeability effect depends on the imposed hydraulic boundaries of the face. Combination of decreased pore pressure values at the face and increased permeability seems to result in excessive deformation. The reason of that parameter's greater effect for support pressure case A=0.5 lies on the deformation mechanism which cannot be recognized easily in the contours. Resulting extrusion from analyses for A=0.5 seem to have a very different form comparing to those for A=1.0 due to unfavorable seepage effects caused by permeability variation. Extrusion for A=1.0 seems to be practically constant irrespective of the face elevation, implying a uniform dilatant tendency (especially in low permeable soil). On the contrary, extrusion for low face pressure values (=low pore pressure values) are localized at the upper part of the section due to loss of hydraulic equilibrium.

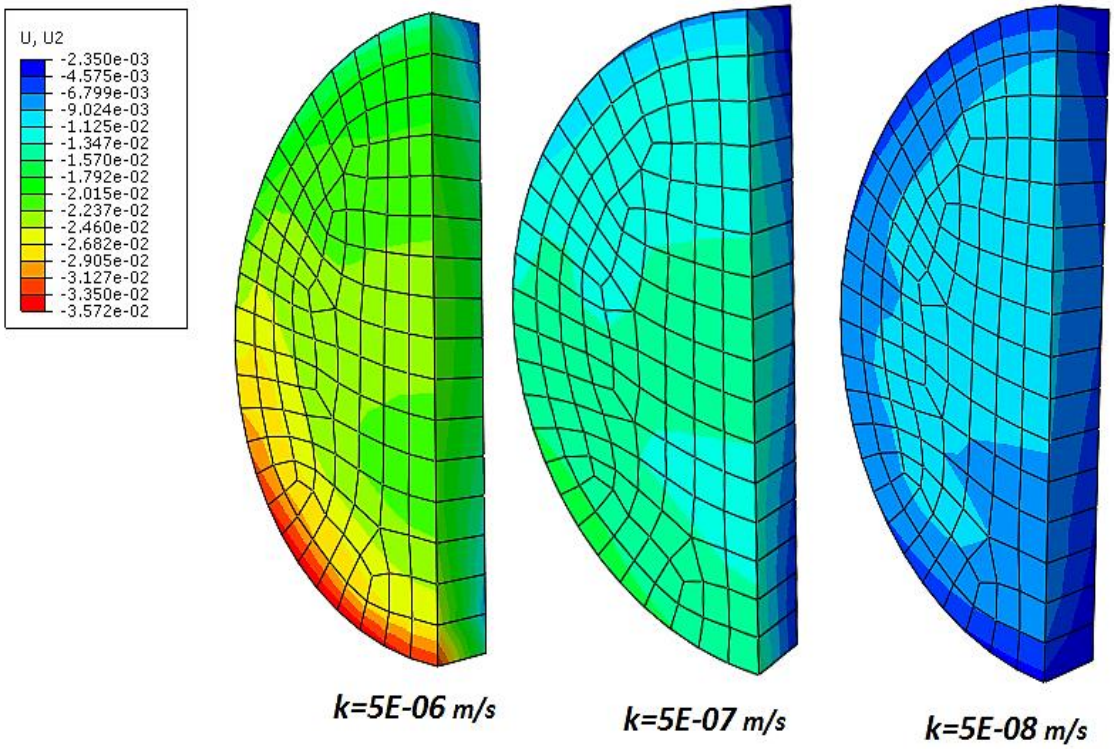


**Figure 47:** Resulted extrusion contours (in m) of the investigated section **(x=0)**, for the three (3) investigated values of permeability, **A=1.0**, **AR=0.67**m/h and soil profile **c**. Negative sign indicate opposite direction in relation to that of tunnel advance.

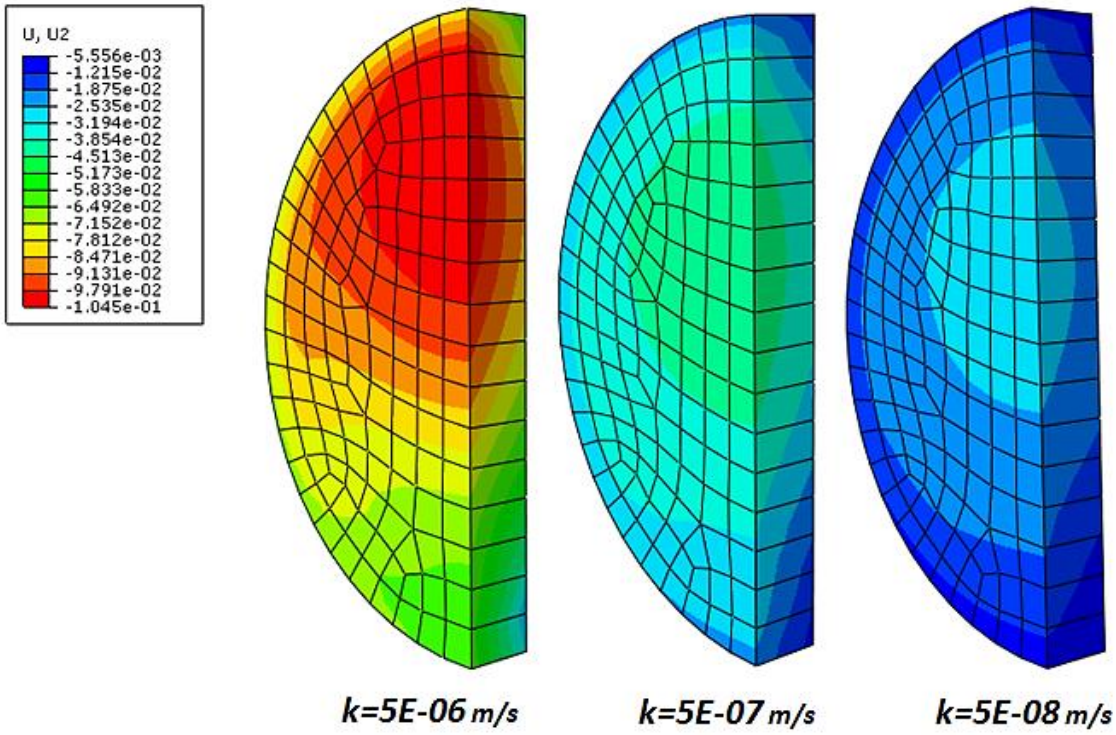


**Figure 48:** Resulted extrusion contours (in m) of the investigated section **(x=0)**, for the three (3) investigated values of permeability, **A=0.5**, **AR=0.67**m/h and soil profile **c**. Negative sign indicate opposite direction in relation to that of tunnel advance.

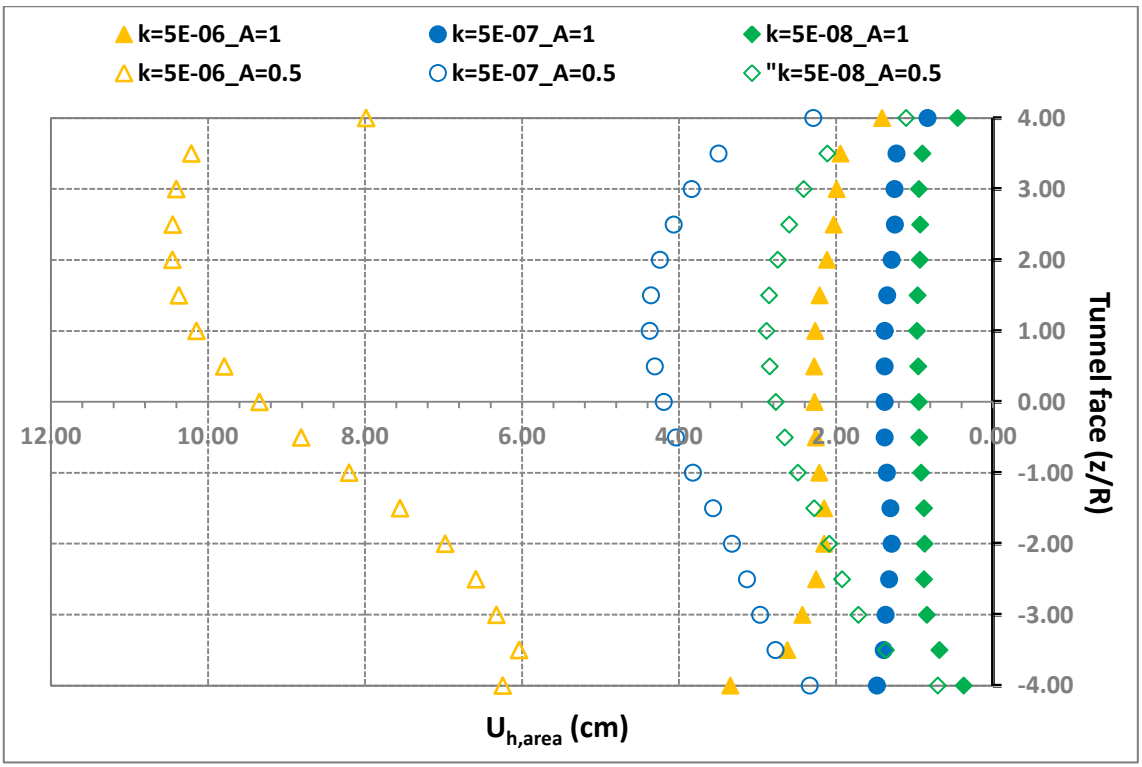


**Figure 49:** Indicative face extrusion profiles along tunnel's diameter, for the three (3) investigated values of permeability (in m/s), support pressure **A=0.5 & 1.0**, **AR=0.67**m/h and soil profile **c**.

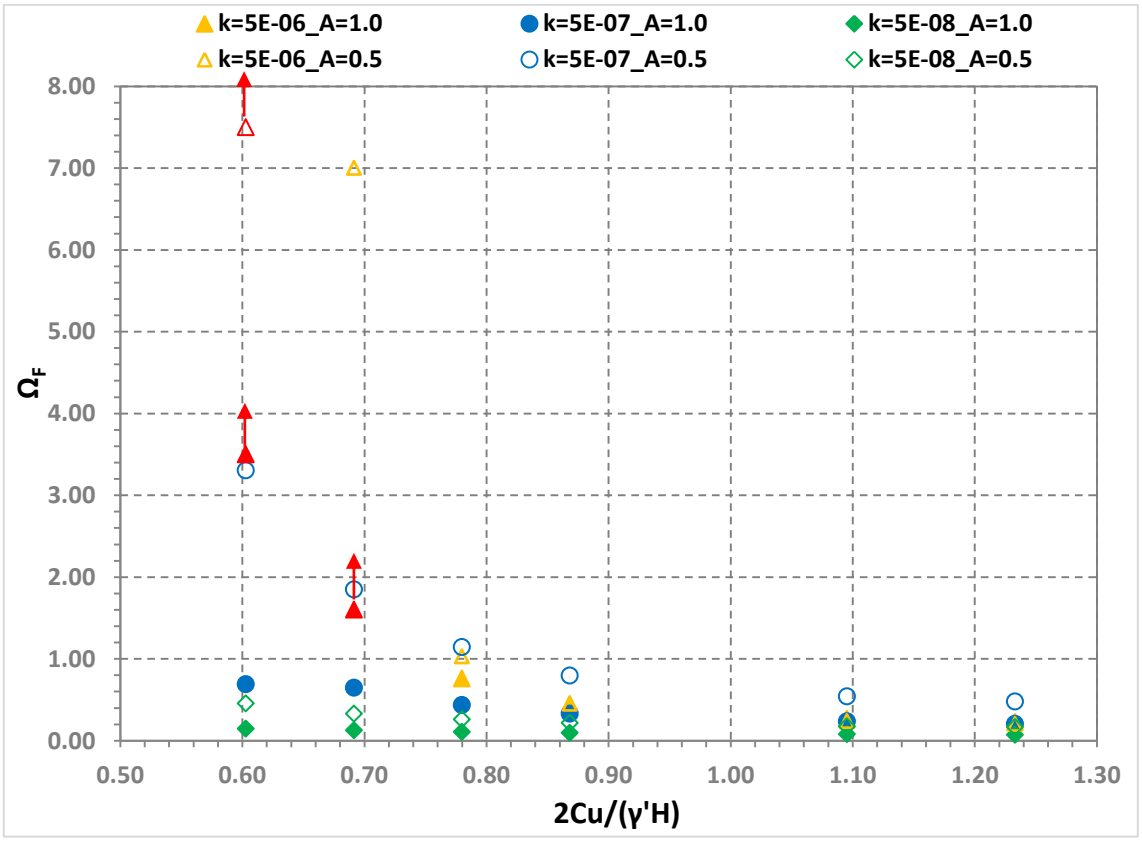


**Figure 50:** Average face extrusion versus the stability ratio 2Cu/γ'H, for the three (3) investigated values of permeability (in m/s), support pressure **A=0.5 & 1.0**, **AR=0.67**m/h and various geotechnical conditions (**a-f**). Uncompleted analyses (3) are depicted with red color at the last successfully completed step.

Figure 50 shows the variation of extrusion factor $\Omega_F$ versus the stability ratio $2C_u/\gamma'H$. Analyses for higher pressure values and/with lower permeability values indicate a stable face regardless of the geotechnical conditions. Unfavorable combinations of poor geotechnical conditions ($2C_u/\gamma'H<0.8$) – increased permeability (k=5E-06m/s or higher) may lead to considerable extrusion while other plotted results from the analyses could not be completed due to severe numerical instabilities caused by excessive deformation. The plotted face extrusion values are obtained at the last successfully completed step of the analyses. Of course they cannot be assumed as final and as a result their incremental tendency is indicated by red arrows.

Coupled analyses include time-dependent, interrelated mechanisms. Based on the assumption made regarding muck's condition, decrease of support pressure means decrease in pore pressures at the excavation boundary affecting the hydraulic head distribution at the surrounding soil. It is known that, lower hydraulic head in the chamber compared to that of undisturbed soil results in water seepage, the magnitude of which depends primarily on permeability. The higher the soil's permeability, the more increased are the seepage forces towards the tunnel face and consequently its deformation.

In an attempt to recognize the latter in the present study, water flow velocity contours for low face pressure (A=0.5) and soil profile **c** are depicted in Figure 51. It seems that the expected extrusion (Figure 47, Figure 48) is partially attributed to seepage effects. When the hydraulic head in the chamber is lower than that ahead of the face (blue areas) seepage tends to occur towards the face causing higher extrusion values. Higher values of permeability cause higher flow velocities, that is higher seepage forces which eventually result in even higher extrusion values (case k=5E-06m/s). In case of k=5E-07m/s (basic value) seepage is restricted only where loss of hydraulic balance is not in favor (upper part). Finally, for k=5E-08m/s the effect of hydraulic conditions on tunnel face stability is quite interesting. Although face support pressure is low, the permeability is not high enough to permit water to drain towards the face. As a result, the face is deformed (dilatant behavior) but the water is not able to fill the "unsaturated" voids within the available amount of time and therefore negative pore pressures are developed (suction). Although, pore pressures are presented afterwards (§4.4.3) yet resulting positive flow velocities verify it. The latter increases the effective stresses, so extrusion is limited. Suction phenomena and short-term self-support of clayey formations are also important in other geotechnical applications such as open

trenches. The aforementioned available amount of time depends on the loading/unloading rate of the soil which in our case is expressed through the applied rate of advance. This issue as well as its effect will be addressed in the next section.

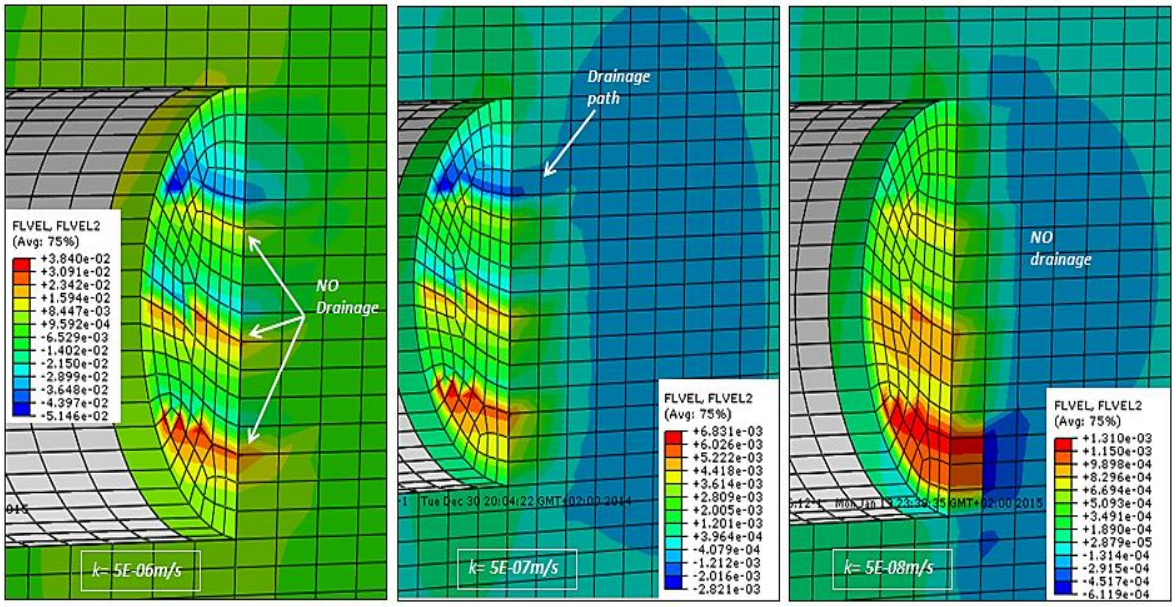


**Figure 51:** Water flow velocity contours (in m/h) at the vicinity of the tunnel face for the three (3) investigated values of permeability, **A=0.5**, **AR=0.67m/h** and soil profile **c**. Negative sign indicate water flow **towards** the tunnel face.

### 4.4.2. Face Convergence - Preconvergence

Face convergence was found closely related with face extrusion for different support pressure cases. In a similar way, evolution of convergence (preconvergence) along with its final value at the investigated face chainage (face convergence) was investigated for the same three (3) permeability values and also for two (2) different support pressure values (A=0.5 & 1.0).

Initially, transversal cross-section (z-x) of tunnel's face deformed state is presented for support pressure A=1.0 & 0.5 (Figure 52 & Figure 53). Radial convergence values are again presented 10 times multiplied for clarity reasons. It should be repeated that interest is not drawn on the absolute value of deformation but on the relative effect of parameters on it. Convergence results come in perfect agreement with those of extrusion validating that they constitute two closely inter-related deformation mechanisms. As permeability raises, convergence also raises. The rate of increase is again regulated by the applied pressure at the face. Permeability variation is found to be significant only for support pressure case A=0.5,

thus denoting the importance of hydraulic boundaries as an unfavorable gradient may lead to serious instabilities.

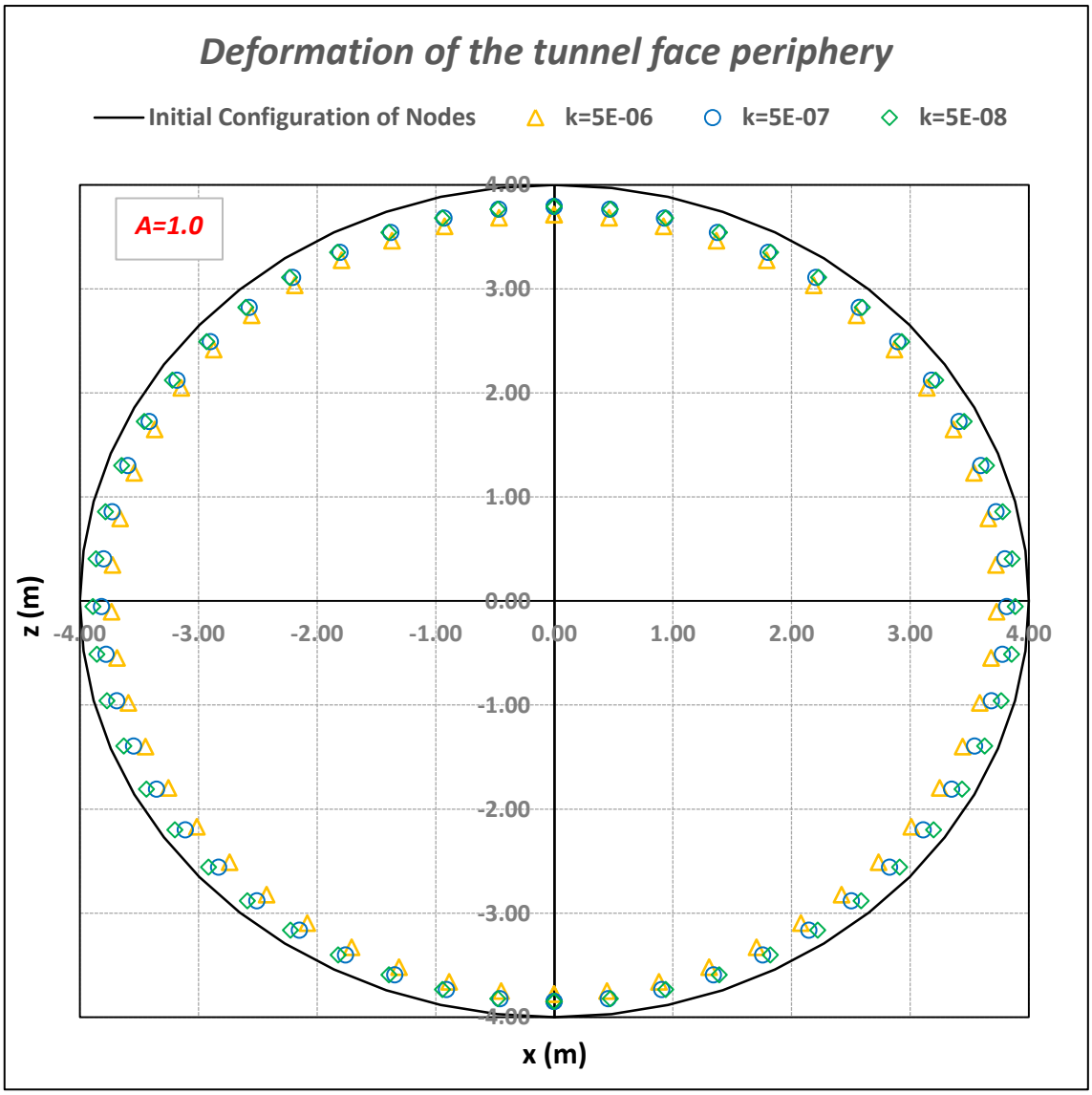


**Figure 52:** Illustration of 10-fold radial convergence at face chainage x=0 for the three (3) investigated values of permeability (in m/s), support pressure **A=1.0**, soil profile **c**, and **AR=0.67**m/h.

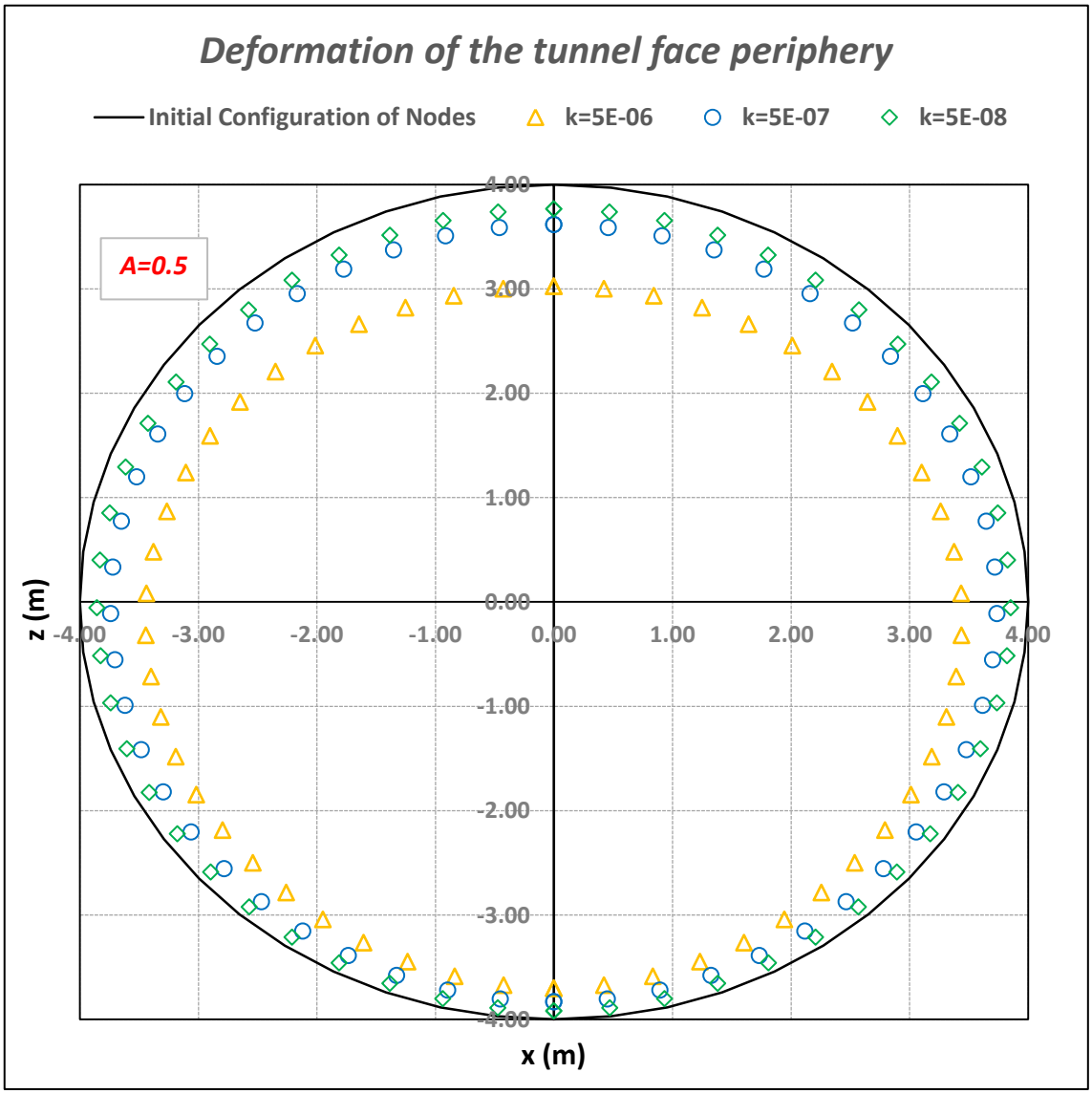


**Figure 53:** Illustration of 10-fold radial convergence at face chainage x=0 for the three (3) investigated values of permeability (in m/s), support pressure **A=0.5**, soil profile **c**, and **AR=0.67**m/h.

In Figure 54 the average radial convergence of the tunnel versus the normalized distance from the face (x/R) is depicted in a longitudinal cross-section for specific geotechnical conditions. Increase of convergence is more abrupt for support pressure A=0.5 and it is mainly observed in a distance x=2R=D verifying previous assumption regarding the length of the advance core. The abrupt increase at face chainage x=0 is in good agreement with the form of final radial convergence (Figure 52, Figure 53).

Finally, normalized convergence $\Omega_R$ is plotted versus the stability ratio $2C_u/\gamma'H$. Unstable face conditions are expected for $2C_u/\gamma'H<0.8$ and k=5E-06m/s or higher for both face pressure cases. Red colored values correspond to the three (3) aforementioned semi-completed analyses which indicate face instability.

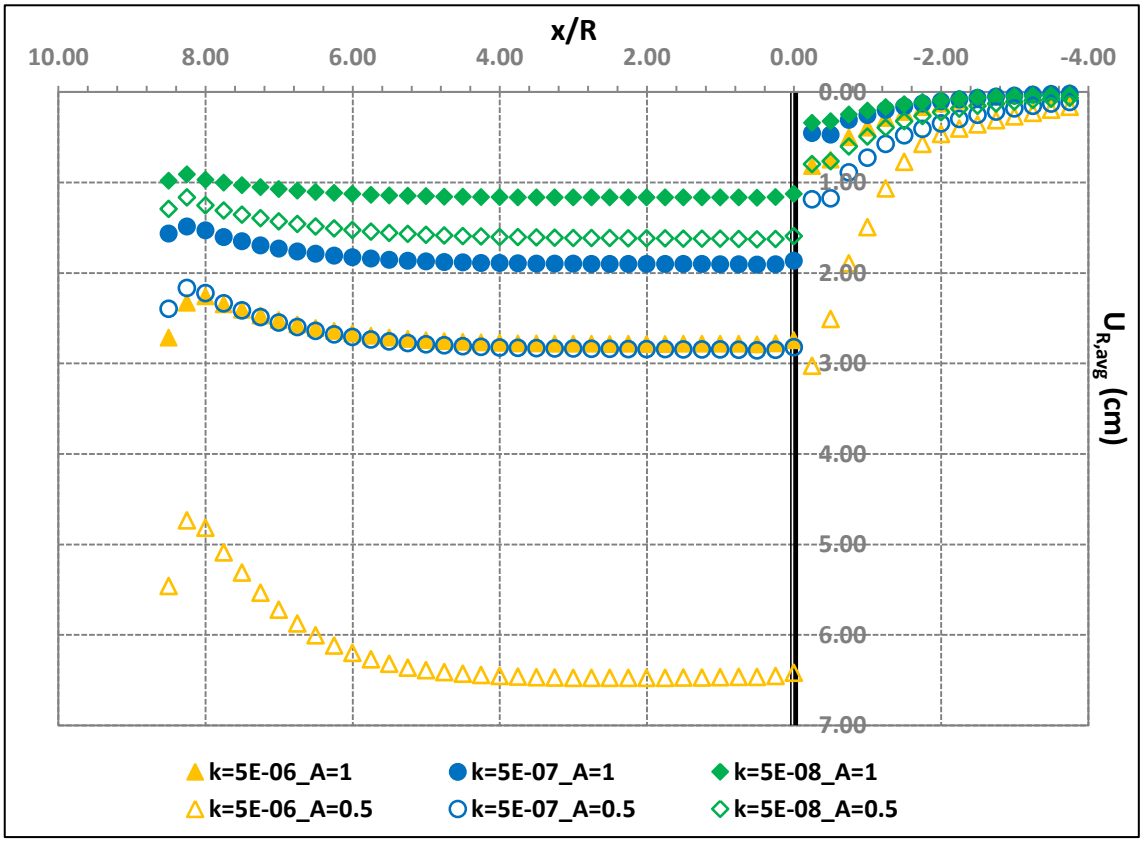


**Figure 54:** Indicative longitudinal profile of average radial convergence, ahead and behind the face for the three (3) investigated values of permeability (in m/s), support pressure **A=0.5 & 1.0**, **AR=0.67**m/h and soil profile **c**.

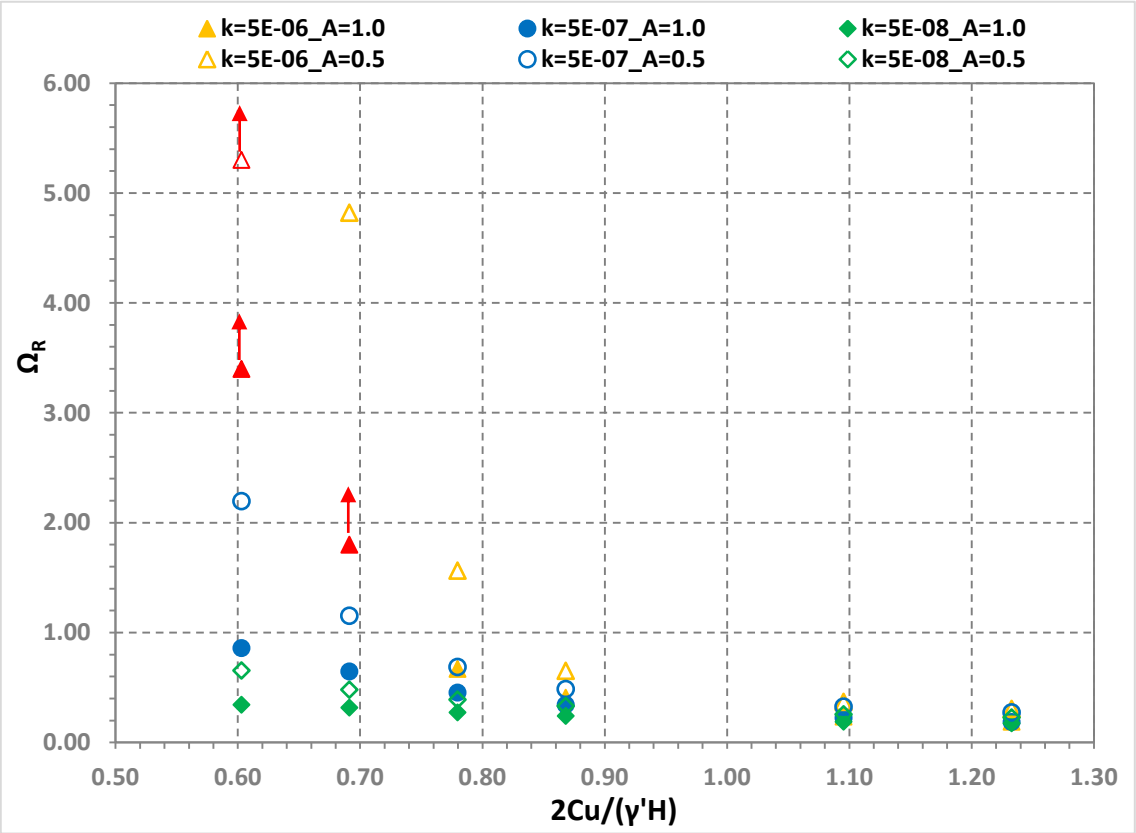


**Figure 55:** Average radial convergence at face chainage x=0 versus the stability ratio 2Cu/γ'H, for the three (3) investigated values of permeability (in m/s), support pressure **A=0.5 & 1.0**, **AR=0.67**m/h and various geotechnical conditions (**a-f**). Uncompleted analyses (3) are depicted with red color at the last completed step.

### 4.4.3. Excess Pore Pressures ahead of the face

Variation of permeability modifies or even alters the drainage conditions and consequently the pore pressures build up. Figure 56 presents the distribution of excess pore pressures ahead of tunnel face, along the horizontal axis (y) of the tunnel for the three (3) investigated values of permeability and for two (2) different applied face pressures. It was found that the initial pore pressure value at the face (x=0), coincides with the applied pore pressure value of the central node. By carefully observing Figure 56 the following can be derived:

- Pore pressure distribution ahead of the face is mainly controlled by the applied support pressure and the imposed hydraulic boundaries. Nevertheless, permeability variation has a significant effect on it.

- Excess pore pressures for low permeable soils tend to dissipate more abruptly just as for high support pressure values. Restricted disturbance of the stress and hydraulic field is the most likely cause.
- In the case of permeability k=5E-07m/s or lower, negative excess pore pressures (suction) are developed in a relatively short distance from the face containing as it was explained before, the expected deformation.
- Suction phenomena are not observed for permeability k=5E-06m/s or higher. On the contrary, pore pressure raise is developed close to the face.
- A bizarre raise of positive excess pore pressures (~13kPa) is observed for k=5E-06m/s and A=1.0 in front of the face.

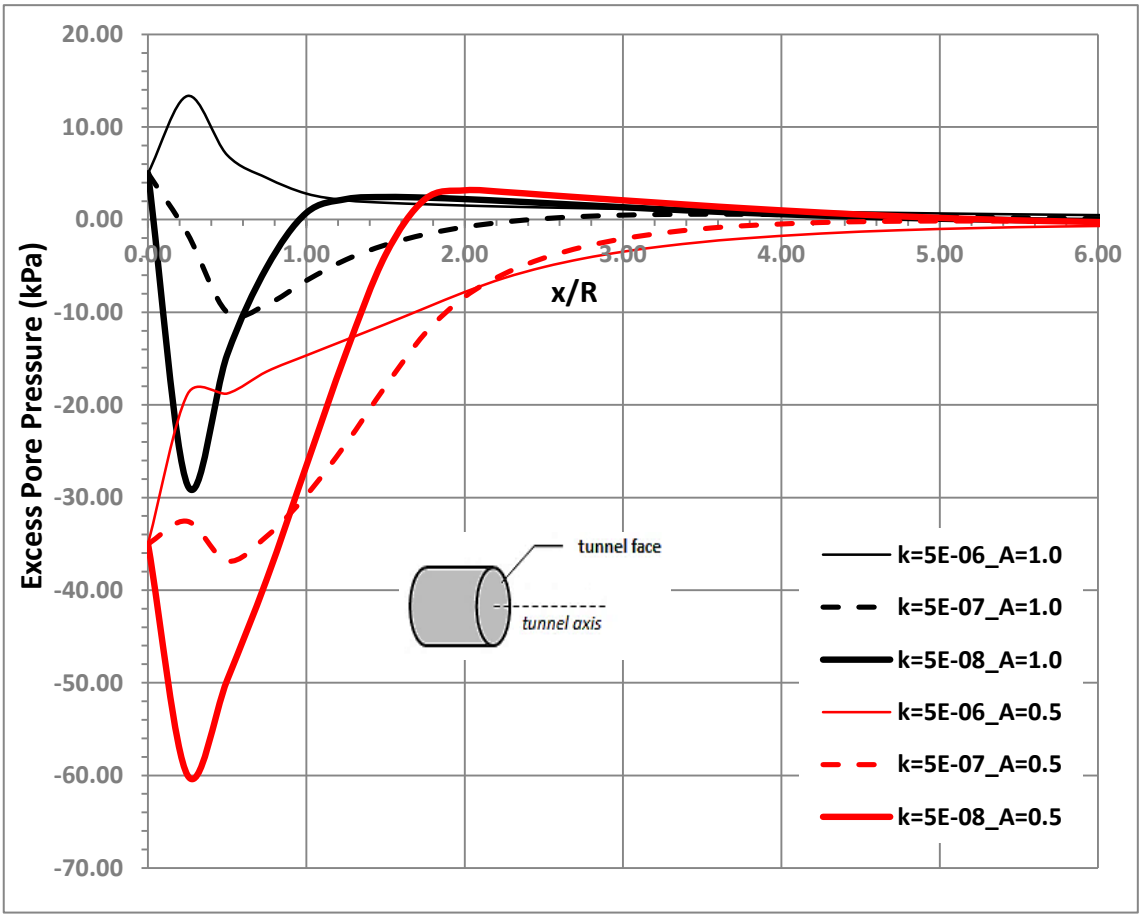


**Figure 56:** Excess pore pressures ahead of the tunnel face, calculated on the horizontal tunnel axis versus the distance (x/R), for the three (3) investigated values of permeability (in m/s), support pressure **A=0.5 & 1.0**, **AR=0.67**m/h and soil profile **c**.

Attempting to explain the last observation, we tried firstly to assess the sensitivity of results in soil's dilatancy. Dilatancy angle was taken as a constant fraction of friction angle (i.e. $\delta=\phi/6$). For this reason an additional set of analyses (8) was indicatively carried out,

assuming two (2) extreme cases, i.e. **δ=0** & **δ=ϕ**. In Figure 57, results of excess pore pressure distribution are plotted for the two extreme cases. Reasonably, increase of dilatancy results in pore pressure decrease and vice versa. Nonetheless, excess pore pressure observed cannot be attributed to the low dilatancy angle assumed (δ=3,33deg). Pore pressure results from the analysis assuming k=5E-06m/s and δ=0 (–) are not presented in Figure 57 because it did not succeed to terminate due to numerical instabilities resulting from the combination of parameters selected. However, it does not seem to influence the conclusions as it most likely follows the same trend of the other two curves. Afterwards, since a single soil profile is examined (soil **c**), sensitivity of results in geotechnical conditions was investigated. It was noticed that regardless of the geotechnical properties, the same trend existed and in addition to that more competent soil profiles (e.g. soil **f**) developed greater values.

Concluding, excess pore pressure build up in front of the working face is most probably related to the extent of deformation and the applied pore pressure boundaries. It is known that, increase of permeability facilitates water seepage. Since deformation for support pressure A=1.0 is restricted, pore water that seeps towards the tunnel is locally squeezed resulting in the aforementioned spike. Despite that, it should be highlighted herein that the distribution presented concerns the developed pore pressures in a characteristic but **single** node-row in front of the tunnel. Consequently, any conclusions should be treated with caution.

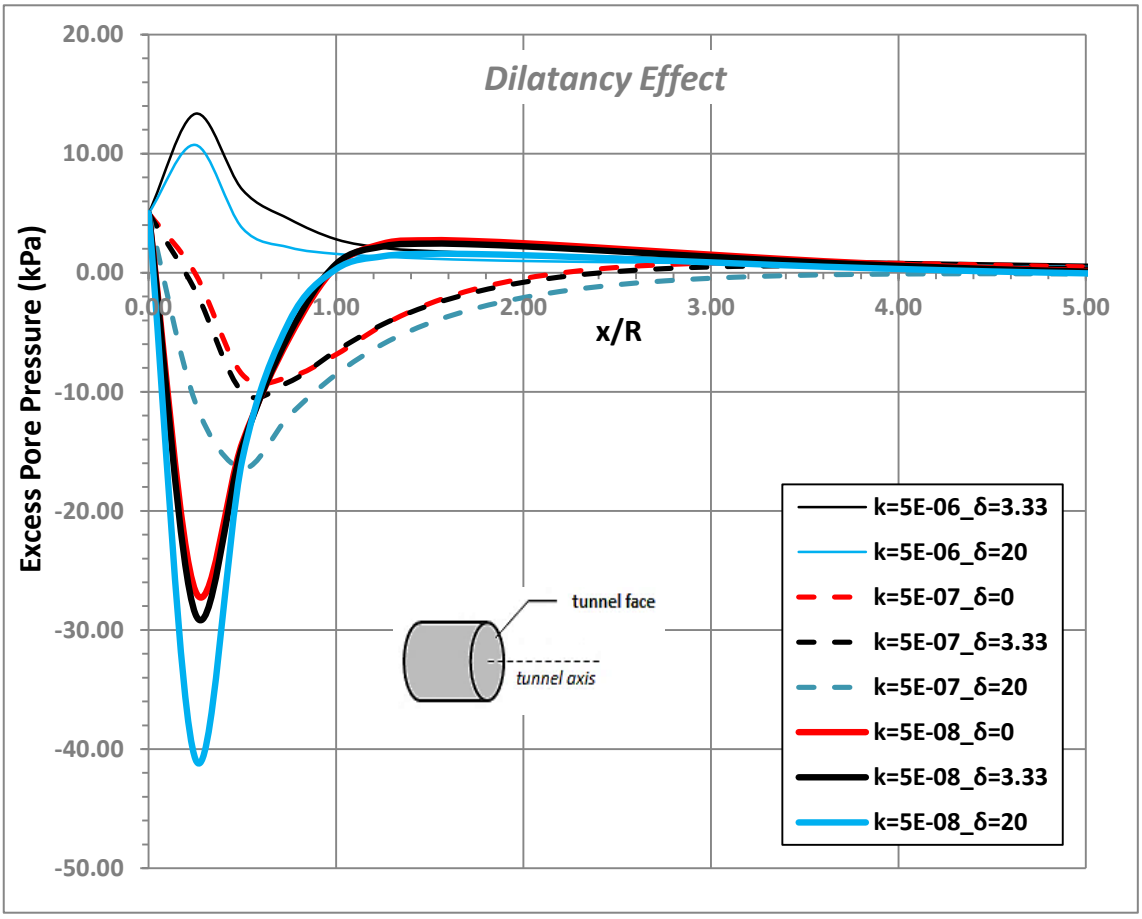


**Figure 57:** Excess pore pressures ahead of the tunnel face, calculated on the horizontal tunnel axis versus the distance (x/R), for the three (3) investigated values of permeability (in m/s) and angles of dilatancy (in degrees), support pressure ratios **A=1.0**, **AR=0.67**m/h and soil profile **c**.

## 4.5. Advance Rate effect on face stability

Advance rate and permeability variation is considered to affect both the drainage conditions and the hydraulic head field distribution and are connected with time dependent phenomena in low permeable soils (e.g. consolidation). In the present section, results from parametric investigation of advance rate effect are presented. Although advance rate in common EPBM practice does not vary a lot, three (3) different values of advance rate were investigated to cover the whole application range (AR=0.5, 0.67 & 1.0m/h[17]). The results correspond to analyses for various geotechnical conditions **(a-f)** and for two (2) different applied face pressures (**A=0.5 & A=1.0**).

[17] 12, 16 & 24m/day

### 4.5.1. Face extrusion

Initially, extrusion contours of investigated section (x=0) are presented for the three (3) investigated advance rate values and for specific geotechnical conditions (Figure 58 & Figure 59). It is evident that results resemble significantly with those of the permeability investigation (Figure 47 & Figure 48), verifying the view that both parameters affect the same phenomena. Increase of advance rate results in decrease of extrusion because drainage and its consequences are hindered. Regarding the distribution of extrusion on the face surface, its effect is reasonably localized at the central/upper part of the section where the face is lower supported. However, the magnitude of this variation is indisputably much smaller comparing to permeability.

Moreover, comparing the effect of the two pressure cases it can be derived that its effect also depends on the assigned pore pressure boundaries. The latter is much clearer in Figure 60 where extrusion profiles of soil **c** for the three (3) investigated values of advance rate and for two (2) different face support pressures are shown. Advance rate effect on resulting extrusion for support pressure case A=1.0 is negligible while for support ratio A=0.5, advance rate variation seems to have a small impact on the expected extrusion.

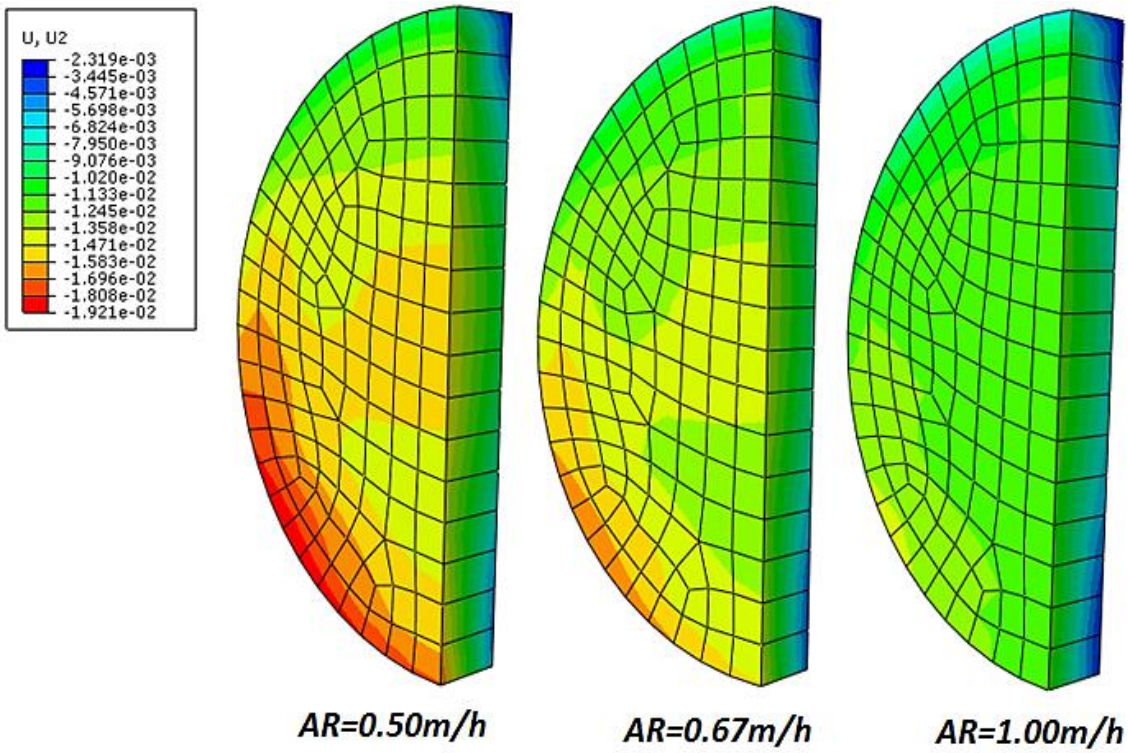


**Figure 58:** Resulted extrusion contours (in m) of the investigated section **(x=0)**, for the three (3) investigated advance rate values, **A=1.0**, **k=5E-07m/s** and soil profile **c**. Minus sign indicate opposite direction in relation to that of tunnel advance.

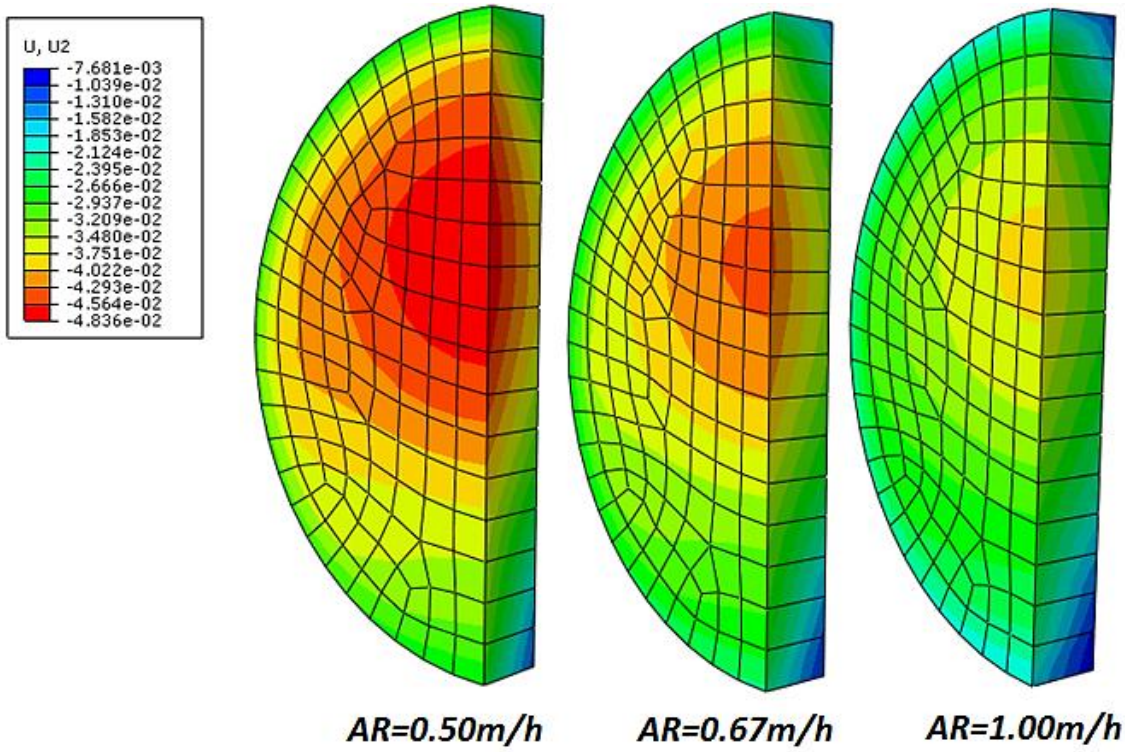


**Figure 59:** Resulted extrusion contours (in m) of the investigated section **(x=0)**, for the three (3) investigated advance rate values, **A=0.5**, **k=5E-07m/s** and soil profile **c**. Minus sign indicate opposite direction in relation to that of tunnel advance.

The reason of parameter's greater effect on expected extrusion for support pressure case A=0.5 lies on the deformation mechanism which cannot be recognized easily in contours. Resulting extrusion from analyses for A=0.5 seem to have a very different form comparing with those for A=1.0 due to local alteration of the hydraulic field. Extrusion for A=1.0 seems to be practically constant irrespective of the face elevation implying a uniform dilatant tendency. On the contrary, extrusion for low face pressure values (=low pore pressure values) are localized at the upper part of the section due to the unfavorable piezometric head and therefore to minimal development of seepage forces **towards** the face.

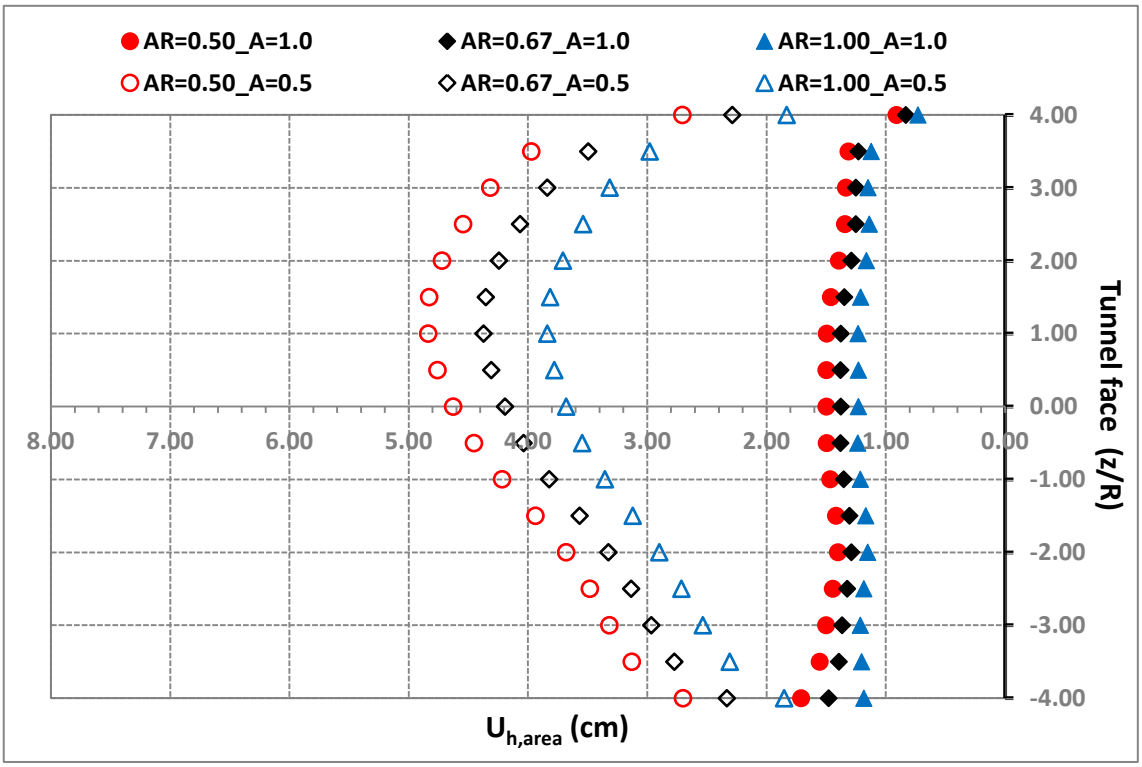


**Figure 60:** Indicative face **extrusion** profiles along tunnel's diameter, for the three (3) investigated values of advance rate (in m/h), support pressure ratios **A=0.5 & 1.0**, **k=5E-07**m/s and soil profile **c**.

Finally, Figure 61 depicts the variation of extrusion factor $\Omega_F$ versus the stability ratio $2C_u/\gamma'H$. It seems that for face support pressure A=1.0 the excavation face remains stable regardless of the applied advance rate and the assumed geotechnical conditions. The latter proves again that support pressure applied at the face along with prevailing hydraulic boundaries at the face is the factor that practically controls the stability of the face. Advance rate effect is noticed only in unstable conditions (i.e. $2C_u/\gamma'H<0.8$ and A=0.5) but it is not considered significant as instability is caused anywise by lack of sufficient support.

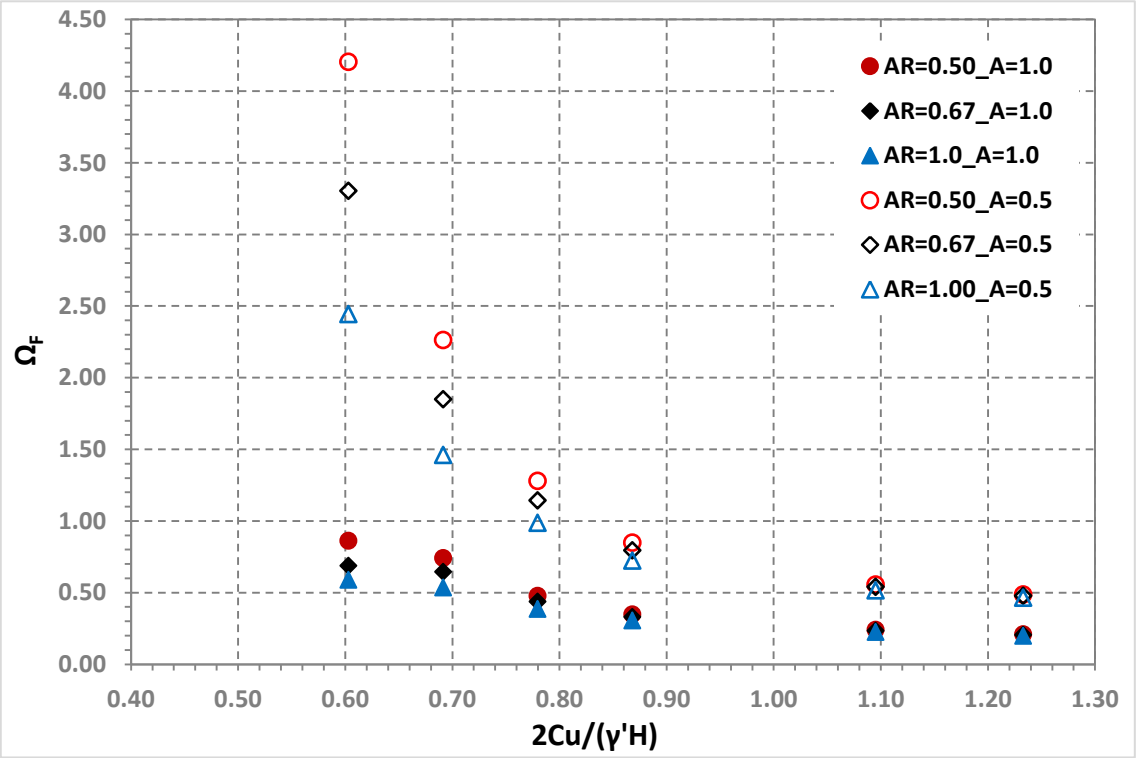


**Figure 61:** Average face extrusion versus the stability ratio 2Cu/γ'H, for the three (3) investigated values of advance rate (in m/h), support pressure ratios **A=0.5 & 1.0**, **k=5E-07**m/s and various geotechnical conditions (**a-f**).

### 4.5.2. Face Convergence

In the present paragraph, evolution of convergence (preconvergence) along with its final value at the investigated face chainage (face convergence) is presented for the three (3) investigated advance rates and also for two (2) different support pressure values (A=0.5 & 1.0). To begin with, transversal cross-section (z-x) of tunnel's face deformed state is presented for support pressure A=1.0 & 0.5 (Figure 62 & Figure 63). Radial convergence values are always presented 10 times exaggerated for clarity reasons. A common observation for both support pressure cases is that variation of advance rate hardly affects the final convergence value at the working face. The same conclusion is reached regarding its evolution (preconvergence) as it is shown in Figure 64.

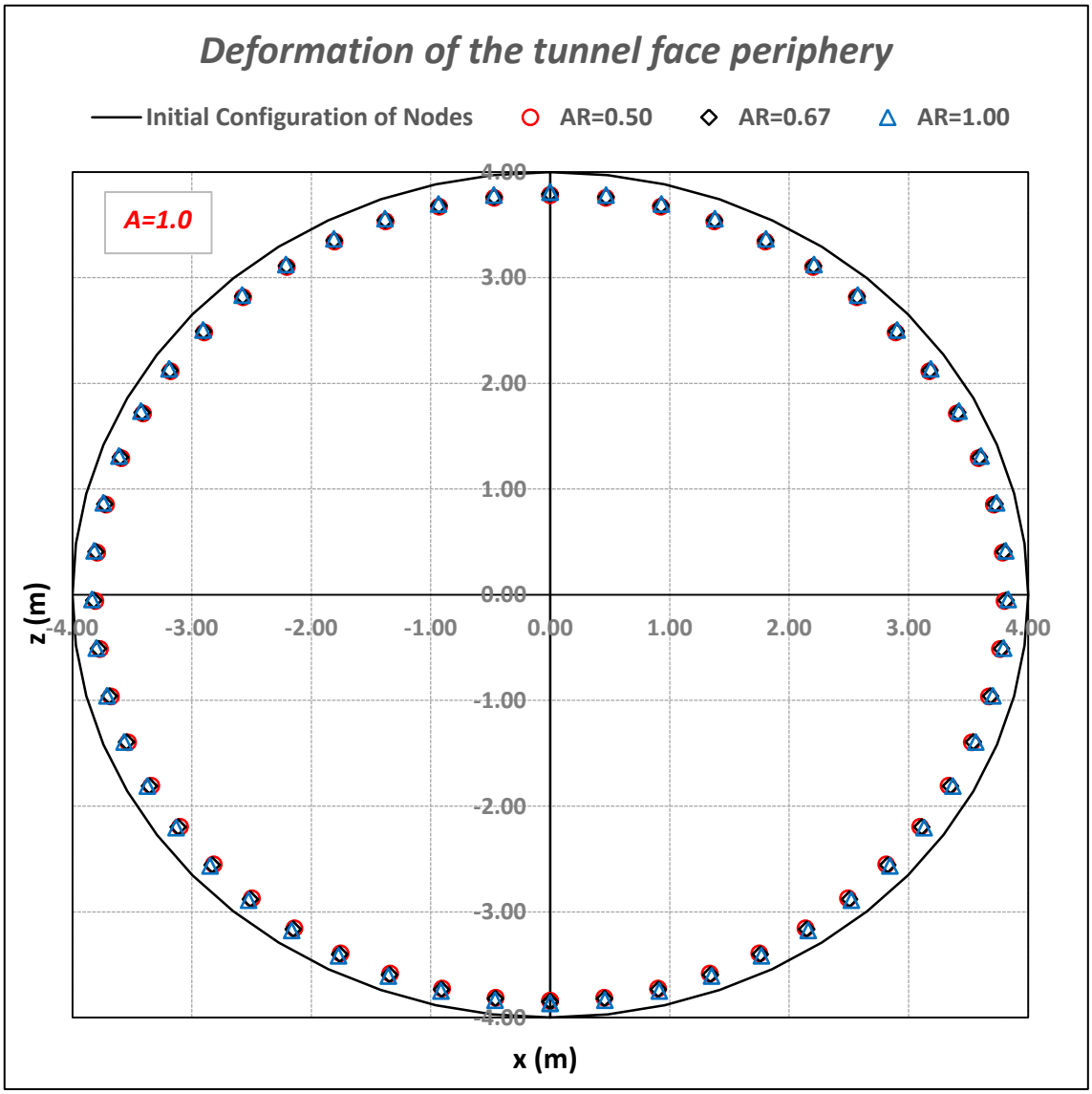


**Figure 62:** Illustration of 10-fold radial convergence at face chainage x=0 for the three (3) investigated values of advance rate (in m/h), support pressure **A=1.0**, soil profile **c** and **k=5E-07**m/s.

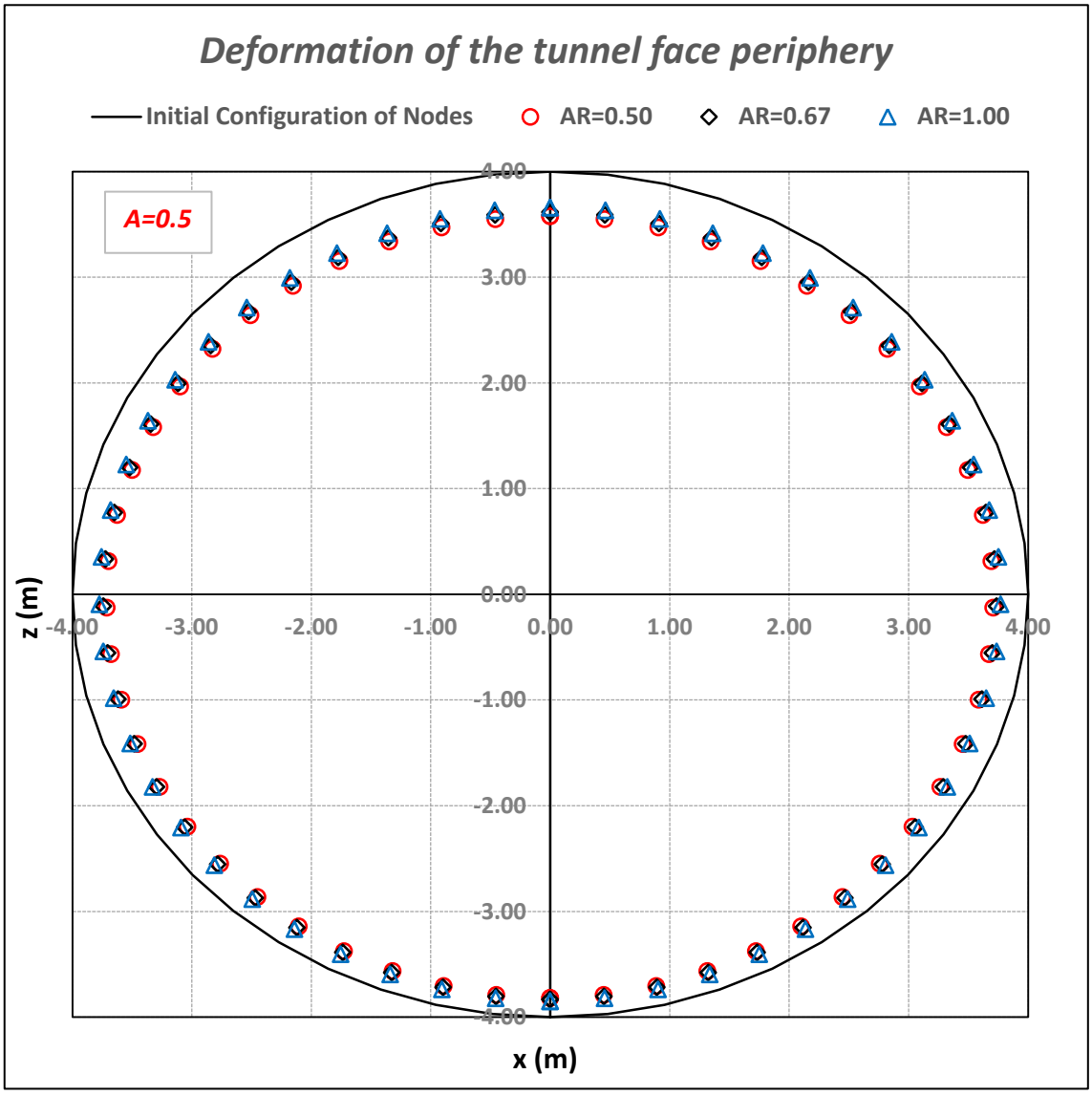


**Figure 63:** Illustration of 10-fold radial convergence at face chainage x=0 for the three (3) investigated values of advance rate (in m/h), support pressure **A=0.5**, soil profile **c** and **k=5E-07**m/s.

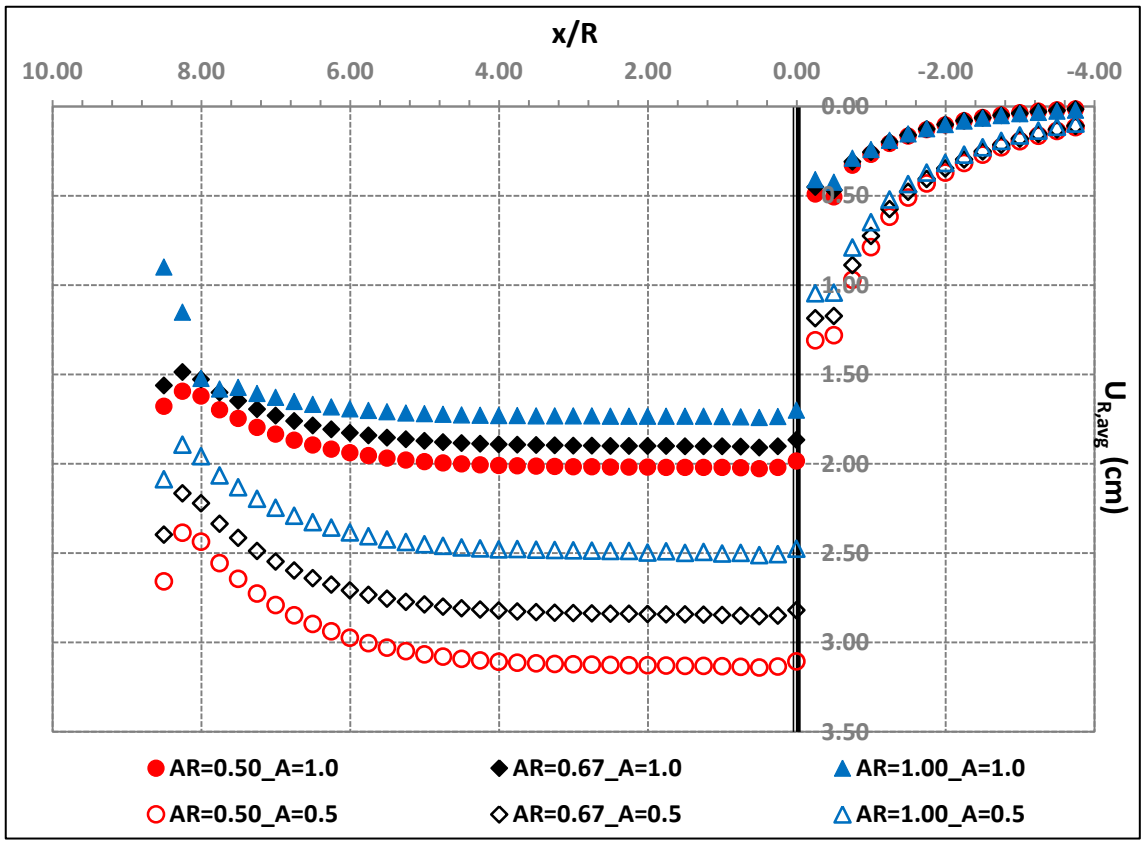


**Figure 64:** Indicative longitudinal profile of average radial convergence, ahead and behind the face for the three (3) investigated values of advance rate (in m/h), support pressure ratios **A=0.5 & 1.0**, **k=5E-07**m/s and soil profile **c**.

Finally, distribution of radial convergence factor $\Omega_R$ versus the stability ratio $2C_u/\gamma'H$ is depicted in Figure 65. Two (2) areas can be observed. For $2C_u/\gamma'H>0.8$ the working face remains stable as for permeability variation, with no effect of advance rate on the expected radial convergence. For ratio values less than 0.8, stability conditions are aggravating with a restricted effect by advance rate variation. Concluding, it should be mentioned that investigation of a wider range of advance rate may lead to completely different results regarding its effect on the problem. Nonetheless, given that advance rate variation is somehow constrained in practice, something like that would be unrealistic.

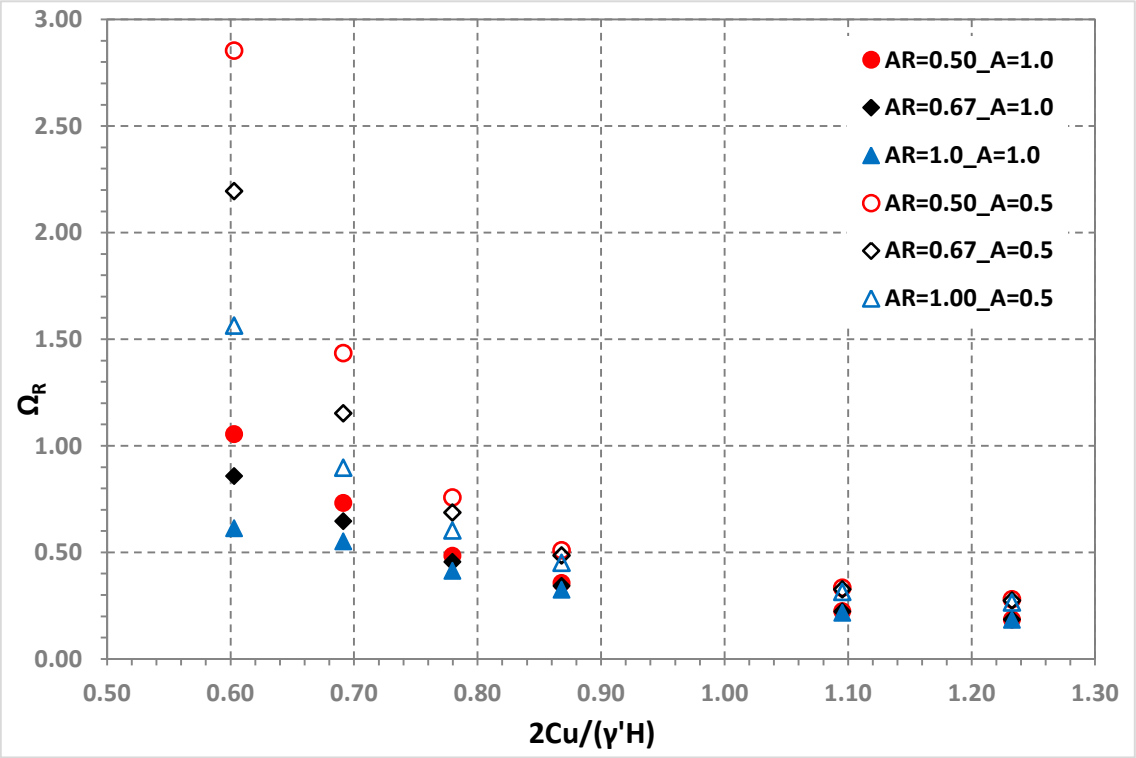


**Figure 65:** Average radial convergence at face chainage x=0 versus the stability ratio 2Cu/γ'H, for the three (3) investigated values of advance rate (in m/h), support pressure ratios **A=0.5 & 1.0**, **k=5E-07**m/s and various geotechnical conditions **(a-f)**.

### 4.5.3. Excess Pore Pressures ahead of the face

Apart from advance rate variation effect on deformation, hydraulic head field distribution is also affected locally due to possible modification of drainage conditions. In Figure 66, excess pore pressure distribution ahead of the face is shown, calculated along the horizontal tunnel axis.

Typical for practically undrained conditions, rise of advance rate leads to pore pressure decrease due to suction. However, the effect on pore pressure build up and its dissipation distance is practically negligible which comes to verify the aforementioned conclusions regarding the effect on the expected deformation.

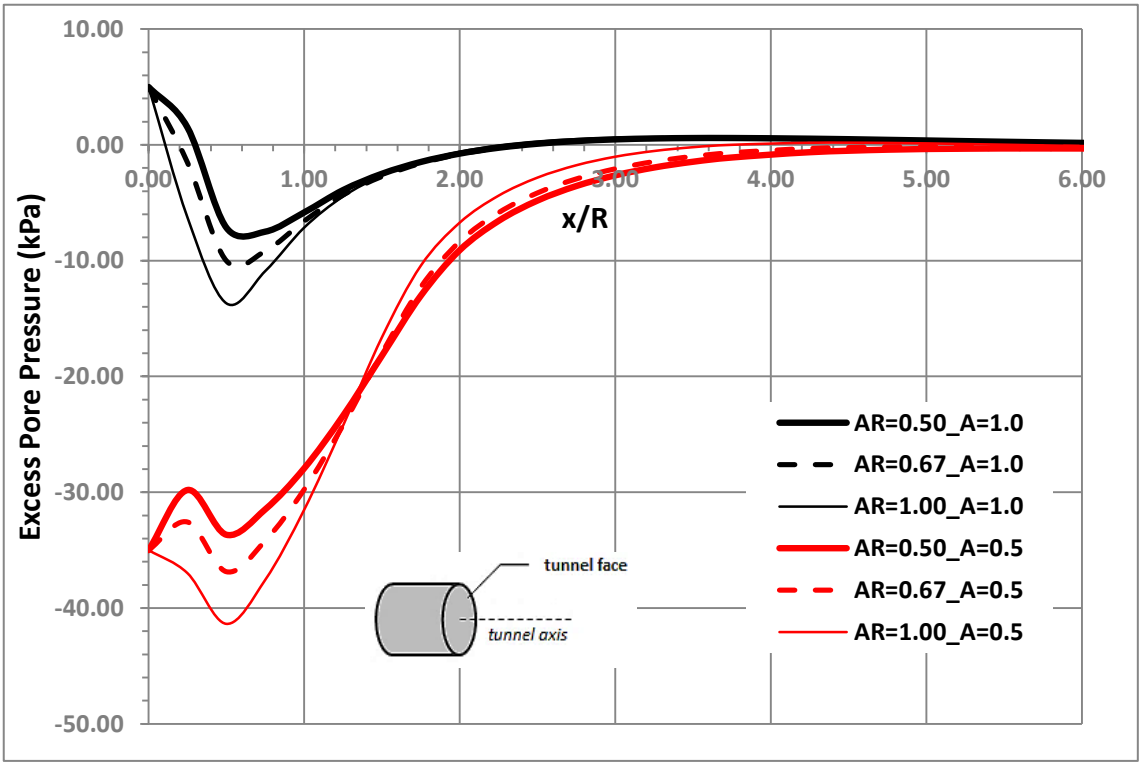


**Figure 66:** Excess pore pressures ahead of the tunnel face, calculated on the horizontal tunnel axis versus the distance (x/R), for the three (3) investigated rates of advance (in m/h), support pressure ratios **A=0.5 & 1.0**, **k=5E-07**m/s and soil profile **c**.

## 4.6. Verification analysis of simplification on pressure assignment

As it was mentioned in §2.5, in order to reduce modelling and computational time, a simplification was adopted regarding the application of pore pressure values at the excavation face. In more detail, instead of assigning at each node of the face a unique pore pressure value equally corresponding to the applied support pressure, the face surface was divided in four (4) node-sets, each one having a constant pore pressure value (Figure 25). Figure 26 presents an indicative sketch of the simplification made for the case of absolute pressure $P_0$ at the crown equal to the hydrostatic one (A=1). In order to validate that the results are not affected by this simplification, a random verification analysis was carried out where at each face node was assigned its unique pore pressure value. The results of this analysis are presented herein.

Figure 67, Figure 68 & **Σφάλμα! Το αρχείο προέλευσης της αναφοράς δεν βρέθηκε.** depict compared results of extrusion, convergence and pore pressure build up ahead of the

tunnel face respectively. It is evident that the simplification made regarding the pore pressure assignment at the face is valid as the results do not seem to be practically affected.

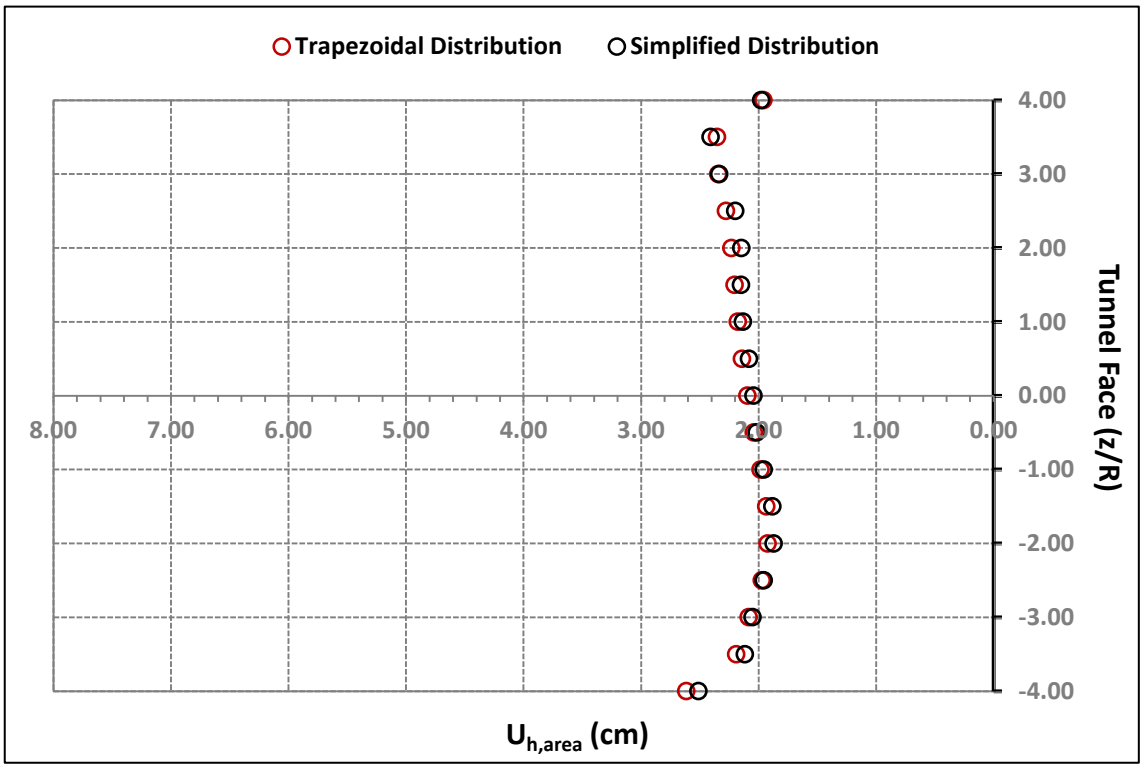


**Figure 67:** Comparison of extrusion profiles assuming precise (trapezoidal) and simplified distribution of pore pressure values at the face of a random analysis.

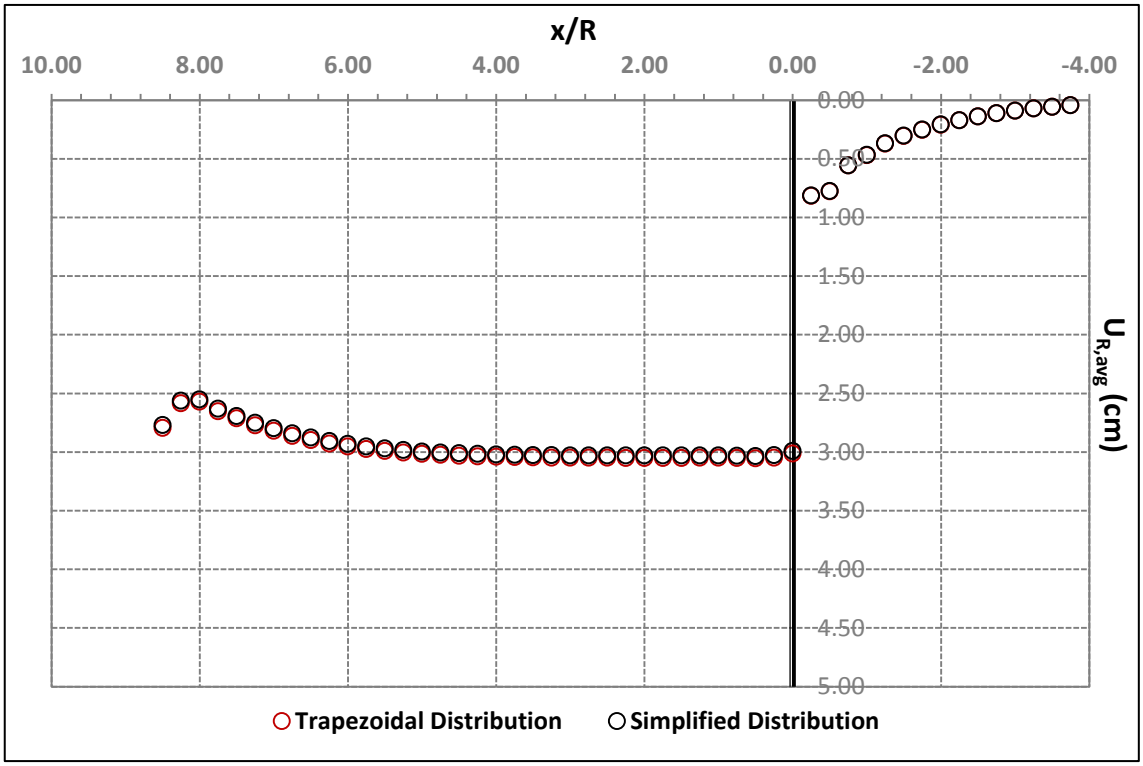


**Figure 68:** Comparison of average convergence profiles, assuming precise (trapezoidal) and simplified distribution of pore pressure values at the face of a random analysis.

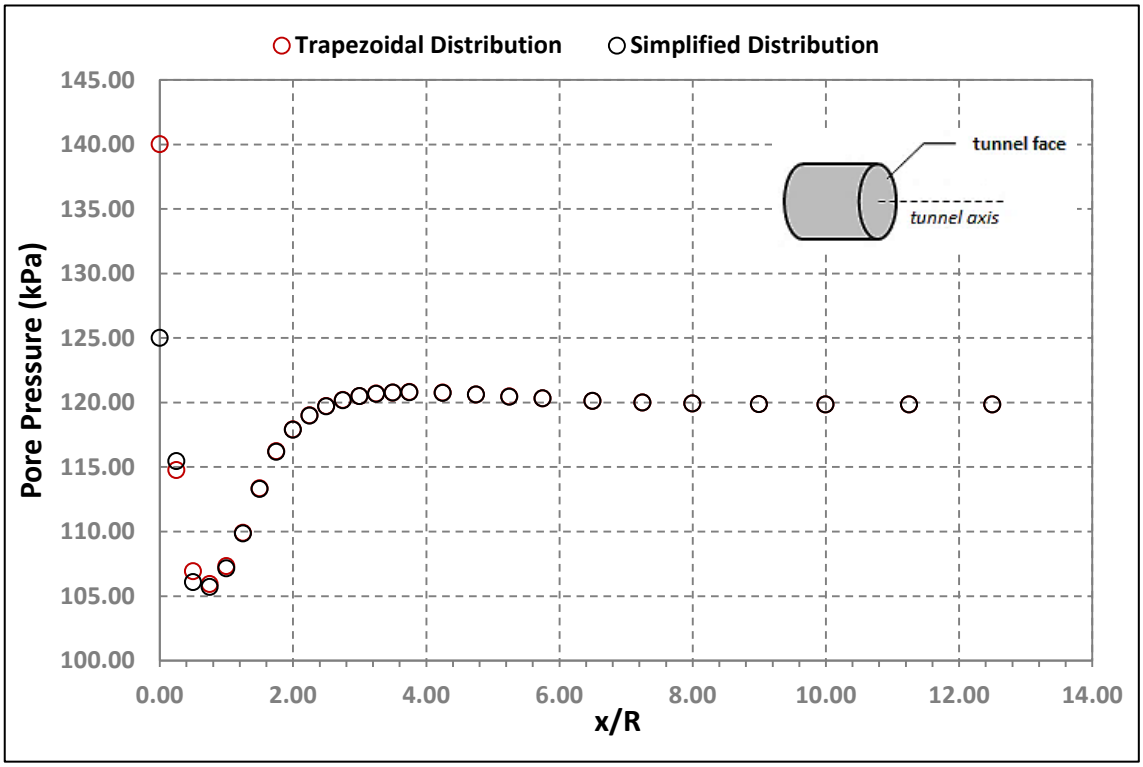


**Figure 69:** Comparison of pore pressure development ahead of the tunnel face versus the distance (x/R), assuming precise (trapezoidal) and simplified distribution of pore pressure values at the face of a random analysis.

# 5
# Conclusions & Suggestions

In the present postgraduate Thesis, results from a significant number of 3D hydro-mechanical FEM analyses are presented and evaluated aiming to investigate parameters that may alter the hydraulic conditions and affect the stability of the excavation face of shallow, EPB-bored tunnels, in fully saturated, clayey soils. In more detail, the effect of three (3) main parameters was explicitly studied, namely:

- the applied face support pressure,
- the ground permeability &
- the excavation rate, mostly known as rate of advance.

The performed FEM analyses concern specific geometrical characteristics (H/D=1.5), hydrostatic initial stress field ($K_0$=1) and various geotechnical conditions (soil strength & compressibility). Deformation results were expressed through the resulting average extrusion and radial convergence at the investigated section and they were plotted versus a newly proposed stability factor $2C_u/\gamma'H$. It is evident that utilization of the undrained shear strength of the excavated ground implies that the selected simulation parameters correspond to undrained excavation conditions. The validity of this assumption was continuously checked and found to be valid as the value of the void ratio hardly showed any variation during the analyses. Finally, the excavation-induced disturbance of the hydraulic status in the vicinity of the tunnel face was studied by monitoring the pore water pressure distribution and the water flow velocities ahead of it. The most significant conclusions reached through this work are summarized below:

- Applied face pressure was found to be decisive regarding the magnitude of deformations. In the case of support pressure greater than the hydrostatic, the face remains stable even in poor geotechnical conditions whereas when serious pressure drop is combined with unfavorable geotechnical conditions ($2C_u/\gamma'H<1.0$), excessive deformation is triggered. Unity was found to be a marginal value between the two stability states. Higher extrusion is reasonably observed at the low-supported, upper part of the section.

- Permeability variation consistent to low-permeable soils indicate that the face stability may be aggravated by permeability increase in poor geotechnical conditions even for adequate face pressure. The latter effect is regulated by the hydraulic boundaries at the excavation face and possible development of unfavorable seepage forces.
- Advance rate variation within the common range of EPB practice showed that drainage conditions are not practically affected and thus its impact on face stability compared to that of permeability is considerably smaller.
- Face extrusion and convergence were proven to be closely related and inter-dependent as the results show perfect agreement. Low face pressures values, higher values of ground permeability or/and low rates of advance also lead to higher convergence values localized mostly near the tunnel crown.
- Extrusion is affected by the face pressure variation in greater degree than the convergence as extrusion and face pressure both refer to the same axis (y).
- Investigation of hydraulic boundaries' modification caused by consolidation of the muck showed that even a significant rise of effective stresses in the chamber is not adequate to affect neither the anticipated deformations nor the hydraulic head distribution. However the latter refers to a certain permeability value and given the sensibility of coupled FEM analyses, it should be investigated further in order to reach a "safe" conclusion.
- The disturbance on the local hydraulic head field is regulated by the hydraulic boundaries at the excavation face. Pore pressure distribution ahead of the face as well as seepage forces are in accordance with the deformation results and the prevailing drainage conditions. Excess face pressure results in excess pore pressure build up (+) ahead of the face which tend to dissipate in relatively short distance due to limited deformation. On the contrary, negative (-) excess pore pressures are developed due to suction when the face is deformed under undrained conditions (low permeability – insufficient face pressure – high rate of advance). Suction acts in favor of the stability as it leads to temporary rise of effective stresses. Indeed, aggravation of geotechnical properties or permeability rise when face pressure is considered adequate did not seem to affect the stability of the face.

- Considerable seepage forces were not anticipated due to the flow constraint. Despite that, examination of flow velocity vectors ahead of the face showed that increase of hydraulic gradient due to decrease of pore pressure boundaries contributes to further increase of extrusion.

**Prospectively**, further research may be based on the present including the following:

- Application of different constitutive laws and more consistent to clayey-low permeable soils, such as the Modified Cam-Clay constitutive model.
- Investigation of different overburden heights and/or tunnel diameter (H/D ratios).
- Investigation of different $K_0$ coefficients in order to accommodate the initial stress field effect.
- Apart from the boring cycle, other phases of the procedure such as a standstill of the machine such as the ring erection or maintenance works of the cutter wheel could be studied regarding the effect of hydraulic conditions on tunnel face stability (advanced consolidation phenomena). In order to accommodate such downtimes, increase of duration of computational iterations would be sensible.
- Given that undrained conditions and related phenomena (e.g. suction) act in favor of tunnel face stability, further research could be conducted regarding the allowable stand-up time of the soil formation, the critical face pressure etc.

Over the last years, sophisticated methods have been developed to accommodate ground water presence and its effects on tunnel face stability. Numerical methods and their constantly reduced computational time thanks to technological advance have been well established both in research and design phase while efforts such as the present one constitute a further step towards better comprehension and reliable prediction of soil behavior. However, it is important to realize that even an advanced and implicit modelling in a numerical 3D coupled analysis can only give an indication of the excavation-induced outcome. Soil-water-tunnel interaction can be really difficult to be evaluated due to its complex nature and the high degree of uncertainty of the input parameters. Consequently, previous experience, field observation and in-situ measurements remain key factors for a successful tunnelling project.

# REFERENCES


Abaqus, D. (2011) Abaqus/Standard Analysis User's Manual, USA. Available at citeulike-article-id:6641735

Anagnostou G., Kovari K. (1994). Stability Analysis for tunnelling with Slurry and EPB Shields. *"Gallerie in condizioni difficili"*. Torino, Italy.

Anagnostou, G. (1993). Modelling Seepage Flow during Tunnel Excavation. *EUROCK '93.* Rotterdam: Ribeiro e Sousa & Grossman.

Anagnostou, G. (1995). The influence of tunnel excavation on the hydraulic head. *International Journal for Numerical and Analytical Methods in Geomechanics*, 725-746.

Anagnostou, G. (2002). Urban Tunnelling in water bearing ground - Common problems and soil-mechanical analysis methods. *Proceedings of 2nd International Conference on Soil Structure Interaction in Urban Civil Engineering.* Zurich.

Anagnostou, G. (2008). The Effect of Tunnel Advance Rate on the Surface Settlements. *Proceedings of 12th International Conference of International Association for Computer Methods and Advances in Geomechanics (IACMAG).* Goa, India.

Anagnostou, G. (2014). *Muir Wood Lecture 2014 - "Some Critical Aspects of Subacqueous Tunnelling".* Avignon: ITA-AITES.

Arnau O., Molins C. (2012). Three dimensional structural response of segmental tunnel linings. *Engineering Structures 44*, 210-221.

Babendererde, L. (2003). *Problems of TBMs in Water Bearing Ground.* Nordseetaucher GmbH: Hyperbaric Tunnelling Technical Report.

Bakker K.J., Teunissen E.A.H., van den Berg P., Smits M., Th. J.H. (2003). K100 research at the second Heinenoord tunnel. *Proceedings of 31st ITA-AITES World Tunnel Congress.* Amsterdam: Taylor & Francis plc.

Bezuijen A., Joustra J.F.W., Talmon A.M., Grote B. (2005a). Pressure gradients at the tunnel face of an Earth Pressure Balance shield. In E. Y. Solak T., *Underground Space Use: Analysis of the Past and Lessons for the Future.* London: Taylor & Francis Group.

Bezuijen A., Pruiksma P.J., van Meerten H.H. (2006). Pore pressures in front of tunnel, measurements, calculations and consequences for stability of tunnel face. In S. T. ErdemY., *Tunnelling. A Decade of Progress. Geodelft 1995-2005* (pp. 27-33). Bezuijen A. & van Lottum H.

Bezuijen A., Talmon A. (2006). Calculation Models based on Monitoring during Tunnel Construction. In H. v. A. Bezuijen, *Tunnelling. A Decade of Progress. GeoDelft 1995-2005.* London: Taylor & Francis Group plc.

Bezuijen A., Talmon A.M. (2008). Processes around a TBM. *Proceedings of the 6th International Symposium IS-Shanghai 2008.* Shanghai, China: Taylor & Francis plc.

Bezuijen A., Talmon A.M. (2014a). Soil pressures at the cutting wheel and the pressure bulkhead of an EPB-shield. In P. S. Yoo C., *Geotechnical Aspects of Underground Construction in Soft Ground* (pp. 523-531). Shanghai: Taylor Francis Group.

Bezuijen A., Talmon A.M. (2014b). Soil pressures on both sides of the cutter wheel of an EPB-shield. *Proceedings of the 40th WTC 2014.* Iguassu Falls, Brazil.

Bezuijen A., Talmon A.M., Joustra J.F.W., Grote B. (2005b). Pressure gradients and muck properties at the face of an EPB. *Proceedings of the 5th International Symposium TC28.* Amsterdam, 15-17 June: Taylor & Francis plc.

Bezuijen, A. (2006). The influence of soil permeability on the properties of a foam mixture in a TBM. In H. v. A. Bezuijen, *Tunnelling. A Decade of progress. Geodelft: 1995-2005* (pp. 35-41). London: Taylor & Francis plc.

Bowles, J.E., (1997). "*Foundation Analysis and Design*". 5th Edition, McGraw Hill

Broere W., van Tol A.F. (2000). Influence of Infiltration and Groundwater Flow on Tunnel Face Stability. In F. K. Kusakabe O., *Geotechnical Aspects of Underground Construction in Soft Ground* (pp. 339-344). Tokyo, Japan.

Broere W., van Tol. A.F. (2001). Time-dependant infiltration and groundwater flow in a face stability analysis. In T. K. Adachi T., *Modern Tunneling Science and Technology* (pp. 629-634). Kyoto, Japan.

Broere, W. (2001). Tunnel Face Stability & New CPT Applications. *PhD Thesis*. Delft: Deft University of Technology.

Chern, J.C., Yu, C.W., and Shiao, F.Y. (1998). "Tunnelling in squeezing ground and support estimation." Proc. Reg. Symp. Sedimentary Rock Engineering, Taipei, 192-202

EFNARC (2005). Specification and guidelines for the use of specialist products for mechanized tunneling (TBM) in soft ground and hard rock

Feng, Q. L. (2004). Soil Conditioning for modern EPBM drives. *Tunnels & Tunnellinh International*, 18-20.

Horn, M. (1961). Horizontaler Erddruck auf senkrechte Abschlußflächen. *Landeskonferenz der Ungarischen.* Budapest: Übersetzung ins Deutsche durch.

In-Mo Lee, Seok-Woo Nam. (2004). Effect of tunnel advance rate on seepage forces acting on the underwater tunnel face. *Tunnelling and Underground Space Technology*, 273-281.

Jancsecz S., Steiner W. (1994). Face Support for large Mix-Shields in Heterogeneous ground conditions. *Proceedings Tunnelling '94* (pp. 531-550). London: Chapman& Hall.

Kavvadas M. (2014). Computational Methods of Underground Project Analysis Master Course, 10th Lecture (in Greek), Design & Construction of Underground Works, Cross-Departmental Postgraduate Diploma, School of Civil Engineering – Mining & Metallurgy, N.T.U.A

Kavvadas M., Litsas D., Fortsakis P., Prountzopoulos G., Tzivakos K., Chortis P. (2013). Report on the State-of-Art with Collection of Data from TBM Tunnelling. *Deliverable 9.3 for the European Research Program NeTTUN (New Technologies for Tunnelling & Underground works. Status: Confidential*. Athens, Greece: NTUA.

Kavvadas M., Litsas D., Sitarenios P., Chortis P., Kalos A., Rachmani A. . (2015). Report on Results of Non-Linear Finite Element Analyses of Face Stability and Deformation. *Deliverable 9.8 for the European Research Program NeTTUN (New Technologies for Tunnelling & Underground works). Status: Confidential*. Athens, Greece: NTUA.

Krause, T. (1987). Schildvortrieb mit flüssigkeits- und erdgestützter Ortsbrust. Dissertation TU Braunschweig. (in German)

Leca, E. & Dormieux, L. (1990). Upper and lower bound solutions for the face stability of shallow circular tunnels in frictional material. Géotechnique, Vol. 40, p. 581-606.

Leca, E. & Panet, M. (1988). Application du Calcul à la Rupture à la stabilité du front de taille d' un tunnel. Revue Française de Géotechnique, Vol. 43, p. 5-19 (in French).

Lunardi, P. (2000). The design and construction of tunnels using the approach based. *Tunnels and Tunnelling International*, Special Supplement.

Michalakopoulos T. (2014), Mechanized tunnelling Master Course, 7th Lecture (in Greek), Design & Construction of Underground Works, Cross-Departmental Postgraduate Diploma, School of Civil Engineering – Mining & Metallurgy, N.T.U.A

Panet, M. (1993). Understanding Deformations in Tunnels. In B. E. Hudson J.A., *Compehensive Rock Engineering* (pp. 663-690). London: Pergamon.

Panet, M. (1995). *Calcul des Tunnels par la Methode de Convergence-Confinement.* Paris: Presses de l' Ecole Nationale des Ponts et Chaussees.

Peila, D. (2014). Soil Conditioning for EPB Shield Tunnelling. *KSCE Journal of Civil Engineers*, vol.18, 831-836.

Peila D., Borio L. (2010). *Training Session on Construction Methods for Tunnelling.* Buenos Aires: ITACET Foundation.

Piaskowski, A., Kowalewski, Z. (1965). Application of Thixotropic Clay Suspensions for Stability of Vertical Sides of Deep Trenches without Strutting. Proc. Int. Conf. SMFE, Vol. III, Montreal;

Prountzopoulos G. & Kavvadas M. (2014). An indirect method for the design of reinforced tunnel faces. *Proceedings of 2nd Eastern European Tunnelling Conference (EETC 2014).* Athens.

Prountzopoulos, G. (2012). *Investigation of the excavation face stability in shallow tunnels.* Athens, (in Greek): Doctoral Thesis, National Technical University of Athens .

S. Babendererde, E. Hoek, P.G. Marinos, A.S. Cardoso. (2005). EPB-TBM Face Support Control in the "Metro do Porto" Project, Portugal. *Proceedings 2005 Rapid Excavation & Tunnelling Conference.* Seattle.

S. Redmond, V. Romero. (2011). Pressure Face TBM Case Histories. *2011 Rapid Excavation & Tunnelling Conference Proceedings* (p. 1028). San Francisco: Society for Mining, Metallurgy and Exploration.

Sitarenios P. Kallivokas G., Prountzopoulos G., Kavvadas M. (2014). Investigation of Tunnel Face Stability and Deformation using Critical State Plasticity. *Proceedings of 2nd Eastern European Tunnelling Conference (EETC 2014).* Athens.

Sitarienos P., Litsas D., Papadakos A., Kavvadas M. (2015). Effect of Hydraulic Conditions in controlling the Face in EPB Excavated Tunnels. *ITA WTC 2015 Congress & 41st General Assembly.* Dubrovnik, Croatia.

Thewes M., Budach C. (2010). Soil Conditioning with foam during EPB tunnelling. *Geomechanics and Tunnelling Vol.3*.

Vermeer P.A., Ruse N., Marcher T. (2002). Tunnel Heading Stability in Drained Ground. *Felsbau 20*, No.6.

Maidl, U. 1995. Erweiterung der Einsatzbereiche des Erddruckschildes durch Bodenkonditionierung mit Schaum, *Dissertation, Ruhr-Universität Bochum.* (in German)

www.herrenknecht.com

www.facesupport.org

# APPENDIX

**Figure 70:** Field observation of EPB's conveyor belt of Athens Metro Line 3 Extension Project at Ag. Varvara Station (1).

**Figure 71:** Field observation of EPB's conveyor belt of Athens Metro Line 3 Extension Project at Ag. Varvara Station (2).